Interim Report No. 1

STUDY TO DEVELOP A TECHNIQUE FOR MEASUREMENT OF HIGH ALTITUDE OZONE PARAMETERS

Prepared for
National Aeronautics and Space Administration
Electronics Research Center
575 Technology Square
Cambridge, Massachusetts 02139
Attention: KI/Instrumentation Laboratory

Contract NAS12-137

EOS Report 7087-IR-1 15 May 1967

Prepared by

J. A. Duardo

Approved by

F. M. Johnson, Manager
Quantum Electronics Department

Approved by

A. O. Jensen, Manager
Electro-Optical Technology Laboratory

ELECTRO-OPTICAL SYSTEMS, INC. — PASADENA, CALIFORNIA
A Subsidiary of Xerox Corporation

CONTENTS

CONTENTS (contd)

CONTENTS (contd)

ILLUSTRATIONS

ILLUSTRATIONS (contd)

SECTION 1

INTRODUCTION

Although ozone is present in the earth's atmosphere only as a minor constituent, it has a profound influence on atmospheric dynamics by virtue of the fact that it is an extremely efficient absorber of solar UV radiation. The distribution of ozone in the atmosphere essentially governs the rate of absorption of solar radiation as a function of altitude, latitude, longitude, and solar zenith angle. The resultant atmospheric temperature gradients in turn provide one of the principal driving forces for the atmospheric wind fields. As evidenced by the discussions in this report and the numerous literature articles referenced in the bibliography (Section 9), a great amount of observational data has been compiled concerning ozone distributions at numerous locations. The fundamental principles of the atmospheric circulation-ozone distribution interrelationship are well understood. However, in order to extend this knowledge and to provide a means of tracing the atmospheric circulation on a global scale, measurements of the ozone distribution should be performed on a continuous basis with worldwide coverage.

The atmospheric ozone content and its vertical distribution have been measured by optical techniques since Fabry and Buisson first demonstrated in 1913 that ozone was responsible for the atmospheric solar cutoff at 3000Å. Since then, a great number of spectroscopic investigations of the absorption properties of ozone have also been

conducted in the laboratory. As a result of the laboratory measurements, the numerous and extensive measurements of atmospheric concentrations, and the thorough analyses which have been performed in the reduction of observational data, the optical techniques for determining total ozone concentrations have been highly refined. The resolution with which the vertical distribution of ozone can be determined from the ground is still, however, rather poor. Among the major objectives of this program is the determination of how the established optical techniques for measuring the vertical distribution of ozone can be adapted so they can be performed from an orbiting satellite. The limits of accuracy for these techniques are also to be established by analyses which adopt reasonable values of anticipated measurement errors.

The studies performed to date on this program have confirmed the basic feasibility of using optical means for the continuous measurement of atmospheric ozone from an orbiting satellite. Two techniques, in particular, appear to offer great promise for implementation in the near future. That is, it is not anticipated that a long instrument, or device, development period would be required for the utilization of these two techniques aboard orbiting spacecraft. The principles of these techniques are discussed in some detail in Sections 6 and 7 of this interim report. Discussions and evaluations of these techniques are presented in this report.

Another program objective is to evaluate the optical techniques for their ability to determine wind motion in the upper atmosphere. In particular, major emphasis will be placed on the feasibility of utilizing the optical techniques to monitor ozone-air mass motion from the equator to the poles. In this connection, the theories with have been advanced concerning the use of ozone as a

tracer for wind motion have been reviewed and are discussed in detail in Section 2.

These theories are being critically analyzed since they will prove to be major considerations in the fulfillment of another of the program requirements, namely, to recommend the optimum satellite orbits and positions of supporting ground stations for the attainment of information concerning atmospheric winds. This task will be performed in the forthcoming second-year effort.

During the period covered by this report, a major effort was expended in compiling and evaluating a comprehensive bibliography of articles relating to the absorption properties of ozone and to optical techniques for measuring the concentrations of atmospheric ozone. The contents of these articles served as a basis for selecting the optical techniques which offer the greatest promise for the atmospheric ozone measurements. The large number of articles which have been published in this field justifies their inclusion, in the form of a list of references, as a separate section of this report. Accordingly, Section 9 contains a bibliography of ozone articles classified according to whether the primary emphasis is on atmospheric photochemistry, atmospheric dynamics, spectroscopic properties, or the determination of atmospheric concentrations. Sections 3 and 4 of this report summarize the information, obtained from the articles on ozone spectroscopy and atmospheric measurement, that is pertinent to the analyses being performed during the present program.

SECTION 2

METEOROLOGICAL ROLE OF ATMOSPHERIC OZONE

Although the total amount of ozone in a vertical column above the earth's surface corresponds to only about 0.3 cm when reduced to standard temperature and pressure (STP), this chemical species exerts a powerful influence on meteorological processes, principally by virtue of the high efficiency with which it converts incident solar ultraviolet radiation into heat. This can be illustrated, superficially, by considering that a nonuniform distribution of ozone in the earth's atmosphere, and the resultant nonuniform heating, will lead to temperature gradients which can in turn create atmospheric wind fields. However, a redistribution of ozone by atmospheric winds will lead to an alteration of the temperature and wind patterns so that a complex relationship between ozone distribution and wind patterns can generally be expected.

The objectives of the discussions appearing in this section are: (1) to demonstrate the intimate role that ozone plays in meteorological processes, with special emphasis being placed on atmospheric wind-ozone relationships, and (2) to establish the value of continuous monitoring of the worldwide distribution of ozone for the purpose of tracing large scale air mass motions and simultaneously obtaining information concerning other meteorological parameters.

2.1 PHOTOCHEMICAL PRODUCTION OF OZONE

A consideration of the photochemical processes in the earth's upper atmosphere which are responsible for the ozone content is important for the following reason: The transport and circulation of ozone by atmospheric winds was first recognized as an important process when the measured vertical ozone distributions were found to deviate from those which had been predicted by photochemical theory. For this reason, a brief review of the photochemistry which results in the formation and destruction of atmospheric ozone is presented here.

Since Chapman[1*] first outlined the principal features of the photochemical processes involved in the creation of atmospheric ozone, several analyses have been performed to determine the ozone content that would be anticipated on the basis of photochemical equilibrium. Although these latter analyses take into account factors not included in the original theory, the general scheme as presented by Chapman nevertheless remains valid.

Recent reviews of the photochemical production of atmospheric ozone have been published by B. G. Hunt[2,3] and by Whitehead, et. al.[4] The latter authors considered only those photochemical reactions which would occur in an atmosphere of ozone (O_3) and atomic and molecular oxygen (O and O_2) in the presence of inert third bodies. The most important of these reactions are considered to be:

$$O_2 + h\nu \rightarrow O + O; \quad \lambda < 2424\text{Å} \tag{2-1}$$

$$O_3 + h\nu \rightarrow O_2 + O; \lambda < 11{,}800\text{Å} \tag{2-2}$$

$$O + O_2 + M \rightarrow O_3 + M \tag{2-3}$$

$$O + O_3 \rightarrow 2\,O_2 \tag{2-4}$$

$$O + O + M \rightarrow O_2 + M \tag{2-5}$$

*See Section 9.6 for cited references

where M is any third body, presumably N_2 in most cases. The additional reactions

$$O_3 + O_3 \rightarrow 3\ O_2 \tag{2-6}$$

$$O_3 + O_2 \rightarrow O + 2\ O_2 \tag{2-7}$$

are not considered to significantly affect the equilibrium concentrations of ozone.[5]

The quantities required for a numerical calculation of the equilibrium amounts of atmospheric ozone due to the above photochemical reaction scheme are: (1) the flux of solar radiation within the pertinent wavelength bands that is incident on the top of the earth's atmosphere, (2) the absorption cross-sections per molecule of O_2 and O_3 in the pertinent wavelength bands, (3) the values of the rate coefficients, k, for the above reactions, (4) the density distribution with altitude of O_2 and N_2. In addition, the solar zenith angle must be taken into account.

Reasonably reliable values for the solar radiation flux are now available as a result of rocket measurements. The absorption cross-sections of both ozone and molecular oxygen have been carefully measured. There exists some question, however, as to the cross-section value of O_2 that should be used in the ozone calculations, since absorption by oxygen is known to be pressure dependent.[6] The rate coefficients are difficult to measure in the laboratory, and, moreover, some of them are strongly temperature dependent. So-called standard distributions are usually employed for the densities of air molecules. In spite of the necessity for adopting values of these parameters that are somewhat uncertain, there is no doubt about the photochemical origin of ozone.

The calculation of equilibrium amounts of ozone has been performed by various investigators including Paeltzold,[7-12] Nicolet,[13] Frenkiel,[14] Craig,[6] Blamont and Donahue,[15] Chapman,[1,16] Wulf and Deming,[17] and by Whitehead, et. al.[4] Although the calculations performed by these different authors differ in such details as the values assumed for the above-named reaction parameters, all are in general agreement with the following conclusions:

1. The amounts and vertical distributions of ozone in the upper stratosphere can be accounted for by the existence of an equilibrium among the photochemical reactions (2-1) through (2-5).
2. The ozone content of the lower stratosphere cannot be accounted for by in situ photochemical production, but must have its origin in the upper stratosphere. It is presumably formed in the photochemical equilibrium region (above about 40 km) and transported by vertical wind motions to the lower stratosphere, where it is relatively protected from photodecomposition.
3. No significant diurnal variation in the total ozone content is anticipated on the basis of the photochemical reaction scheme. In particular, no significant changes in the total ozone content are expected to occur during the night when the sunlight is absent. Although the concentrations in the uppermost layers may change during the night, the amount of ozone in these layers represents only a small fraction of the total ozone.
4. Minimum amounts of total ozone should be associated with large solar zenith angles. This follows from the fact that the path length for a solar ray through any given layer becomes greater as the zenith angle increases. This results in a proportionately greater absorption of solar radiation in the upper layers and a decrease in the intensity incident on the lower layers. The net effect is to reduce the equilibrium concentrations of ozone.

Whereas the investigators cited above considered only the five listed reactions, Hunt,[2,3,18] Hampson[19] and Roney[20] also included a set of reactions involving H_2O, OH and HO_2. By adopting improved values of k_3 and k_4 given by Bensen and Axworthy and the value of k_5

determined by Reeves, Mannella, and Harteck,[21] Hunt also concludes that the atmospheric concentrations of ozone above about 40 km are consistent with photochemical theory. He attributes the fact that other investigators have previously arrived at this conclusion by considering only reactions 2-1 through 2-5 as being due to a fortuitous choice of erroneous values for k_3, k_4, and k_5. The errors in the assumed values just offset the error in ignoring the reactions involving hydrogen-containing compounds, according to Hunt. In any case, it is generally accepted that the ozone concentrations in the upper portion of the ozonosphere are in accord with the photochemical reaction mechanisms defined by Chapman.

2.2 OBSERVED OZONE DISTRIBUTIONS

The ozone distributions of interest are: (1) Variations in the total (integrated) amount of ozone in a vertical column (of unit area cross-section area) which extends upward from the earth's surface through the entire atmosphere. These include diurnal, daily and seasonal variations over any given location, as well as latitudinal and longitudinal variations at any given time. (2) The vertical distribution of ozone content with altitude, i.e., the vertical profile, which also exhibits temporal and geographical fluctuations. These two types of distributions are measured by different methods and, in general, much more extensive data are available concerning variations in the total ozone content than variations in the vertical distributions.

2.2.1 VARIATIONS OF TOTAL OZONE CONTENT

Craig[6] in 1950 summarized the results of total ozone measurements that had been obtained until that time. Substantial additional data have become available since 1950, and especially during the IGY.

These were summarized in 1960 by Godson[22] as shown graphically in Fig. 2-1. The solid contours in this figure describe the mean distribution of total ozone (in 10^{-3} cm NTP) as a function of month and latitude in the Northern Hemisphere. The amounts shown were arrived at after considerable averaging over a large number of observations and smoothing of data were performed. Several features of the observed variations in total ozone content are conveniently illustrated by means of this figure. It is seen that the total amount of ozone is a maximum in spring and a minimum in autumn with the largest amplitude of variation at high latitudes. There is also very little seasonal variation in the vicinity of the equator, with only a slight maximum being observed in the late spring or early summer. During most of the year, the total amount of ozone increases from the equator to a maximum at about 60°N. In the spring, the maximum occurs at or near the pole. It is to be noted that the observation of a spring maximum at the pole is in disagreement with conclusion (4) of Subsection 2.1, which was based on photochemical considerations. This observation was instrumental in pointing to the importance of atmospheric mass motions in redistributing the photochemically produced ozone from the equator to the poles (see subsection 2.3.1). (Relatively fewer measurements of the total ozone content have been made in the Southern Hemisphere. However, the measurements that have been made indicate that the seasonal and temporal variations in the two hemispheres are quite similar.[23,24])

Evidence for longitudinal variations in the Northern Hemisphere has been given London[25,26] who observed that at all seasons there is more ozone over eastern North America, eastern Asia and central Europe than at other longitudes. These differences become especially pronounced in spring. Kulkarni, et. al.,[27] have noted the amounts of ozone at Tateno, Japan (36°) are consistently larger than at

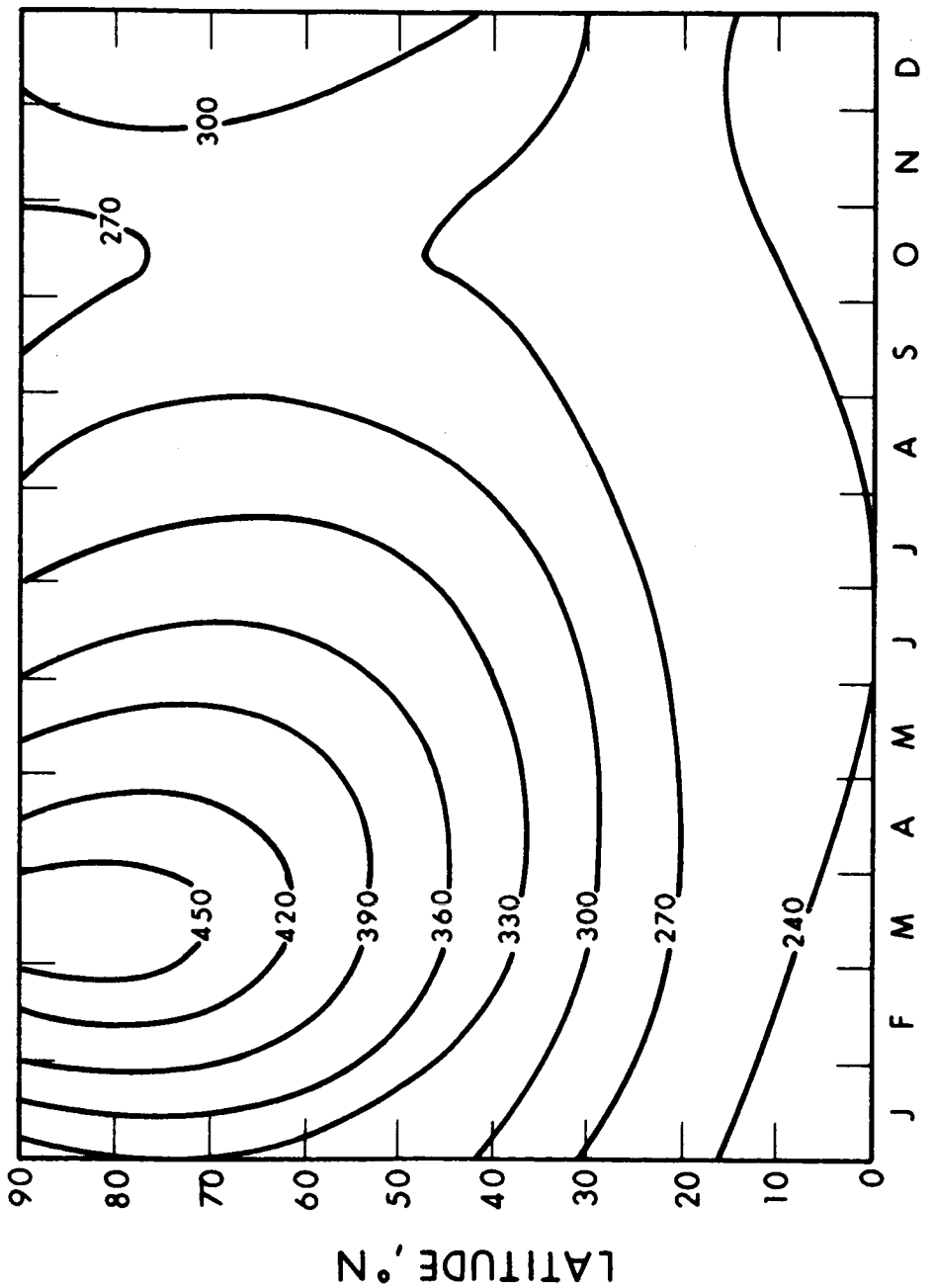

Figure 2-1. Mean Distribution of Total Ozone (units) as a Function of Month and Latitude (Godson, 1960)

Srinagar, India (34°N), particularly during the late winter and spring.

Temporal variations include long-term fluctuations, e.g., month-to-month, and the shorter term fluctuations which are superimposed on these, such as, for example, day-to-day fluctuations. Perl and Dütsch[28] have published extensive data concerning the annual variation of total ozone over Arosa, Switzerland which were obtained during a unique series of measurements made between 1926 and 1958, with minor interruption. These data allowed long-term average values to be determined for each calendar month. These average values appear in Fig. 2-2 as circle points.

The vertical lines shown attached to the points in the figure represent the root-mean-square values of the deviations of individual monthly means from the long-term mean for each month. It is seen that these deviations can be rather sizeable, amounting to 23 X 10^{-3} cm NTP in February, for example. The deviations for June through November, on the other hand, range from 10-12 X 10^{-3} cm NTP. In addition to the monthly and annual variations there occur large and striking deviations of individual daily values from the monthly mean. As noted by Craig,[29] the Arosa data can be used to compute the deviation of each daily value from the mean for the month in which it occurs. For the month of March, the root-mean-square value of such deviations from 1949 through 1958 was 33 X 10^{-3} cm NTP, and for the month of October 16 X 10^{-3} cm NTP. The daily deviations are such that it is not unusual for individual daily values of total ozone in autumn to exceed certain individual values during the period of spring maximum. The types of deviations observed at Arosa are considered by Craig[30] to qualitatively represent the behavior at all locations not too near the equator, with variations at higher latitudes being even more pronounced.

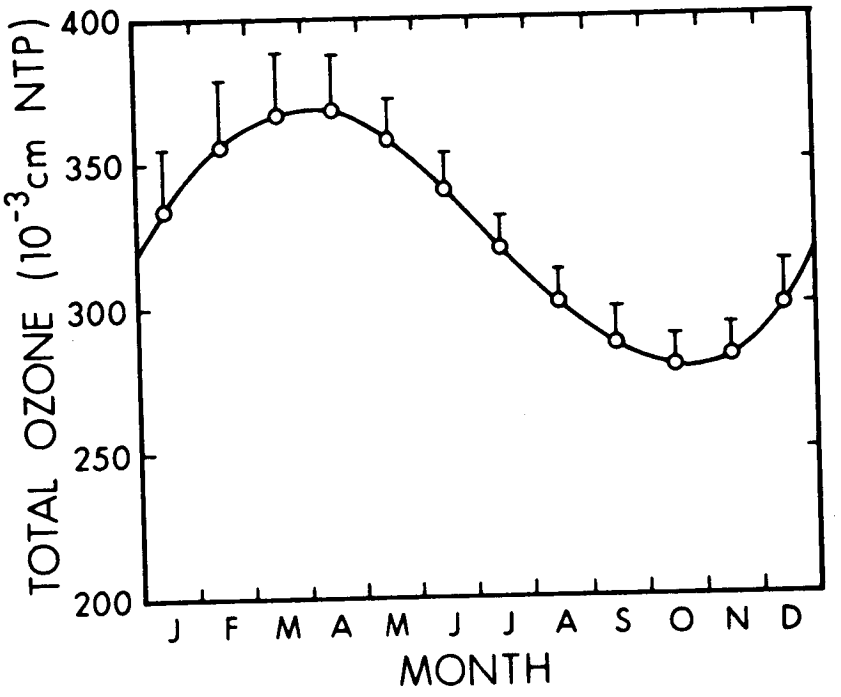

Figure 2-2. Annual Variation of Total Amount of Ozone at Arosa, Switzerland (Perl and Dütsch, 1959)

The above discussions serve to illustrate the types of variations of total ozone content that are known to occur. The data discussed, of course, applies only to the times and locations cited in the examples. However, these examples emphasize the fact that the total ozone content at any given location can only be determined at a given time by direct measurement; the actual amount may differ markedly from mean values.

2.2.2 VARIATIONS IN VERTICAL OZONE DISTRIBUTION

Marked temporal and geographical variations also characterize the vertical distribution of ozone. Figure 2-3 shows five vertical distributions as determined by Mateer and Godson[31] from observations at Moonsonee and Edmonton, Canada, during different seasons. The vertical profiles were computed from Umkehr data (see section 4) which does not allow the distributions to be determined with great resolution and necessarily smooths out small-scale features. However, the principle features shown in the figure are typical of all vertical ozone distributions which have been observed at high latitudes. The maximum density of ozone is found in the lower stratosphere, usually between 15 and 30km. The ozone density above 30km decreases rapidly with height. Below the tropopause, i.e., below approximately 10 km , the ozone density is small and relatively constant. Of special importance is the fact that variations of total ozone amounts are mainly accounted for by variations in the lower stratosphere.

Dütsch[32] has published similar seasonal curves for Aroza, Switzerland, which is situated at a lower latitude than the Canadian stations. As is seen in Figure 2-4, the vertical distribution and its seasonal variation at Aroza is qualitatively the same as at the higher latitudes. One notable difference is that the seasonal variations in the lower stratosphere are smaller. In the figure there is also shown a vertical distribution which was measured at Leopoldville in the Congo. As

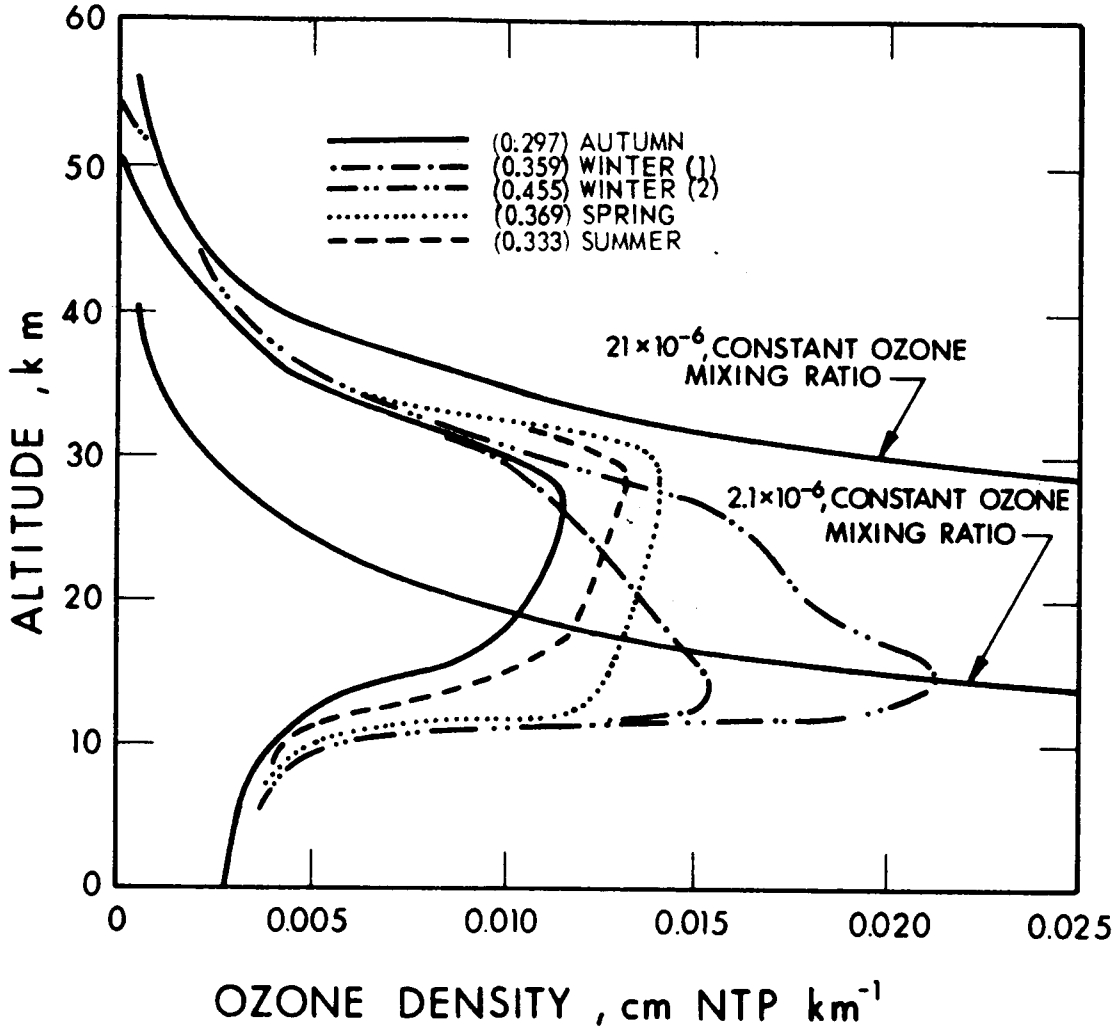

Figure 2-3. Average Vertical Distributions of Ozone at Moosonee and Edmonton, Canada, for Different Seasons of the Year (Mateer and Godson, 1960)

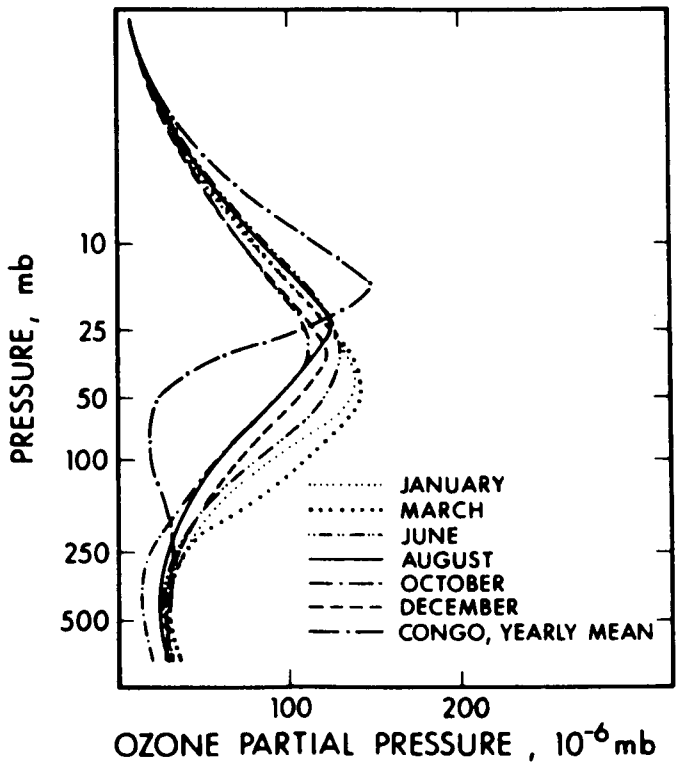

Figure 2-4. Average Vertical Distributions of Ozone at Arosa for different Months of the Year (Dutsch, 1962)

in most measurements made near the equator, there is little seasonal variation at any altitude and the maximum density occurs at a higher altitude.

The above examples show that there is a direct correlation between seasonal variability in the vertical distributions and in the total ozone amounts. This is due to the previously noted fact that changes in total ozone amounts are due mainly to changes in the ozone concentrations in the lower stratosphere. It will be seen in later discussions that this variability is governed by transport mechanisms involving large-scale atmospheric wind motions.

One feature of vertical ozone distributions which is not shown in Figs. 2-3 and 2-4, is the tendency for the occurrence of double maxima in the vertical profile on days of large total amounts of ozone. That is, when the integrated ozone content is unusually large, a primary maximum in concentration is observed between 20 and 35km, and a secondary maximum between 10 and 20km. The existence of the second maximum was first suggested by Gotz[33], and then later confirmed by Ramanathan and Karandikar[34]. From observations at Tromso, Tronsberg and Langlo[35] also obtained evidence for a double maximum. Durand[36], et.al., deduced two marked maxima at 17 and 25KM from the data from a V2 rocket flight over New Mexico in October 1947. Regener[37] has also observed double maxima in the results of balloon flights over New Mexico. Normand[38] has shown that the secondary maximum, if analyed in terms of the ozone-to-air mixing ratio, can provide valuable information concerning the vertical component of stratospheric winds. (see Subsection 2.3.1)

2.3 EVIDENCE FOR TRANSPORT OF OZONE BY ATMOSPHERIC WINDS

Three types of arguments or evidence have been advanced to establish the value of monitoring ozone distributions over wide areas as a means of

tracing atmospheric winds. These are: (1) an argument based on the observed deviations of ozone distributions from those predicted by photochemical theory, (2) analyses, including numerical computations, which show that non-uniform distributions of ozone in the atmosphere will result in differential heating and, therefore, temperature gradients of sufficient magnitude to cause air mass motion, and (3) observational data which provide direct correlations to be made between ozone distributions and atmospheric wind fields which are simultaneously measured.

In order to illustrate the value of continuous ozone monitoring as a means of providing information about air mass motions, the three types of evidence mentioned above will be reviewed here.

2.3.1 DEVIATION OF OZONE DISTRIBUTIONS FROM PHOTOCHEMICAL EQUILIBRIUM PREDICTIONS

The first type of deviation to be noted was discussed in Section 2.1, where it was stated that the ozone concentrations in the lower stratosphere did not agree with equilibrium predictions. In addition to failing to predict the correct absolute concentrations, the photochemical theory cannot account for the great variability observed in the lower stratospheric ozone content. It is only by invoking a combination of vertical air displacements and horizontal advection* that the observed concentrations, and their variations, can be reconciled with photochemical theory.

The effect of a vertical component of air flow on the vertical profile depends not only on the original ozone distribution, but also on the photochemical stability of ozone at the level in question.

---

* The horizontal shifting of a mass of air, considered especially as a means of transfer of heat.

Wulf and Deming[17], Nicolet[13], Craig[6], and Dütsch[39], among others have examined the stability or life of ozone, i.e., the efficiency with which the photochemical processes at any given level will respond to a perturbation due to winds, etc., to restore the ozone content to its equilibrium value. The main conclusion from these studies is that the times for half restoration is of the order of hours or less for levels above about 35km, but may be weeks or more below 20km (due mainly to the low efficiency of O_2 and O_3 dissociation at the lower altitudes). Dütsch[39], for example, concludes that the photochemical time constants may vary from minutes at 55km to years at 20km. Wulf and Deming[17] arrived at similar conclusions and used these to show that if a parcel of air containing ozone is transported, for example, from the altitude at which the amount in photo-equilibrium with solar radiation is a maximum to a level considerably above this, the solar radiation rapidly reduces the ozone content to the equilibrium amount at this latter level. However, if this ozone is transported to a level considerably lower than that of the maximum concentration, it is appreciably screened from the action of solar radiation. At the same time, the deficit of ozone at the point from which it was transported downward is rapidly restored by photochemical action. This observation has led to the widely accepted conclusion that downward movement of air in the stratosphere will lead to an increase in total ozone while upward movement of air will tend to bring ozone to a minimum amount.

Normand[38] made the very significant observation that the ozone mixing ratio (not density) in the lower stratosphere is a conservative property of a parcel of air and is determined mainly by the past history of that parcel of air. Along an isobar in the lower stratosphere, the ozone mixing ratio should increase in subsiding air and decrease in ascending air. Normand also notes that the secondary maxima in the vertical tend to occur on days of high total ozone content and that

if the ozone were plotted in terms of its mixing ratio vs altitude, the secondary maxima would appear as a change of slope on the curve. He concludes that if the vertical distribution of the mixing ratio were known from day-to-day over a large area, valuable information would be obtained concerning the vertical component of wind in the lower stratosphere. (Special note is taken of this conclusion at this point, since the optical technique which is recommended in Section 6 allows the simultaneous measurement of ozone and air concentrations, i.e. the mixing ratio, to be determined as a function of altitude.). Reed[40] demonstrated that measured atmospheric vertical displacements are of sufficient magnitude to at least partially account for the day-to-day fluctuations in both the total ozone content and its vertical distribution. Figure 2-5 shows the results of a sample calculation performed by Reed, which illustrates the extent to which the vertical profile of the ozone mixing ratio can be altered by allowing vertical displacements to operate on an assumed initial distribution. Curve I in the figure represents an initial distribution which corresponds to a total ozone amount of 0.132 cm (NTP). This latter curve is allowed to be displaced downward by a distribution of vertical velocities resulting in the new distribution represented by Curve II. The length of the ordinates between the two curves indicates the assumed displacements. Not only is the vertical distribution altered, but, with the assumed displacements, the total ozone content increases from 0.132 cm to 0.156 cm. Reed concludes that this increase of 0.024 cm is close to the theoretical maximum that can be accounted for when the magnitude of known vertical motions is considered. Larger increases than this can be explained only by assuming that horizontal advection also contributes to the increase.

The discussions of this subsection up to this point have emphasized the discrepancy between observed vertical ozone distributions and those predicted from photochemical theory. Equally significant, as

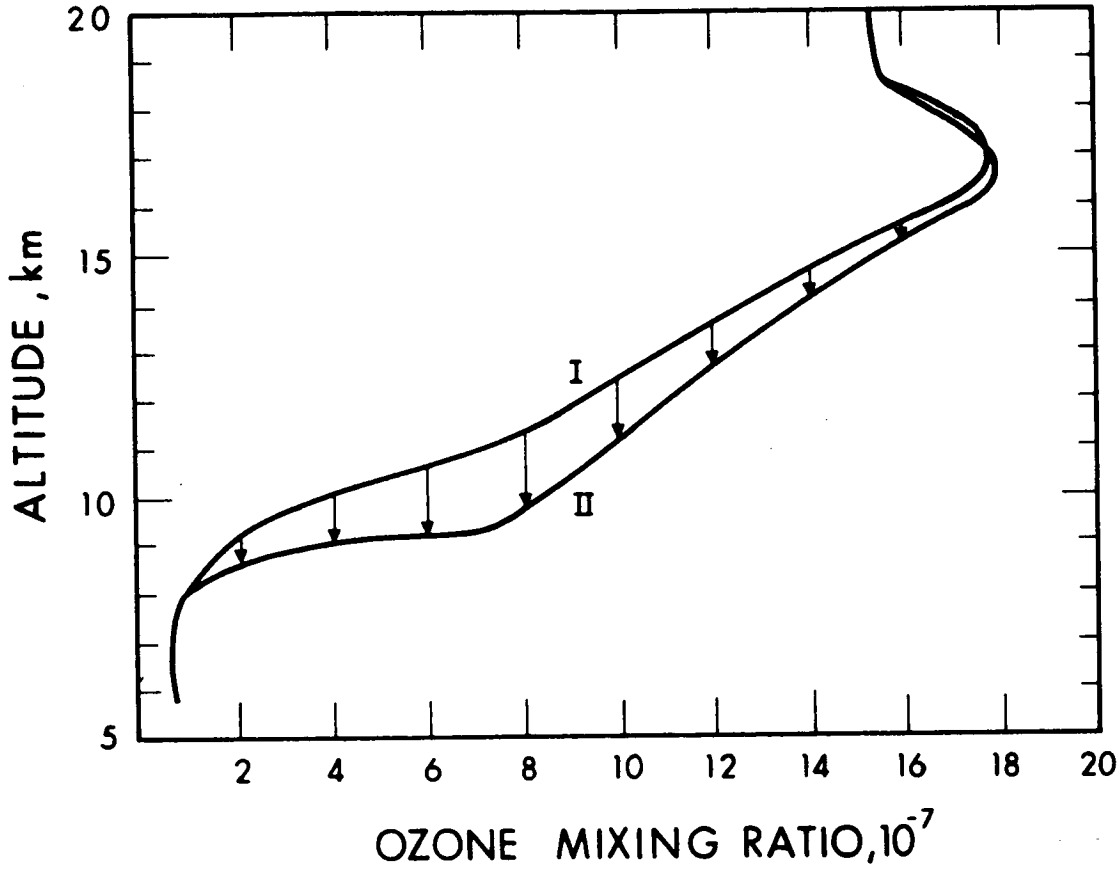

Figure 2-5. Alteration in Mixing Ratio Vertical Distribution Caused by Vertical Displacements (Reed, 1950)

indications of the importance of ozone redistribution by atmospheric motions, are the discrepancies between the observed latitudinal ozone distributions and those predicted by theory. As was noted in Subsection 2.2.1, the occurrence of a maximum in the total ozone content over polar regions in the spring was in contradiction to conclusion (4) of the photochemical discussion (subsection 2.1). Craig[6], among others, has pointed out that neither the latitudinal nor the seasonal variations of ozone concentrations could be explained in terms of variations in the solar zenith angle. Wulf[41] was apparently the first to point out that the spring polar maximum could be explained in terms of a general circulation pattern which includes both vertical transport and a meridional component of circulation. This pattern is illustrated in very simplified form in Fig. 2-6, in which the ozone density is schematically represented by the dark shading. Wulf pointed out that the meridional circulation pattern illustrated in the figure was consistent with the known temperature distribution in the stratosphere. The meridional component causes air to descend in the atmosphere over the equator and to move northward in the lower stratosphere. At the poles the stratospheric air would rise again, while the tropospheric air would descend in the manner shown in the figure. Air rising over the poles would have its ozone sharply reduced by solar radiation, while air descending over the poles would lead to a large concentration of ozone in the cold artic air. As this air works its way southward over the earth's surface, the ozone content will diminish to an extent which depends on the amount of contact with the surface. Meanwhile, the air rising over the equator will be relatively free of ozone because of solar action, which ensures the integrated amount of ozone will be a minimum in this region. Kellogg and Schilling[42] have elaborated somewhat on Wulf's proposed circulation pattern, showing that the general pattern agrees with a large number of observational results and theoretically deduced features of the upper atmosphere.

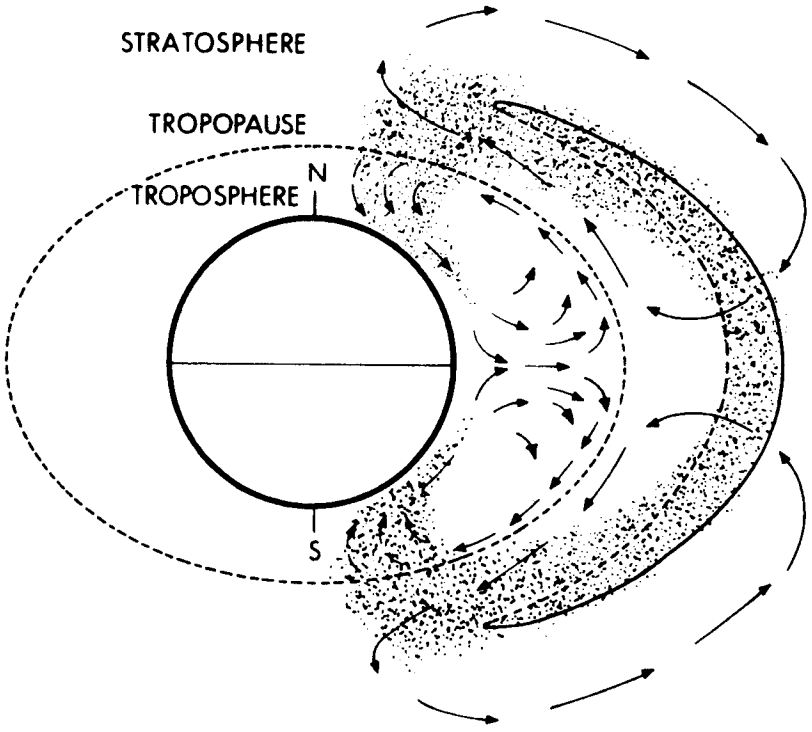

Figure 2-6. Atmospheric Circulation Pattern Leading to Latitudinal Redistribution of Ozone (Wulf, 1945)

While Wulf's circulation pattern is now widely accepted, there is some question as to the relative importance of horizontal and vertical motions in explaining variations in ozone distributions at any given time and place. Paetzold[43] concludes that spring fluctuations are dominated by vertical motions and mixing. Ramanathan[44] states that ozone variations associated with weather systems are most marked in the period October to June. Goody and Roach's[45] results of ozone IR emission measurements tend to confirm that fluctuations in total ozone amount are not due to the same causes at all seasons. Others who have discussed observed ozone distributions and/or have attempted to evaluate the relative importance of horizontal and vertical motions are cited in References 46 through 70. There is unanimous agreement among all authors who have investigated this problem about the need for a greater amount of observational data with which to compare the results of theoretical analyses and computations.

2.3.2 HEATING DUE TO OZONE ABSORPTION AS A DRIVING FORCE FOR WINDS

The discussion in the preceding subsection was intended to demonstrate the manner in which ozone photochemical considerations and atmospheric circulations could account for the observed ozone distributions and their variations. In actual fact, the problem is much more complicated, since the atmospheric distribution of ozone is one of the principal factors governing the magnitude and direction of atmospheric mass motions. In analyzing the response of the earth's atmospheric circulation to the solar heat input in the stratosphere, Webb[71] considers the distribution of ozone to be the most important variable, aside from the simple geometry of the sun-earth relationship and possible fluctuations in the solar UV flux.

The role that ozone absorption plays in the general circulation pattern can be illustrated in simplified form as follows: During the equinoctal

period, when the sun's incident radiation is perpendicular to the earth's surface at the equator, there exists considerable symmetry between two hemispheres, with respect to the angle of incidence of solar radiation. In particular, the input of solar energy into the upper atmosphere is symmetric in both directions away from the equator, if it is assumed that the opacity is uniform. This latter assumption implies identical latitudinal distributions of ozone in the two hemispheres. Ultraviolet radiation of a given wavelength should penetrate to a maximum depth at the equator; i.e., reach a minimum altitude before it is absorbed. At points away from the equator towards either pole, the penetration decreases or the minimum altitude increases. A well defined meridional gradient of heat input into the stratosphere thus develops at the time of equinox. This, in turn, results in a decrease of temperature at any given constant altitude surface from the equator to the poles which would cause low pressure centers at each pole and westerly winds over the entire globe.

This very simple picture can be extended to other periods, when the subsolar point moves away from the equator and can qualitatively explain many of the gross features of the global circulation pattern[72-76]. That this circulation pattern is also strongly dependent on the vertical distribution of ozone can be seen in the following summary form[42]: The important mechanisms for heating of the atmosphere below about 80km are the absorption of solar radiation by ozone and of infrared radiation by water vapor and carbon dioxide. Detailed calculations of the radiative budget of each layer between 50 and 70km show that there is a net gain of heat due to absorption at the bottom part of this layer and a loss at the top. This condition can only lead to a convective transport of heat to counteract the radiative unbalance. The magnitude of the convection at any time and location in the atmosphere will obviously depend strongly on the prevailing ozone distribution and on the solar zenith angle.

The above examples serve to emphasize the close interrelationship that exists between photochemical, radiative, and dynamical processes. Many authors have analyzed the role of ozone in the atmospheric heat budget by using assumed or "standard" distributions of ozone[71-86]. Others have attempted to calculate ozone concentrations theoretically by using observed air densities and temperatures.

Leovy[72] notes that not only does the temperature depend on the ozone distributions, but the converse is also true[87]. He performed an iterative type of calculation which simultaneously took into account the photochemical and radiative aspects of the problem and which resulted in the simultaneous determination of ozone and temperature distributions. This analysis and many others[71-87] demonstrate that if the actual ozone distribution could be measured at a given time and location, the heat budget and temperature profile appropriate to that location could be computed. This information could in turn be incorporated into hydrodynamic models which relate atmospheric motion to the temperature field. Details of the analytical procedure for calculating the velocity field from a knowledge of the differential heating have been set forth by Lindzen and Goody[88], who took into account the various forms of couplings between ozone concentrations, temperatures, radiative and photochemical effects, and wind motions. This latter work and those of Davis[83] and Bekoryukov[47] in particular, show that given sufficient data concerning ozone distribution over large areas, analytical techniques can be used to deduce the atmospheric response, in terms of atmospheric circulations, to the non-uniform solar heat input.

2.3.3 DIRECT CORRELATIONS BETWEEN ATMOSPHERIC OZONE AND AIR CIRCULATIONS

In recent years, it has been possible to perform simultaneous measurements of ozone vertical distributions, temperatures, and atmospheric

wind velocities. Breiland[89] has examined the results obtained with the chemiluminescent ozone soundings during weekly balloon flights at a network of stations in North America. By direct correlation, it was established that significant changes in the temperature lapse rate or in the wind field frequency are associated with correspondingly significant changes the partial pressure of ozone. In particular, the stratified nature of the atmospheric wind field and thermal structure is reflected to a high degree in the ozone soundings.

Sticksel[90] and Paetzold[49] have shown that there exists a relationship between ozone content and the position of the subtropical jet stream relative to the location of the observations. With few exceptions, the jet stream, a core of winds with speeds in excess of 50 knots, was found to the south of the ozonesonde station whenever double maxima were found in the vertical profile. Sticksel, by taking in account several meteorological criteria, analyzed this relationship in terms of the atmospheric dynamics which are responsible for the double maxima.

More recently, Hering[61,91] has demonstrated the value of broadscale ozone determinations in diagnostic studies of atmospheric circulation processes. By virtue of a network of 12 ozonesonde stations distibuted over North America, ozone concentrations were systematically measured at the same time that data pertaining to pressure, temperature, and humidity were taken at the various stations. The results, as reported by Hering, leave no doubt that continuous observations of ozone concentrations taken simultaneously over several geographic locations could serve to assess the importance and correctness of the several proposed relationships between ozone and atmospheric circulation which have appeared in the literature.

The studies which have been cited in this section are being carefully analyzed in order to determine the optimum satellite orbits, the

range of latitudes and altitudes of ozone distribution measurements,etc., which would prove to be of the greatest value in diagnosing global scale air mass motion.

2.3.3.1 Correlations Between Ozone and Other Atmospheric Parameters

In the course of the study performed during this program effort, an impressive number of literature articles were found which describe observed correlations between atmospheric ozone content and various meteorological parameters. The main objective of this study was to demonstrate the value of monitoring the ozone distributions on a world-wide basis as a means of tracing large-scale atmospheric motions. The relationship of ozone to other meteorological properties was therefore not examined in detail. However, references to the articles which relate evidence for these correlations are included in Section 9.3.

The existence of these correlations suggest that ozone measurements may be of value not only for tracing winds, but also for providing indirect information concerning the values of other atmospheric parameters. That is, once the exact nature of the correlations are established, a remote ozone measurement may allow the values of other parameters to be inferred. An indication of how the total ozone content can be related, for example, to temperature at a given pressure level is seen in Figs. 2-7 and 2-8. These figures were taken from Godson's work[22] in which the correlations at different latitudes were compared. Other investigators[40,66,92,93] have discussed the relationship between temperature and total ozone amounts as a function of latitude and season, and in terms of horizontal advection and vertical motion. The relationship is a complex one but, as Figs. 2-7 and 2.8 and Godson's discussions indicate, it can be analyzed and understood on a semi-empirical basis.

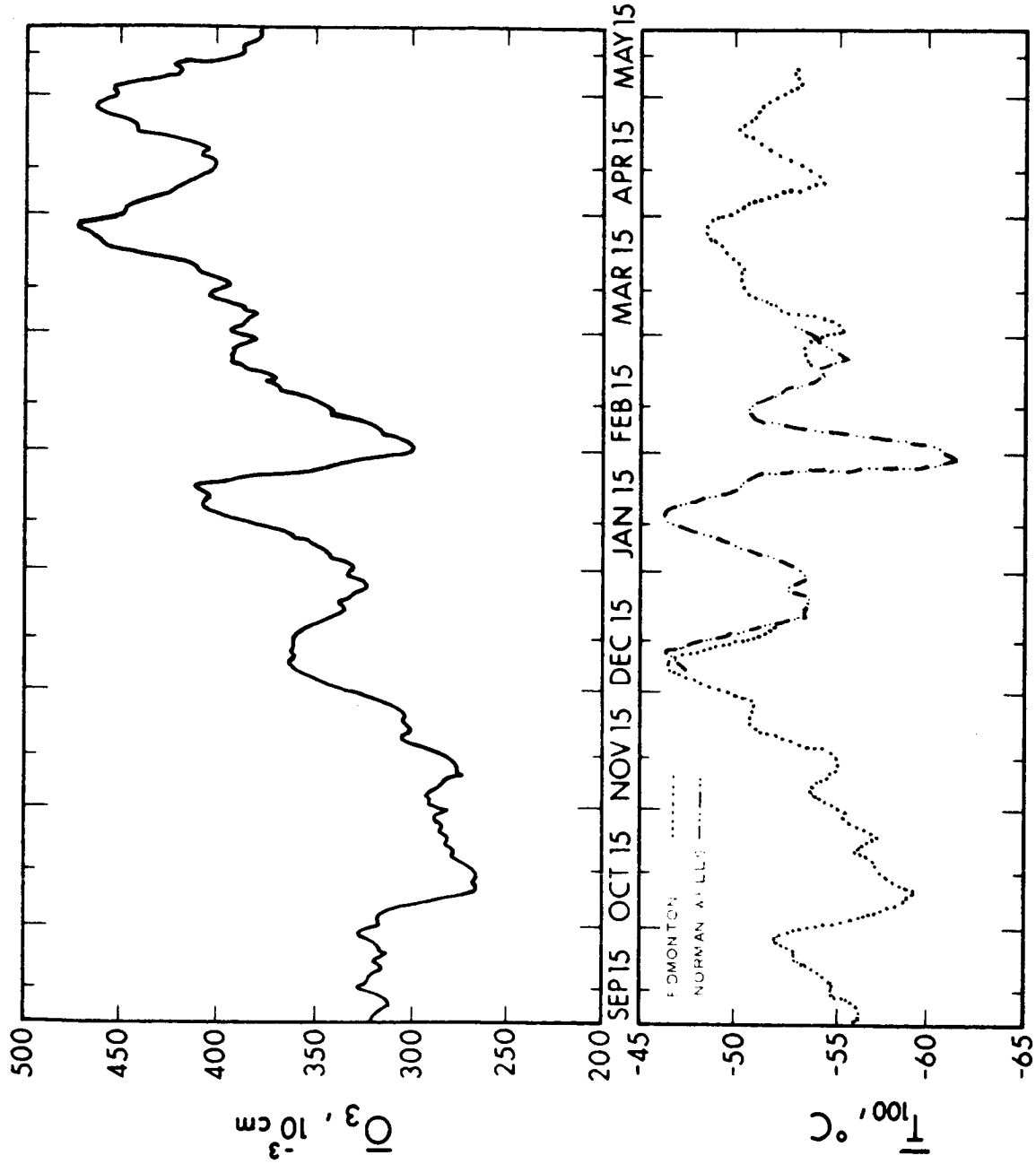

Figure 2-7. 10-Day Running Means of 100 mbar Temperature and of Total Ozone for 1953-54 Winter at Edmonton, Canada (Godson, 1960)

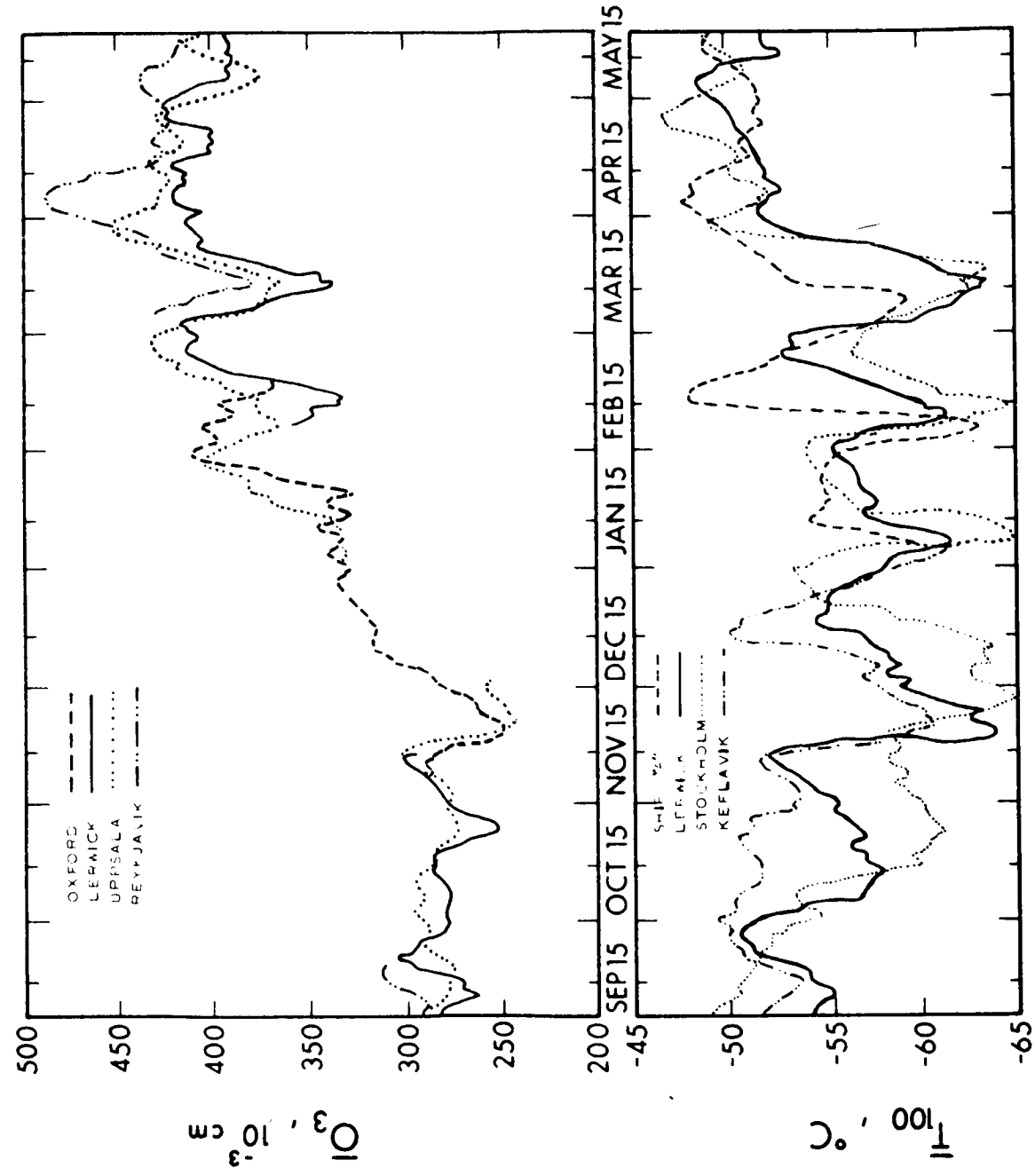

Figure 2-8. 10-Day Running Means of 100 mbar Temperature and of Total Ozone for 1953-54 Winter European Ozone Stations Near 60° N (Godson, 1960)

Correlations between ozone and other meteorological parameters are too numerous to discuss here; the titles of the articles referred to in Section 9, however, serve to illustrate the varied nature of the correlations which have been observed.

2.4 OZONE MONITORING AS A MEANS OF TRACING ATMOSPHERIC AIR MASS MOTIONS

The results of the many investigations cited above show that there is a dual connection between the distribution of atmospheric ozone and atmospheric circulations: (1) the atmospheric circulation effects a transfer of ozone from regions of high content to regions of low content, or vice-versa, and, together with photochemical processes, accounts for the observed distributions and their variations, and (2) absorption of solar radiation by non-uniform latitudinal, longitudinal, and vertical distributions of ozone provides one of the principal driving forces for the atmospheric circulation in the form of temperature gradients. The atmospheric circulation-ozone interrelationship has been extensively investigated by numerous workers, and the basic physical and meteorological principles involved are believed to be well understood. It is reasonable to assume that by incorporating empirical correlation data into circulation computations which are based on photochemical-radiative-hydrodynamical models, the role that ozone plays in meteorological processes will be understood in detail. The need at present is for increased observational data on the distribution of ozone, particularly on a continuous basis and on a global scale. It is evident that the study of atmospheric ozone has advanced to such a stage that, given such data, it can lead to a complete definition of the atmospheric circulation-ozone interrelationship.

SECTION 3

OZONE SPECTROSCOPY

Any optical technique that is to be developed for the quantitative measurement of ozone concentrations will depend on an accurate knowledge of the absorption properties of the ozone molecule. The certainty with which the absorption coefficients of ozone in the infrared, ultraviolet, and visible spectral regions are known will be one of the factors determining the accuracy of atmospheric ozone measurements. For this reason, an extensive search of the literature was conducted to compile all available material on the spectroscopic properties of ozone. This literature search resulted in a vast amount of information concerning the visible, UV, and IR absorption bands of ozone, as is indicated by the lengthy bibliography in Subsection 9.4.

A discussion of the absorption bands of ozone should also include a brief review of the chemical structure and vibrational and electronic energy levels of the molecule, since these properties strongly influence the changes in the band structure that accompany changes in temperature and pressure. These properties have recently been reviewed by G. Herzberg.[94] These factors will have a strong bearing on the interpretation of spectroscopic measurements in terms of absolute ozone concentrations. Conversely, by properly accounting for the effects of temperature and pressure it appears possible to extract, from the ozone measurement data, values of atmospheric pressure and temperature at the same altitudes for which ozone

concentrations are obtained. These possibilities were not examined in detail during this program effort, however, the main emphasis being placed on an evaluation of the reliability of the several sets of published values for ozone absorption coefficients. The objective of this present section is to fully describe the absorption spectrum of ozone for reference, as analyses of the measurement techniques are discussed in subsequent subsections of this report. As will be seen, a great wealth of information concerning ozone absorption has been obtained by numerous investigators, so that the values of the molecular quantities which are required in any optical measuring technique, i.e., absorption coefficients, can be considered to be known to a high degree of accuracy. Furthermore, the fact that they are known over a wide spectral range and under a variety of conditions promises great versatility for optical ozone measurement techniques.

3.1 CHEMICAL STRUCTURE AND VIBRATIONAL AND ELECTRONIC ENERGIES

Trambarulo et al,[95] and Robinson[96] have reviewed the chemical structure and energy levels of the ozone molecule and analyzed the electronic configuration in terms of valence-bond and molecular orbital theory. The best data indicates that the three atoms of oxygen in an ozone molecule form an isosceles triangle with an apex angle of 116° 49min. ± 30min. The two end oxygen atoms are connected to the central atom by chemical bonds which can be considered to be intermediate in character between single and double oxygen-oxygen bonds. The two equal bond lengths have been measured at 1.278Å by both microwave[97] and electron diffraction[98] methods.

Figure 3-1 consists of a partial electronic energy diagram of the ozone molecule. The levels shown are labelled by standard spectroscopic notation, the assignments being made in accordance with

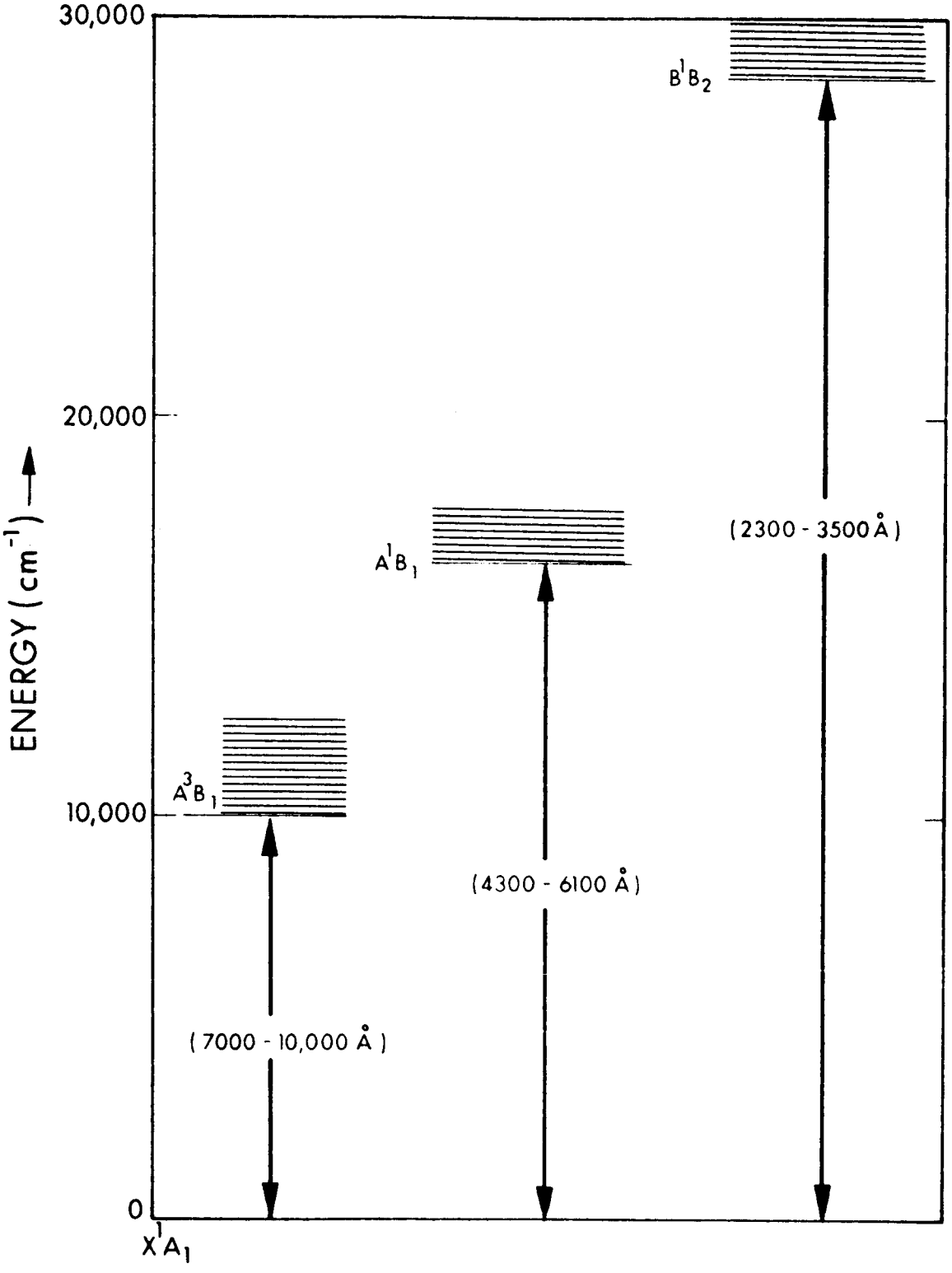

Figure 3-1. Electronic Energy Level Diagram for Ozone

theoretical predictions. It must be emphasized that the assignments are tentative and that little is known concerning the nature of the excited electronic states, $A\ ^3B_1$, $A\ ^1B_1$, and $B\ ^1B_2$.

The electronic transitions from the ground state, $X\ ^1A_1$, to the $B\ ^1B_2$ state give rise to the wide absorption bands (Hartley-Huggins bands) that appear in the region between 2300Å and 3500Å and which account for the atmospheric solar cutoff. The diffuseness of the absorption band is due partly to the unresolved vibrational and rotational structure of the band, but mostly to the inherent diffuseness of the $B\ ^1B_2$ state. Similarly, the Chappius bands at 4300 to 6100Å and the near-infrared bands between 7000 to 10,000Å are diffuse due to the inherent widths of the $A\ ^1B_1$ and $A\ ^3B_1$ states, respectively. This diffuseness corresponds to a predissociation of the ozone molecule. That is, following the act of absorption of radiation there is a large probability that the ozone molecule will instantaneously undergo a radiationless transition into a dissociative state which consists of an oxygen molecule and an oxygen atom. Thus, the absorption of ultraviolet, visible, and near-IR radiation results, at least to a high degree, in the decomposition of the ozone molecule. The significance of this, from the point of view of ozone measurements, is that the ozone molecule does not reemit the same radiation that it absorbs. There is no evidence in the literature for a fluorescence band between 2300Å and 3500Å which corresponds to the inverse transition, $B\ ^1B_2 \rightarrow X\ ^1A_1$, of the Hartley-Huggins bands. Nor has any fluorescence been reported in the vicinity of the Chappius or near-IR absorption bands. All ozone detection and measuring schemes which depend on a fluorescence-type backscattering phenomena are, therefore, excluded from consideration, with the possible exception of the IR transition at 9.6μ.

The best available data indicate that two of the fundamental vibrational frequencies of ozone are at 710 cm^{-1} and 1043 cm^{-1}.

These assignments are consistent with the infrared (vibrational) data, and also with the observed temperature dependence of the vibrational structure in the ultraviolet (electronic) absorption bands. These values could conceivably be used to advantage in the measurement of upper atmospheric temperatures concurrently with the ozone measurements.

That is, if the band structure in the atmospheric ultraviolet absorption bands could be analyzed in terms of its temperature dependence, it would provide a measure of the temperature at the ozone altitudes. While this is an interesting possibility that should be kept in mind in future analyses, the present conclusion is that the complex structure of the UV bands has not yet been unambiguously interpreted in terms of individual vibrational transitions.

3.2 ABSORPTION SPECTRA OF OZONE

The absorption spectra of ozone in the visible, ultraviolet, and infrared spectral regions have been measured by literally dozens of workers.[99-152] The absorption bands of interest are illustrated and discussed in this section.

3.2.1 VISIBLE ABSORPTION BANDS

Figure 3-2 shows the wavelength variation of the absorption cross section of ozone in the region of the visible Chappius bands[99] as measured by Vigroux.[100] It is noted that there is a strong wavelength dependence of both the ozone cross section and the scattering cross sections of air molecules in this spectral region. This allows the contribution of the air molecules to the total attenuation of solar radiation to be accounted for, and also permits the measurement of ozone concentrations to be made from the measurement of

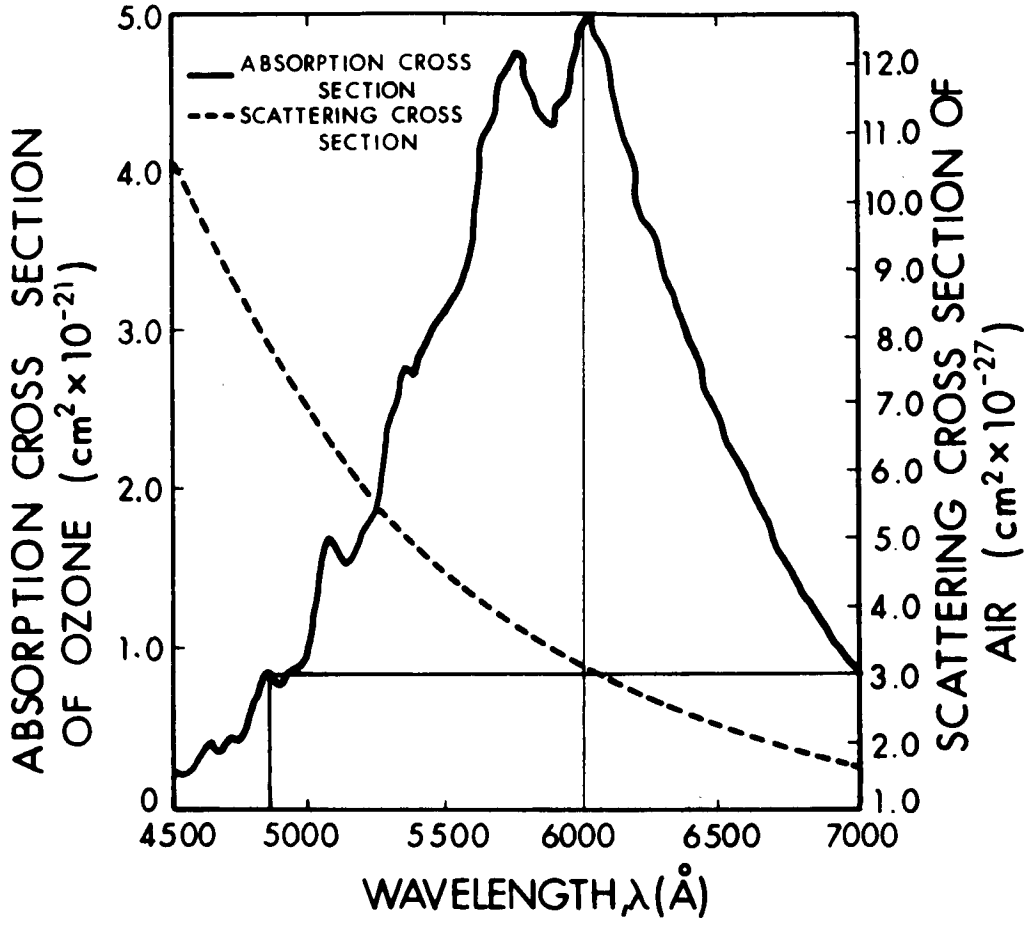

Figure 3-2. Absorption Cross Sections of Ozone and Scattering Cross Sections of Air (cm^2 per molecule) in the Region of the Chappius Bands

relative intensities of transmitted solar radiation at a pair of wavelengths. These points will be elaborated upon in Section 6. The absorption represented by the Chappius band cross section is relatively weak. However, through a path length which traverses the total atmosphere there occurs sufficient attenuation in these bands to measure ozone concentrations. The Chappius bands will prove to be instrumental in the evaluation of some of the active and passive techniques discussed in this report.

3.2.2 ULTRAVIOLET ABSORPTION BANDS

The ultraviolet absorption bands of ozone between 2300Å and 3500Å, are responsible for the atmospheric cutoff of UV solar radiation. In this spectral region, the absorption of solar radiation is extremely strong, and extremely small quantities of ozone could be detected by utilizing these bands. This will prove to be of value in extremely high altitude measurements (35 to 80 km). Three of the absorption curves in the ozone Hartley-Huggins bands, as determined by different authors, are reproduced as the top part of Fig. 3-3. The values of the absorption coefficients are seen to drop off rapidly towards wavelengths longer than those shown in the figure and there is considerably more structure in the bands. This structure is associated with vibrational and rotational transitions of the molecule and is temperature-dependent. It is this portion of the bands which could possibly be utilized in the measurement of temperatures of the upper atmosphere. It is seen that at certain wavelengths the determinations differ by as much as 25%. The values measured by Vigroux[100] have generally been considered to be the most reliable and were adopted by the International Ozone Commission in 1957 for calculation of the amount of atmospheric ozone from measurements by Dobson spectrophotometers. Inn and Tanaka[107] have also endorsed Vigroux's values as representing the most reliable set of ozone absorption coefficients in the 2000-3000Å

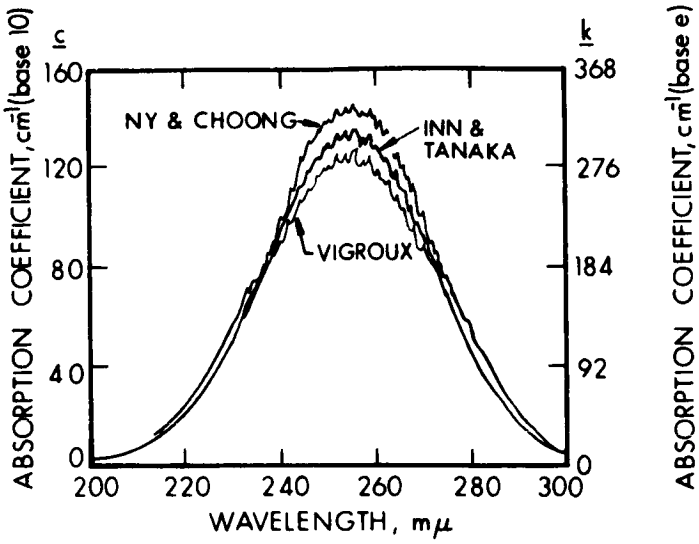

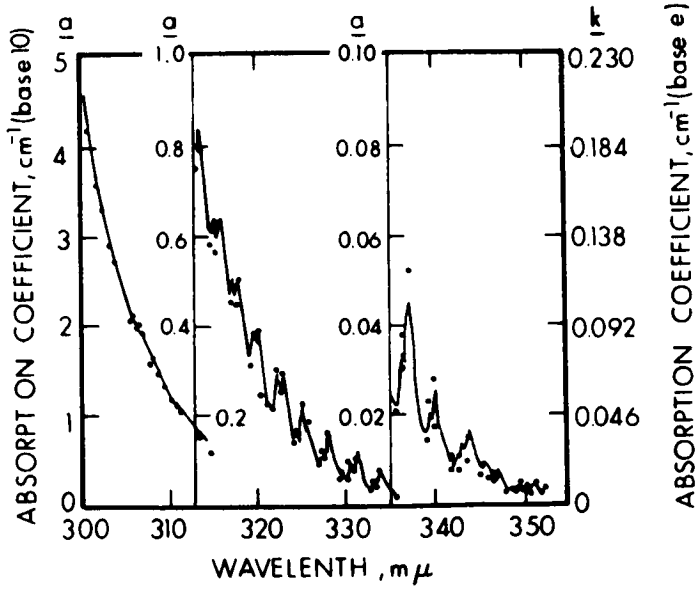

Figure 3-3. The Ultraviolet Ozone Absorption Profiles as Determined by Three Sets of Authors (top). Absorption Coefficients on the Long Wavelength Edge of the Ultraviolet Bands, as Determined by Vigroux

7087-IR-1

region. On the other hand, Dobson[103] and Hamilton and Walker[104] have claimed that Vigroux's measurements are considerably in error and have independently measured ozone absorption coefficients for use in their calculations. In spite of this, Vigroux's values will be used hereafter in this program for two reasons: (1) Vigroux has performed the only detailed set of measurements which yield the temperature dependence of the ozone coefficients; thus, the ozone absorption coefficients which should be used in measuring atmospheric ozone (-40° to -50°C) have been derived[105] from the temperature-dependence data given by Vigroux, and (2) the wavelengths used in the Dobson spectrophotometer technique are in the region between 3055 and 3398Å. This region is characterized by a complex vibrational structure (see Fig. 3-3, lower curve) which has not been completely analyzed , and which would understandably cause difficulty due to the temperature dependence of the absorption profile. The absorption band at wavelengths shorter than 3055Å is truly diffuse and its profile would not exhibit strong fluctuations with changes in temperature. In the passive technique being recommended in this report, measurements in the 3055-3400Å region will also be required in addition to measurements in the diffuse portion of the band (see Section 6).

The temperature dependence will be taken into account by using the aforementioned values of the coefficients which correspond to the low atmospheric temperatures and/or by selecting wavelengths within the band structure for which there is little or no temperature dependence.[106] The order of magnitude as well as the reliability of the absorption coefficient values have been the primary considerations in the choice of wavelength to be used in the proposed optical techniques for ozone measurement. This will be seen in the discussions in Section 6.

3.2.3 INFRARED ABSORPTION COEFFICIENTS

Figure 3-4 is reproduced from a publication by J. Strong[107] who has suggested that this band be used to measure atmospheric pressure simultaneously with ozone content (see subsection 5.1.3). The band is associated with the 1043 cm^{-1} fundamental vibration and, as is seen in the figure, it occurs in a region that is relatively free of absorption by other atmospheric constituents.

As a result of the detailed experimental measurements and the theoretical calculations by Clough and Kneizys[108], the 9.6 micron absorption band can be considered to be completely analyzed. A complete vibrational-rotational analysis, which includes the effect of Coriolis coupling and a second-order distortion interaction, has allowed the contribution that each vibrational transition (ν_1 and ν_3) makes to the 9.6 micron absorption band to be evaluated as a function of wavelength. Figure 3-5 shows this band in greater detail. The portion of the spectrum appearing in the figure shows the agreement obtained between measured and computed values. Since the integrated absorption of the band has been previously calculated by Walshaw[109], the intensities in both bands (ν_1 and ν_3) can be expressed in absolute units. Thus, a set of reliable absorption coefficients is available for use in any optical technique utilizing the 9.6 micron absorption band, whether it involves discrete line absorption or integrated absorption.

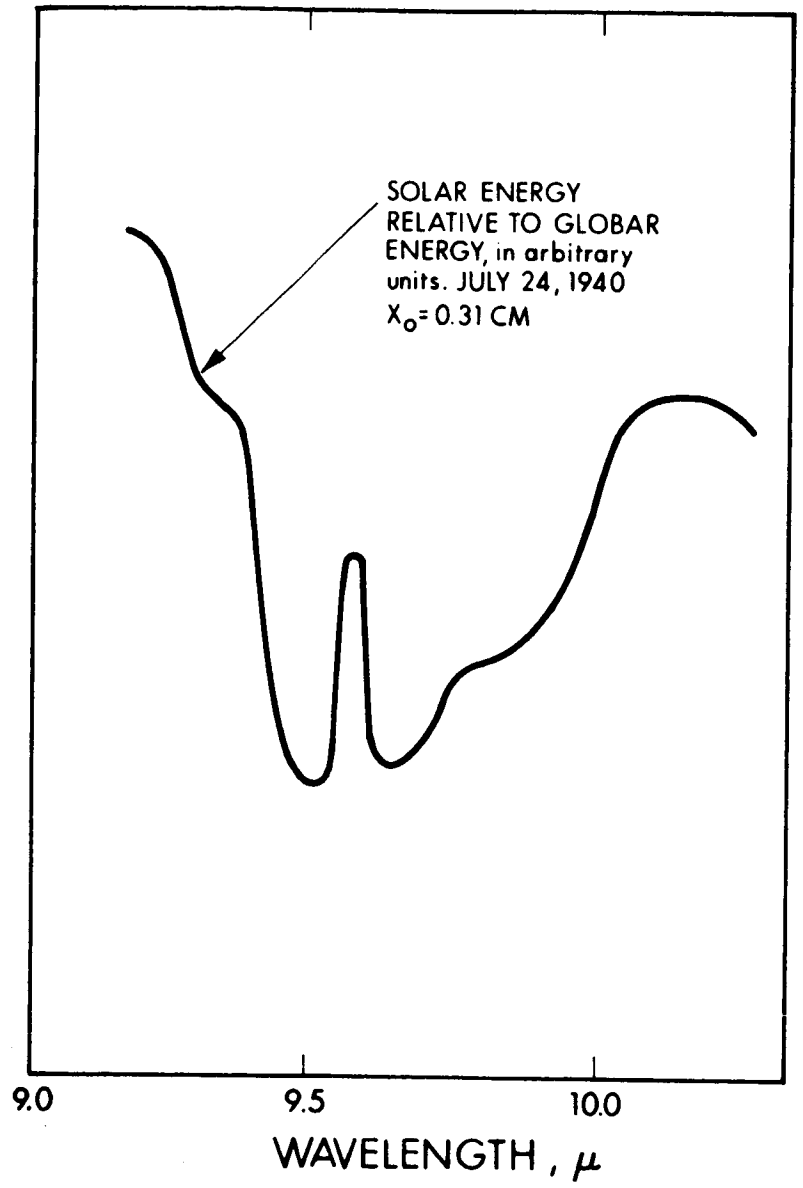

Figure 3-4. 9.6μ Absorption Band of Ozone

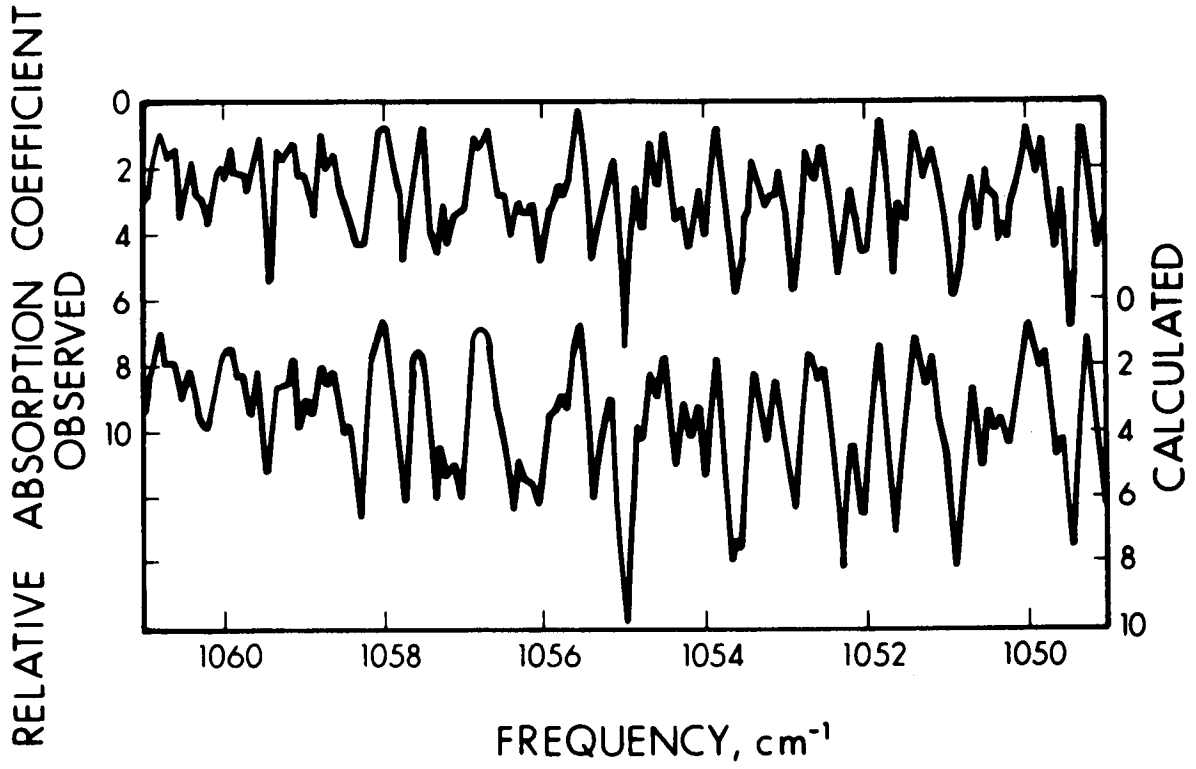

Figure 3-5. A Portion of the 9.6μ Ozone Absorption Band as Measured Under High Resolution (upper curve) and as Reconstructed by Computer Analysis (lower curve)

SECTION 4

METHODS OF ATMOSPHERIC OZONE MEASUREMENTS (NON-SATELLITE TECHNIQUES)

Since the ozone layer was discovered[138] in 1913, a great variety of optical techniques have been employed to measure both the total ozone content and its vertical distribution. The total content can be determined from the ground rather easily by using the sun as a source for the absorption measurements. The vertical distribution can likewise be measured from the ground by means of the so-called "Umkehr" effect,[153-156] but this method suffers due to poor accuracy. Paetzold[157-163] performed a number of measurements by the method of using eclipses of the moon, but measurements can be made by this technique only when the moon is in a favorable position with respect to the sun and an observer on the earth. More recent techniques which have been used include the method of balloon ascents, airplane and V-2 rocket spectroscopy, and satellite reflection spectrometry. These methods are all limited in scope since they allow measurements over only limited ranges of altitudes. Furthermore, in common with most techniques which have been used, these methods can be used only over a limited number of geographic locations at any given time.

In addition to the optical methods, various chemical methods have been developed which yield excellent data concerning vertical ozone distribution above individual ground stations. Subsection 9.5 of this report consists of a list of references to articles which deal with methods of measuring the total atmospheric ozone

content as well as its vertical distribution. These methods range from such early methods as the method employing lunar eclipses to the more recent techniques involving satellites, rockets, balloons and airplanes.

Details of these techniques will not be discussed here, an excellent review having been presented recently by Craig[3]. It suffices at this point to note that an impressive number of detailed descriptions of optical ozone measuring techniques appear in the referenced articles, from which valuable information can be drawn.

For example, the Götz or Umkehr technique is of interest not because of its accuracy, which is, in fact, poor as it pertains to vertical distribution determinations, but because it has been exhaustively refined by Dobson and other workers. In the process of improving the technique, many factors, such as ozone absorption coefficients, wavelengths to be monitored, slit widths and design of the measuring spectrophotometer, etc., were carefully analyzed by these workers. Since these factors also must be considered in the present program, advantageous use can be made of the knowledge that has been gathered as a result of the above previous efforts. Therefore, the Götz technique, as well as other techniques that are represented in the list of references in Subsection 9.5, will continue to be analyzed in order to help evaluate critical parameters that need to be specified in the techniques under investigation in this program.

A chemical technique of particular interest is the chemiluminescent method developed by Regener.[164] This technique makes use of the chemiluminescent reaction of ozone with a disc sensor coated with silica gel and an organic dye, Rhodamin B. The ozone concentration is determined by measuring the light energy released by the reaction.

Due to the extremely rapid response of the device to changes in ozone concentration, very high resolution measurements are made by this technique. The ozonesonde and the conventional radiosonde are flown together in sounding balloons and the ozone signal is telemetered to a ground receiver along with data on temperature, pressure, and humidity. It is with this technique that Hering and co-workers obtained the data at the 12 ozonesonde stations, as discussed in Subsection 2.3.3.3 of this report. This technique is of interest since it is probably the most reliable and well developed technique for taking ozone measurements over a single ground station. Since it is independent of optical techniques, it would appear to be the ideal supplementary technique which could be used as a crosscheck to the advanced concepts which are being evaluated in the current program. That is, once an orbiting satellite is making ozone measurements, ozonesonde balloons could be used at isolated geographical locations for independent measurements of vertical ozone distributions. The results of the two methods could then be directly compared. A system of ozonesonde stations that could compile as much data as a single orbiting satellite would, of course, be highly impractical, if not impossible, to establish.

SECTION 5

ADVANCED CONCEPTUAL METHODS OF OZONE MEASUREMENTS FROM ORBITING SATELLITES

The literature search performed during this program effort has turned up an impressive amount of information relating to the use of optical techniques in the measurement of atmospheric ozone content. A variety of techniques which apply to the measurement of both the total ozone content and its vertical distribution have been critically examined and evaluated.

This survey has shown that there are a number of optical techniques for ozone measurement which could be used in conjunction with an orbiting satellite. These would be essentially independent and supplementary techniques, and it may prove desirable to instrument one satellite to perform the measurements by two or three of these techniques simultaneously.

The techniques which have been considered can be classified as being either passive or active methods. The former involve measurements made of the radiation emitted by a natural source, such as the sun, or by the atmospheric ozone itself. The latter rely on the use of radiation provided by a man-made source, such as a laser, which may either be a ground-based or satellite-borne instrument. The following paragraphs describe briefly the optical ozone-measuring methods which merit consideration for a satellite application.

5.1 PASSIVE TECHNIQUES

The two passive techniques that are seriously being considered for recommendation are (1) the determination of vertical ozone content by a measurement of the differential attenuation of solar radiation which traverses the earth's atmosphere, and (2) the determination of vertical ozone content by analysis and the infrared radiation emitted by the atmospheric ozone. The theoretical principles for both of these techniques have been well developed and a limited amount of observational data has been acquired which confirms the essential correctness of both methods.

5.1.1 DIFFERENTIAL ATTENUATION OF SOLAR RADIATION

This technique depends on viewing the solar rays after they pass tangentially through the earth's atmosphere. The satellite-borne detector monitors the intensities at a number of wavelengths for different geometrical ray paths and the vertical distribution can be deduced from straightforward physical and geometrical considerations. This method involves the use of visible and near ultraviolet radiation, as is described in detail in Section 6.

5.1.2 INFRARED EMISSION BY ATMOSPHERIC OZONE

This technique utilizes infrared radiation which is emitted by the ozone molecule and is analogous to a method which has been used to deduce vertical resolution from ground-based measurements.[45,165,166,167]

5.2 ACTIVE TECHNIQUES WITH OPTICAL PROBES

The use of active probes represents a new concept in ozone measurements principally because such probes have become feasible only since the development of the laser and since it has become possible to

consider the use of a satellite as a transmitting or receiving station. A program of measurements incorporating active probes would offer many advantages including the fact that it would not depend on the position of the sun with respect to the satellite position. It would also be capable of operation during either day or night, thus providing valuable information concerning diurnal variations of the vertical ozone distribution. Such information would be of value in clarifying the role of ozone in atmospheric processes, including horizontal and vertical air transport mechanisms. An active probe technique would be expected to provide at least as much information concerning the vertical distribution of ozone as any of the passive techniques under investigation.

The methods discussed here depend on the availability of high-power laser radiation at wavelengths which can be utilized in the determination of atmospheric ozone. At present, the class of laser most likely to fulfill this need is the so-called Raman laser. This name is derived from the fact that laser-like radiation, i.e., highly intense, pulsed, coherent, monochromatic, and directional radiation, can be produced at a variety of wavelengths by the phenomenon known as stimulated Raman scattering. The production of Raman lasers requires the use of a high intensity, pulsed primary laser such as the ruby or neodymium laser (6943μ and 1.06μ, respectively) or the use of second harmonic laser radiation at 3471Å or 5300Å, respectively.

5.2.1 SATELLITE-BORNE RAMAN LASERS, SATELLITE-BORNE DETECTORS

A Raman laser aboard a spacecraft could be used to provide a source for ozone measurement by absorption techniques. As such, the laser radiation would be a substitute for solar radiation in the first passive technique discussed above if used in a two-satellite configuration. Much more versatility would result by using a laser source,

however, since such a technique would not suffer from geometrical restriction inherent in using solar radiation. The laser source could also be used in a single satellite configuration to measure the ozone content by the well known technique based on back scattering of UV radiation by air molecules.[168-171]

5.2.2 GROUND-BASED RAMAN LASERS, SATELLITE-BORNE DETECTORS

This technique essentially reverses the role of emission source and detector in the ground-based method which determines total ozone content by measuring the attenuation of solar radiation at different incident zenith angles. The use of a laser source again eliminates geometrical limitations which are imposed when the sun is used as a source for absorption measurements.

5.3 SELECTION OF SATELLITE METHODS FOR OZONE MEASUREMENTS

As a result of the survey and preliminary evaluation of optical techniques performed during the first year of this program, two optical techniques have been chosen for detailed analysis. Although others may be seriously considered in later phases of the program, it has been decided to concentrate for the present on one active and one passive technique which both appear to be well within the state of the art. The two techniques are complementary with respect to the type of information they yield. The principal on-board instrumentation requirements for both techniques would be spectral filtering devices and photomultiplier detectors. It is felt that the two types of measurements would be compatible from the point of view of instrumentation on a single satellite, and would allow the atmospheric ozone content to be measured with both high horizontal and vertical resolution.

Progress has been made in demonstrating the feasibility of both of these techniques. This progress is reviewed in Sections 6 and 7 of this report.

SECTION 6

OZONE DETERMINATION BY THE METHOD OF DIFFERENTIAL ATTENUATION OF SOLAR RADIATION

With the development of instrumented satellites, exploratory measurements of ozone profiles over a number of locations have been made[172,173] by the method referred to herein as the differential attenuation of solar radiation. However, the spectral and spatial resolutions which characterize these measurements do not begin to approach the ultimate in the state-of-the-art for satellite-borne instrumentation. The discussions appearing in this section are intended to illustrate the extent to which this method can be improved upon by refining the measurement and data reduction aspects in a satellite application.

The underlying principles of this technique were also used by Venkateswaran, et al[174], to determine the vertical distribution of ozone with the aid of the Echo communications satellite, 1960 Iota I. However, whereas these investigators performed ground-based measurements of solar radiation reflected by the satellite, the technique described here would involve direct measurements of the solar radiation by an instrument aboard a satellite. Several advantages result from the ability to make direct measurements, including increased sensitivity, resolution, and accuracy. Furthermore, depending on the type of orbit, measurements can be made over a selected number of locations around the world on a quasicontinuous basis.

Certain features of the problem, such as the need to correct for the refraction of solar rays by the earth's atmosphere, and the de-

parture of the sun's surface from a point source, while discussed here, will not be treated fully until the subsequent year's effort. The emphasis in the discussion below will be on demonstrating the feasibility and efficiency of the method.

6.1 OPTICAL PRINCIPLES OF THE DIFFERENTIAL ATTENUATION TECHNIQUE

The principles involved can be illustrated by reference to Fig. 6-1. Measurements of solar radiation intensities are taken when the sun's rays are passing tangentially through the earth's atmosphere and the instantaneous position of the satellite is at S_i (during orbital sunrise or sunset). For purposes of illustration, a satellite altitude of 1000 km is shown in the figure, but the technique is valid for a wide range of altitudes. The atmosphere, which is considerably exaggerated in the figure, is divided into a number of shells above the sunset or sunrise point, S_u, and below a height h_1. In the example shown, a model with ten shells, each of 10 km thickness, has been adopted. In principle, any number of shells can be assumed, although a practical limitation will be imposed by the rate at which the satellite-borne instrument can make measurements at the wavelength bands of interest. It can be seen from the discussion below that the greater the number of measurements per sequence, the greater the accuracy with which the vertical distribution can be defined. In the calculations presented later in this section, the model adopted contains 80 spherical shells each of 1 km thickness. Preliminary orbital, detector, and optical analyses indicate that this does not represent an unrealistic rate of measurement taking. The first shell (highest altitude) is bounded by the altitudes h_1 and h_2 (which in the example of Fig. 6-1 take the values of 100 and 90 km, respectively). Similarly, the ith shell is bounded by the altitudes, h_i and h_{i+1}. The satellite can selectively view a ray which, at the local sunset point S_u, passes only through the ith shell. This ray is referred to as R_i and the distance that it traverses in the ith layer is denoted

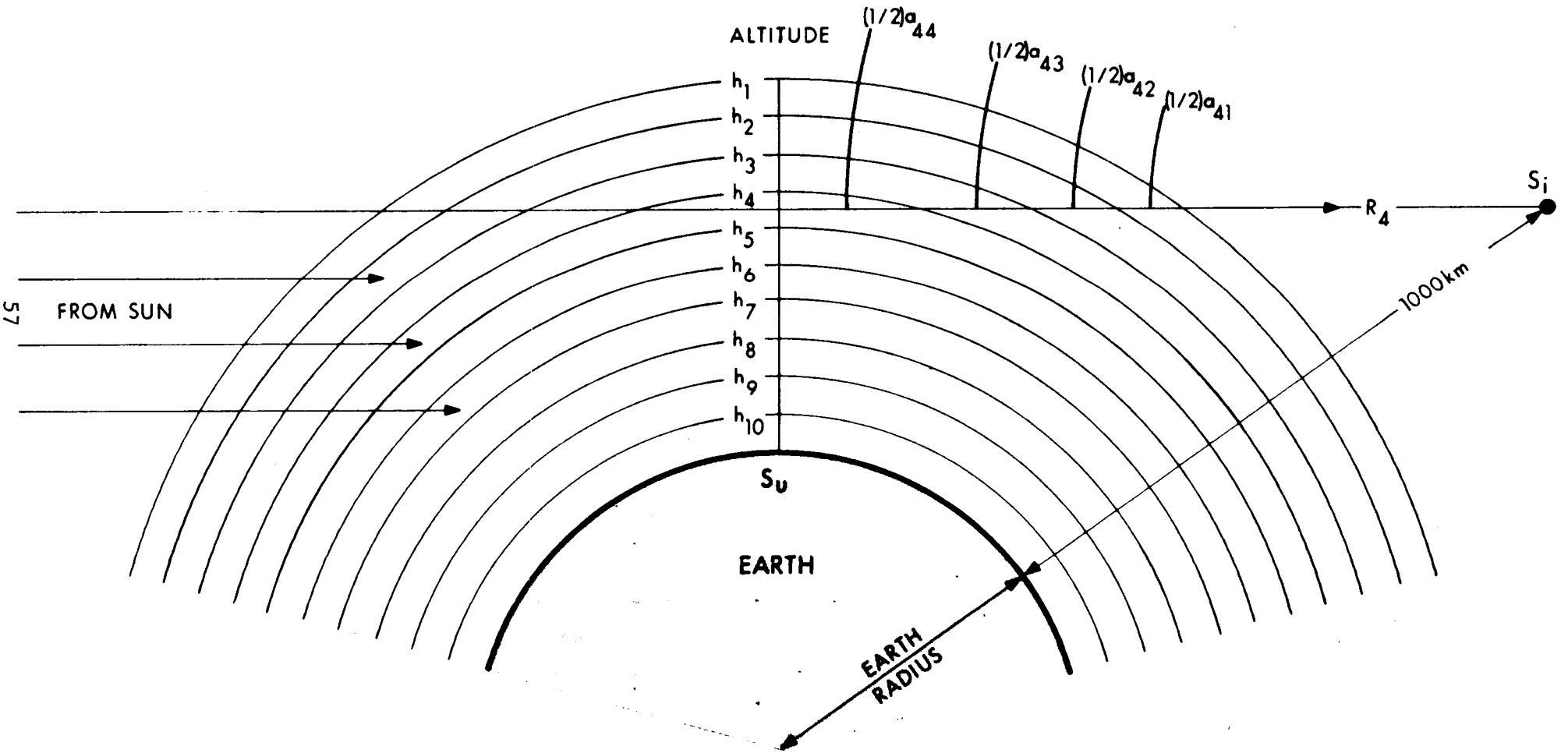

Figure 6-1. Geometry Involved in Direct Measurement of Attenuated UV Solar Radiation

by a_{ii}. However, in passing through the entire atmosphere any ray, other than R_1, will traverse a certain distance, a_{ij}, through the jth layer where j = 1, 2, ..., i-1. The values of a_{ii} and a_{ij} can be determined by geometrical considerations.

The degree of attenuation of any solar ray passing through a tangential path in the atmosphere will depend upon the wavelength and upon the number of absorbing and scattering molecules encountered. The assumption is made that the only significant absorption in the visible and near UV spectral regions is due to molecular ozone, an assumption that is certainly well justified. The Rayleigh scattering can be easily accounted for. The wavelength dependence is, of course, due to the variation with wavelength of the absorption coefficient, or cross section per molecule, of ozone, and the Rayleigh scattering cross-section of air molecules. The number of ozone and air molecules encountered by any tangential solar ray can, for purposes of illustration, be estimated from some adopted model of vertical atmospheric ozone distribution. This has been done for the calculations described in Section 6.2. The motion of the satellite serves as a scanning motion by means of which the attenuation through different atmospheric thicknesses is determined for each wavelength being monitored. The absolute intensities of the solar rays can be determined by direct measurement from a position in which the earth's atmosphere does not intervene. A measure of the differential attenuation is thus obtained for different paths through the earth's atmosphere. Data taken in this manner can be inverted by straightforward computer techniques to yield a vertical profile of the ozone and air distributions.

6.2 DETERMINATION OF MOLECULAR THICKNESSES

As mentioned above, the satellite is allowed to view the solar radiation which passes tangentially through the earth's atmosphere. The

finite size of the sun(which means that it cannot be considered as a point source) and atmospheric refraction are complications which will be discussed in subsequent subsection. For the present, it can be assumed that at any instant, in this portion of its orbit, the satellite views a single ray which passes without refraction at some uniquely defined altitude above the sunset point, S_u. This altitude, which can be determined from a knowledge of the orbital parameters, is denoted by h_{ii}. (The altitude above S_u at which the ith ray passes through the center of the ith atmospheric shell.)

The absolute intensity of the solar radiation, as measured by a satellite-borne detector, will depend on (a) the intensity of solar radiation in the wavelength band being monitored, and (b) the total optical thickness of the earth's atmosphere for the ith ray at the wavelength being monitored. The total optical thickness, τ, is defined here as the exponential factor relating the intensity, $I(\lambda)$, transmitted by the earth's atmosphere to the incident intensity, $I_o(\lambda)$, i.e.,

$$I_i(\lambda_j) = I_o(\lambda_j)e^{-\tau_i} \qquad (6\text{-}1)$$

In equation (6-1) the subscript i is used to emphasize the fact that the optical thickness, and therefore the transmitted intensity, will depend on the particular ray path through the atmosphere; the subscript j is used to indicate that more than one wavelength will be monitored, for reasons to be discussed below.

The optical thickness for any ray of a given wavelength will be determined by the total number of attenuating molecules in the ray's path through the atmosphere. In the wavelength regions which will be used, the only important attenuation mechanisms are Rayleigh scattering by air molecules (N_2 and O_2) and molecular absorption by ozone. For

a given length traversed by a ray at a known altitude, the optical thickness will depend on the prevailing vertical distribution of these attenuating particles. The latter is known to be a variable property of the atmosphere, especially in the case of ozone. The following model vertical distributions of ozone and air therefore, have been adopted for this calculation. The ozone model adopted was the so-called average distribution given by the USAF Handbook of Geophysics, Ch. 8 (1961); the air distribution was taken from the work of Minzner, et. al. (AFCRC-TR-59-267, 1959.) For practical reasons, the earth's atmosphere is considered to consist of 80 concentric shells of one kilometer thickness each (instead of the ten shells shown in Fig. 6-1), and the air and ozone concentrations are assumed to be uniform within each shell. It is also assumed that the satellite can view a ray which passes through the center of each shell above the sunset point, a total of 80 such rays being monitored. (Ray number one is that ray which passes through the outermost, or first, shell at an altitude of 79.5 km above S_u, and the remaining rays and shells are numbered in increasing sequence as the altitude at which each ray passes above the sunset point decreases.) The distance that any ray traverses in each individual shell can be determined through simple geometry. These traversal lengths, a_{ij}, were determined with the aid of a computer program. This program, which will be referred to herein simply as OZONE, is completely flexible with respect to the number of shells and the vertical distribution of particles that can be incorporated into the computation. By weighting each length first by the ozone concentration and then by the air density appropriate to that altitude, the ozone and air thicknesses of each traverse length were determined. The total number of ozone and air molecules encountered by any ray in traversing the entire atmosphere is then simply obtained by summing all of the weighted traverse lengths for that ray.

The results of these computations are summarized in Table 6-1. The first two columns define the ray and sunset point altitude, while the third lists the local values of the air densities which were used. The total number of air and ozone molecules that would be encountered by each ray, with the assumed distributions, are listed in the last two columns. (In these latter columns the letter E denotes the exponent or power of the number 10.)

In the following subsection, a review is given of the manner in which the total molecular thicknesses for each ray are obtained from solar radiation attenuation measurements. Once the molecular thickness for each ray is known, the vertical profile can be computed with the aid of a program which is essentially the inverse of the OZONE program referred to above. This inverse program, or INVOZONE, has been satisfactorily prepared and used in sample computations. It will be modified for future analyses in order to determine the accuracy with which this passive measurement method can reproduce a variety of ozone profiles. This will be done by introducing uncertainties into the total molecular thickness values which reflect errors inherent in the intensity measurements and uncertainties in the ozone cross-section values.

6.3 OPTICAL THICKNESS DETERMINATIONS AND SELECTION OF WAVELENGTHS

Since both the Rayleigh scattering cross-sections for air molecules and the absorption cross-section for ozone vary with wavelength, a given molecular thickness represents a range of optical thicknesses. In this subsection results of optical thickness calculations will be presented. In addition, the manner in which these results help define the wavelengths that should be monitored will be discussed.

The measured quantity, from which the optical thickness of the atmosphere for a given ray is deduced, is the intensity ratio $I_i(\lambda_j)/I_o(\lambda_j)$.

TABLE 6-1

TOTAL MOLECULAR THICKNESSES FOR RAYS 1 - 80

Ray(i)	Altitude h_{ii} (km)	$air(\frac{Molecules}{cm^3})$		Molecular Thickness (Entire Ray) Air		Ozone	
1	79.50	4.811	E14	7.7281	E21	2.803	E15
2	78.50	5.703	E14	1.4818	E22	3.480	E15
3	77.50	6.733	E14	2.1415	E22	4.341	E15
4	76.50	7.916	E14	2.8413	E22	5.432	E15
5	75.50	9.275	E14	3.6142	E22	6.814	E15
6	74.50	1.082	E15	4.4808	E22	8.551	E15
7	73.50	1.259	E15	5.4614	E22	1.073	E16
8	72.50	1.459	E15	6.5724	E22	1.347	E16
9	71.50	1.686	E15	7.8333	E22	1.693	E16
10	70.50	1.942	E15	9.2629	E22	2.129	E16
11	69.50	2.230	E15	1.0882	E23	2.678	E16
12	68.50	2.554	E15	1.2713	E23	3.368	E16
13	67.50	2.917	E15	1.4781	E23	4.238	E16
14	66.50	3.324	E15	1.7097	E23	5.334	E16
15	65.50	3.777	E15	1.9724	E23	6.722	E16
16	64.50	4.282	E15	2.2672	E23	8.462	E16
17	63.50	4.843	E15	2.5973	E23	1.064	E17
18	62.50	5.466	E15	2.9665	E23	1.338	E17
19	61.50	6.156	E15	3.3787	E23	1.688	E17
20	60.50	6.918	E15	3.8380	E23	2.120	E17
21	59.50	7.760	E15	4.3491	E23	2.669	E17
22	58.50	8.687	E15	4.9166	E23	3.330	E17
23	57.50	9.706	E15	5.5457	E23	4.135	E18

TABLE 6-1

TOTAL MOLECULAR THICKNESSES FOR RAYS 1 - 80 (contd)

Ray(i)	Altitude h_{ii} (km)	$\rho_{air}(\frac{Molecules}{cm^3})$		Molecular Thickness (Entire Ray) Air		Ozone	
24	56.50	1.083	E16	6.2426	E23	5.129	E18
25	55.50	1.205	E16	7.0113	E23	6.280	E18
26	54.50	1.340	E16	7.8606	E23	7.717	E18
27	53.50	1.487	E16	8.7962	E23	9.494	E18
28	52.50	1.673	E16	9.8661	E23	1.168	E18
29	51.50	1.884	E16	1.1084	E24	1.438	E18
30	50.50	2.122	E16	1.2463	E24	1.769	E18
31	49.50	2.388	E16	1.4016	E24	2.176	E18
32	48.50	2.694	E16	1.5777	E24	2.678	E18
33	47.50	3.028	E16	1.7751	E24	3.294	E18
34	46.50	3.447	E16	2.0036	E24	4.053	E18
35	45.50	3.933	E16	2.2677	E24	4.984	E18
36	44.50	4.482	E16	2.5702	E24	6.132	E18
37	43.50	5.140	E16	2.9212	E24	7.549	E18
38	42.50	5.886	E16	3.3251	E24	9.288	E18
39	41.50	6.750	E16	3.7903	E24	1.142	E19
40	40.50	7.758	E16	4.3283	E24	1.405	E19
41	39.50	8.936	E16	4.9519	E24	1.728	E19
42	38.50	1.030	E17	5.6741	E24	2.145	E19
43	37.50	1.190	E17	6.5131	E24	2.674	E19
44	36.50	1.375	E17	7.4861	E24	3.343	E19
45	35.50	1.594	E17	8.6211	E24	5.188	E19
46	34.50	1.797	E17	9.8602	E24	5.252	E19
47	33.50	2.153	E17	1.1433	E25	6.532	E19
48	32.50	2.508	E17	1.3268	E25	7.966	E19
49	31.50	2.924	E17	1.5399	E25	9.598	E19
50	30.50	3.432	E17	1.7922	E25	1.157	E20
51	39.50	4.014	E17	2.0875	E25	1.334	E20
52	28.50	4.722	E17	2.4374	E25	1.498	E20

TABLE 6-1

TOTAL MOLECULAR THICKNESSES FOR RAYS 1 - 80 (contd)

Ray(i)	Altitude h_{ii} (km)	$\rho_{air}(\frac{Molecules}{cm^3})$		Molecular Thickness (Entire Ray) Air		Ozone	
53	27.50	5.564	E17	2.8522	E25	1.658	E20
54	26.50	6.573	E17	3.3453	E25	1.819	E20
55	25.50	7.696	E17	3.9188	E25	1.970	E20
56	24.50	9.339	E17	4.6402	E25	2.114	E20
57	23.50	1.069	E18	5.4305	E25	2.132	E20
58	22.50	1.248	E18	6.3479	E25	2.058	E20
59	21.50	1.456	E18	7.4188	E25	1.971	E20
60	20.50	1.710	E18	8.6849	E25	1.875	E20
61	19.50	2.000	E18	1.0164	E26	1.780	E20
62	18.50	2.339	E18	1.1892	E26	1.669	E20
63	17.50	2.737	E18	1.3913	E26	1.563	E20
64	16.50	3.201	E18	1.6276	E26	1.470	E20
65	15.50	3.745	E18	1.9041	E26	1.389	E20
66	14.50	4.382	E18	2.2276	E26	1.320	E20
67	13.50	5.126	E18	2.6059	E26	1.264	E20
68	12.50	5.998	E18	3.0486	E26	1.219	E20
69	11.50	7.019	E18	3.5668	E26	1.179	E20
70	10.50	8.082	E18	4.1521	E26	1.143	E20
71	9.50	9.145	E18	4.7927	E26	1.112	E20
72	8.50	1.031	E19	5.4980	E26	1.083	E20
73	7.50	1.159	E19	6.2775	E26	1.058	E20
74	6.50	1.299	E19	7.1386	E26	1.034	E20
75	5.50	1.451	E19	8.0872	E26	1.013	E20
76	4.50	1.616	E19	9.1297	E26	9.925	E19
77	3.50	1.796	E19	1.1283	E27	9.740	E19
78	2.50	1.991	E19	1.2603	E27	9.567	E19
79	1.50	2.201	E19	1.3320	E27	9.405	E19
80	0.50	2.427	E19	1.3727	E27	9.254	E19

For present considerations, it is assumed that when the transmitted intensity falls within the range

$$0.05\ I_o(\lambda_j) \leq I_i(\lambda_j) \leq 0.95\ I_o(\lambda_j) \qquad (6\text{-}2)$$

the intensity ratio can be measured with sufficient accuracy to determine the optical thickness, $\tau_i\ (\lambda_j)$. (A more exact range of intensity ratios will be specified upon the completion of a detector sensitivity, and signal-to-noise analysis which is discussed in Section 6.6.) The criterion described by the above inequality, when used in conjunction with the data in Table 6-1, serves to define the wavelengths that can be usefully monitored. This can be illustrated by evaluating the optical thickness for the 2900Å component of various rays passing through the earth's atmosphere.

Table 6-2 summarizes the air and ozone molecular thicknesses, for rays number 12 through 31, as well as the contributions to the optical thickness by each type of molecule. The optical thickness of air is the product of the molecular thickness and β, the Rayleigh scattering cross-section per molecule, ($\beta(2900\text{Å}) = 5.763 \times 10^{-26}\ cm^2$.) The ozone optical thickness is the product of the total ozone molecular thickness and the absorption cross-section σ($\sigma(2900\text{Å}) = 1.196 \times 10^{-18}\ cm^2$). The sum of these two products, τ_i or the total optical thickness, gives a measure of the attenuation of the 2900Å component of the ith ray, i.e., as in equation 6-1. The range of values of τ_i which appears in Table 6-2 ensure that the inequality of equation 6-2 is satisfied for the rays 12 through 31. For rays 1 through 11, the transmitted intensity at 2900Å would be greater than 95% of the incident intensity and hence would not be suitable for measuring the optical (and therefore the molecular) thicknesses. For rays 32 through 80, the attenuation rapidly increases and little or no radiation would be transmitted. Thus, it is seen that monitoring solar radiation at 2900Å could provide useful data only for the rays shown in Table 6-2

TABLE 6-2

OPTICAL THICKNESS AT 2900Å FOR RAYS 12-31

Ray (i)	Altitude (km)	Molecular Thickness Air	Molecular Thickness Ozone	Optical Thickness (2900Å) Air	Optical Thickness (2900Å) Ozone	Optical Thickness (2900Å) Total
31	49.50	1.402×10^{24}	2.176×10^{18}	0.0808	2.6025	2.6833
30	50.50	1.246×10^{24}	1.769×10^{18}	0.0718	2.1145	2.1863
29	51.50	1.108×10^{24}	1.438×10^{18}	0.0639	1.7195	1.7834
28	52.50	9.866×10^{23}	1.168×10^{18}	0.0569	1.3969	1.4538
27	53.50	8.796×10^{23}	9.494×10^{17}	0.0507	1.1356	1.1863
26	54.50	7.861×10^{23}	7.717×10^{17}	0.0453	0.9230	0.9683
25	55.50	7.011×10^{23}	6.280×10^{17}	0.0404	0.7510	0.7914
24	56.50	6.243×10^{23}	5.129×10^{17}	0.0360	0.6135	0.6495
23	57.50	5.546×10^{23}	4.135×10^{17}	0.0320	0.4946	0.4978
22	58.50	4.917×10^{23}	3.330×10^{17}	0.0283	0.3983	0.4266
21	59.50	4.349×10^{23}	2.669×10^{17}	0.0251	0.3192	0.3443
20	60.50	3.838×10^{23}	2.120×10^{17}	0.0221	0.2536	0.2757
19	61.50	3.379×10^{23}	1.688×10^{17}	0.0195	0.2015	0.2210
18	62.50	2.966×10^{23}	1.338×10^{17}	0.0171	0.1601	0.1772
17	63.50	2.597×10^{23}	1.064×10^{17}	0.0150	0.1273	0.1423
16	64.50	2.267×10^{23}	8.462×10^{16}	0.0131	0.1012	0.1143
15	65.50	1.972×10^{23}	6.722×10^{16}	0.0114	0.0804	0.0918
14	66.50	1.710×10^{23}	5.334×10^{16}	0.0099	0.0638	0.0737
13	67.50	1.478×10^{23}	4.238×10^{16}	0.0085	0.0507	0.0592
12	68.50	1.271×10^{23}	3.368×10^{16}	0.0073	0.0403	0.0476

(at least for the ozone and air distributions which were used in this sample calculation.) More generally, it can be shown that any wavelength that is monitored will provide useful data for a limited number of rays. The reason for this can be seen by examining the range of values of molecular ozone thicknesses appearing in Table 6-1. Since these values vary in magnitude from about 10^{15} to about 10^{20}, and since the desired optical thickness is of the order of unity, wavelengths should be chosen such that the ozone absorption cross-sections vary in magnitude by about four or five orders of magnitude.

The ozone absorption cross-sections in the visible and UV spectral regions do in fact vary from about 4×10^{-21} cm^2 at 6000Å to about 1×10^{-17} cm^2 at 2600Å. When the Rayleigh scattering attenuation is also taken into account, it can be shown that a wavelength can always be found such that values of $\tau_i(\lambda)$ which are consistent with the criterion expressed by equation (6-2) will be obtained for rays passing as high as 76.5 km above S_u. It can further be shown that only a limited number of wavelengths are required for measuring the optical thicknesses of all of the rays shown in Table 6-1. One such possible set of wavelengths is listed in Table 6-3, together with the ozone absorption cross-sections per molecule and the Rayleigh scattering cross-sections for air molecules.

The wavelengths listed in the above table constitute a representative set. The final selection will take into account such factors as the possible presence of Fraunhofer lines in the solar spectrum, the possible presence of absorption or emission by other atmospheric constituents such as atmospheric sodium or nitric oxide, etc. Detector system requirements and limitations will also have to be considered.

In addition to the need for monitoring different wavelengths because of the spectral dependence of the optical thickness, τ_i, it is required

TABLE 6-3

ATTENUATION CROSS-SECTIONS

λ(Å)	$\sigma(\lambda)$, Ozone(cm^2)	$\beta(\lambda)$, Air(cm^2)
2600	1.0136×10^{-17}	8.922×10^{-26}
2700	6.873×10^{-18}	7.674×10^{-26}
2800	3.405×10^{-18}	6.640×10^{-26}
2900	1.196×10^{-18}	5.763×10^{-26}
3000	3.192×10^{-19}	5.034×10^{-26}
3050	1.604×10^{-19}	5.380×10^{-26}
3100	9.267×10^{-20}	5.739×10^{-26}
4800	0.900×10^{-21}	7.682×10^{-27}
6000	4.355×10^{-21}	3.147×10^{-27}

that two wavelengths be monitored at each instant in order to separate the two individual contributions to the total attenuation. This can bee seen by considering the following two equations:

$$I_i(\lambda_1) = I_o(\lambda_1)e^{-N_i(O_3)\sigma(\lambda_1)+N_i(air)\beta(\lambda_1)} \quad (6\text{-}3)$$

$$I_i(\lambda_2) = I_o(\lambda_2)e^{-N_i(O_3)\sigma(\lambda_2)+N_i(air)\beta(\lambda_2)} \quad (6\text{-}4)$$

In equations (6-3) and (6-4), $N_i(O_3)$ and N_i (air) represent, respectively, the total number of ozone and air molecules, per unit cross-sectional area, encountered by the ith ray in its path through the atmosphere.

If it is assumed that the $\sigma(\lambda_j)$ and $\beta(\lambda_j)$ are known exactly, then equations (6-3) and (6-4) can be solved for the two unknowns, $N_i(O_3)$ and N_i(air). Thus, two wavelengths, for which the inequality of equation (6-2) are simultaneously satisfied, must be monitored for each ray.

Table 6-4 shows that if 2900Å is one of the wavelengths monitored for the rays 12 through 31, the second wavelength could be at 2800Å for some of these rays and/or at 3000Å for others. The table also illustrates that with each of three wavelengths chosen, 2800Å, 2900Å, and 3000Å, measurable attenuations would result for rays 17 through 26. Thus, the possibility exists of obtaining two independent measurements of the air and ozone profiles through the altitude range represented by these rays. This is shown in a more general way in Fig. 6-2 for twelve visible and UV wavelengths. This figure graphically shows that measurable attenuations will result at two or more wavelengths for any tangential ray path through the atmosphere passing as high as 70-75 km above S_u.

TABLE 6-4

TOTAL OPTICAL THICKNESS AND TRANSMISSION

Ray (i)	Altitude (km)	(2800Å) τ	(2800Å) T	(2900Å) τ	(2900Å) T	(3000Å) τ	(3000Å) T
31	49.50	--	.05<	2.6833	0.068	0.7653	0.465
30	50.50	--	.05<	2.1863	0.113	0.6272	0.534
29	51.50	--	.05<	1.7834	0.168	0.5147	0.598
28	52.50	--	.05<	1.4538	0.234	0.4225	0.655
27	53.50	--	.05<	1.1863	0.305	0.3424	0.710
26	54.50	2.6799	0.069	0.9863	0.373	0.2859	0.751
25	55.50	2.1848	0.112	0.7914	0.453	0.2357	0.790
24	56.50	1.7880	0.167	0.6495	0.522	0.1951	0.823
23	57.50	1.4449	0.236	0.4978	0.608	0.1599	0.852
22	58.50	1.1666	0.311	0.4266	0.653	0.1311	0.877
21	59.50	0.9456	0.388	0.3443	0.709	0.1071	0.898
20	60.50	0.7545	0.470	0.2757	0.759	0.0835	0.920
19	61.50	0.6025	0.547	0.2210	0.802	0.0708	0.932
18	62.50	0.4812	0.618	0.1772	0.838	0.0576	0.944
17	63.50	0.3847	0.681	0.1423	0.867	0.0471	0.954
16	64.50	0.3078	0.735	0.1143	0.892		>.96
15	65.50	0.2461	0.782	0.0918	0.912		>.96
14	66.50	0.1931	0.824	0.0737	0.929		>.96
13	67.50	0.1541	0.847	0.0592	0.943		>.96
12	68.50	0.1231	0.884	0.0476	0.954		>.96

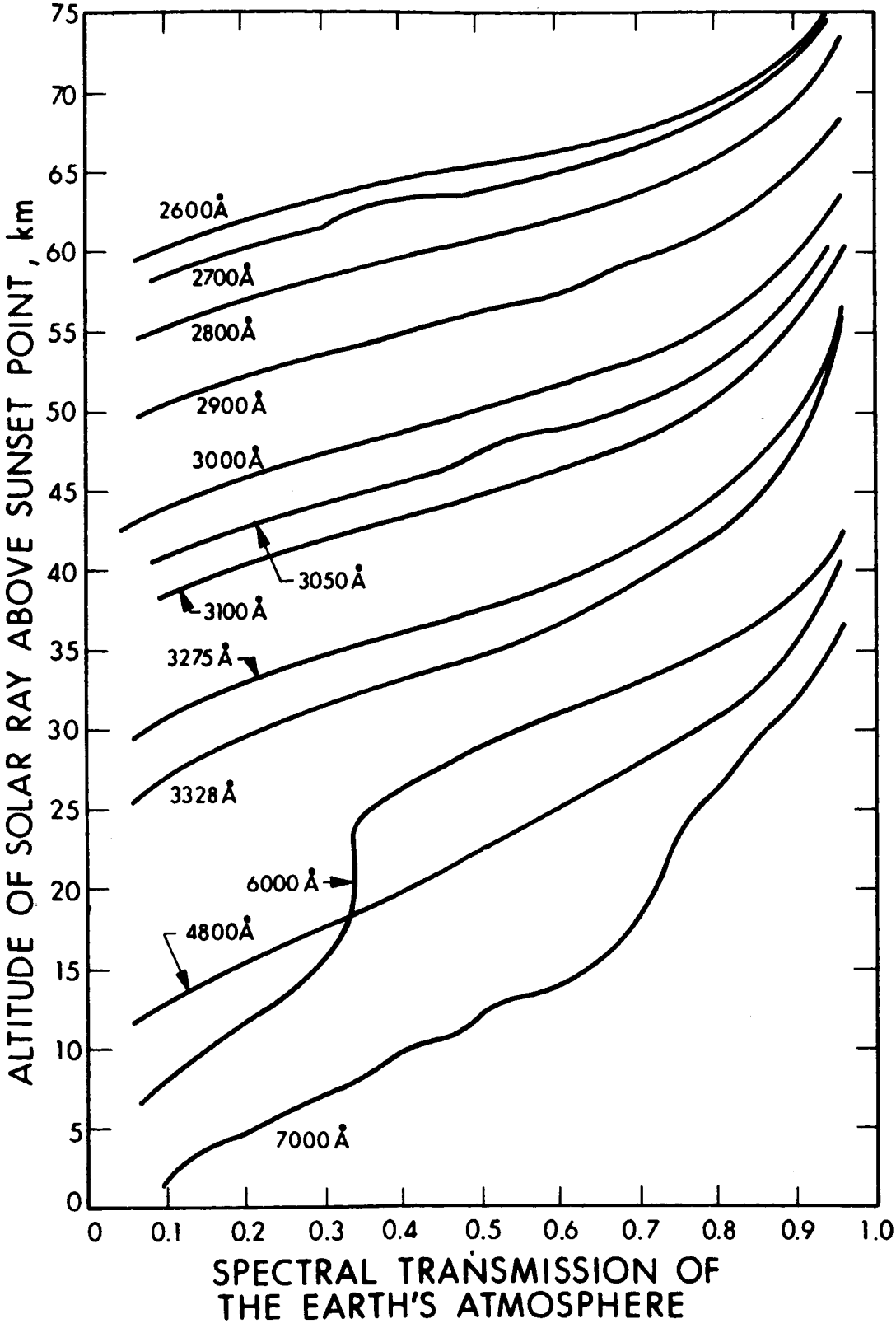

Figure 6-2. Transmission of Earth's Atmosphere for Various Tangential Solar Rays

626197

The above discussion serves to describe the type of analyses which have been undertaken in connection with the method of differential attenuation of solar radiation. In addition to the selection of wavelengths, other aspects under investigation are: (1) an estimate of the accuracy of the technique which takes into account both the inherent uncertainty in the values of the pertinent cross-sections and the accuracy with which the intensity ratios $I_i(\lambda_j)/I_o(\lambda_j)$ can be measured, (2) the number of rays which can reasonably be expected to be measured during a satellite's passage through the sunset and sunrise portions of its orbit, (3) the amount of global coverage that would result from the implementation of such a measurement technique aboard an orbiting satellite. The coverage to be defined will include the number of locations above which the vertical ozone profile would be determined during one day, and the frequency at which such measurements would be made above any given location (4) the analytical techniques which will allow the vertical ozone distribution to be deduced from a measurement of the intensity ratios $I_i(\lambda_j)/I_o(\lambda_j)$. This involves essentially the simultaneous solution of n equations of the type represented by equations (6-3) and (6-4) where n is the number of rays at which the intensity ratio measurements are taken. (The n unknowns are the contributions to $N_i(O_3)$ and $N_i(air)$ made by the n spherical shells for each of the n rays.) This analysis will be performed with the aid of the modified INVOZONE computer program, (5) the complications introduced by the finite size of the sun and by atmospheric refraction are being analyzed, (6) instrument design studies based on the wavelength selection considerations have been initiated. These aspects are discussed in the following subsections.

6.4 IMPLICATIONS OF THE DEVIATION OF THE SOLAR DISC FROM A POINT SOURCE

The fact that the sun cannot be treated as a point source in the application described above has previously been considered to be an inherent

limitation of this measurement technique[172,173,174]. However, an investigation of the problem indicates that the opposite may be true. Rather than representing a limitation, the finite size of the sun's image may be used to advantage due to the fact that the image represents a large number of point (or line) sources with different paths through the atmosphere. The extent of this variation in paths can be appreciated by reference to Fig. 6-3. The position of this satellite is represented by the point B in this figure, and is assumed to be at some known altitude h_s. The extreme rays of the sun are represented by the paths D_1H_1 and QP. The range of altitudes, Δh, directly above the sunset point which is defined by these extreme rays is represented by the line segment K_1K_3. For simplicity, the earth's atmosphere is divided into 3 shells only.

The solar radius, R, from center to limb is known to be equal to $6.957\ (\pm\ .001)\ X\ 10^5$ km. The distance from the earth to the sun, approximately equal to A.U., the astronomical unit, is taken as $1.4953\ X\ 10^8$ km. Therefore, the sun, as observed by a satellite at a distance AB from a location directly above the sunset point, is not a point source but a disc which subtends an angle α at the satellite, where

$$\sin(\alpha/2) = \frac{R}{A.U.+A\ B} \approx \frac{R}{A.U.} = \frac{6.957X10^5}{1.495\ X\ 10^8} = 4.653X10^{-3}$$

$$\alpha/2 \approx 16'$$

$$\alpha=(B_1+\beta_3) \approx 32' \text{ , for AB} \ll \text{A.U.}$$

This represents a vertical range described by the extreme rays of the sun above the sunset point of Δh:

$$\Delta h = 2A\ B\ (4.65X10^{-3})km = 9.30X10^{-3}\ A\ B \text{ km.}$$

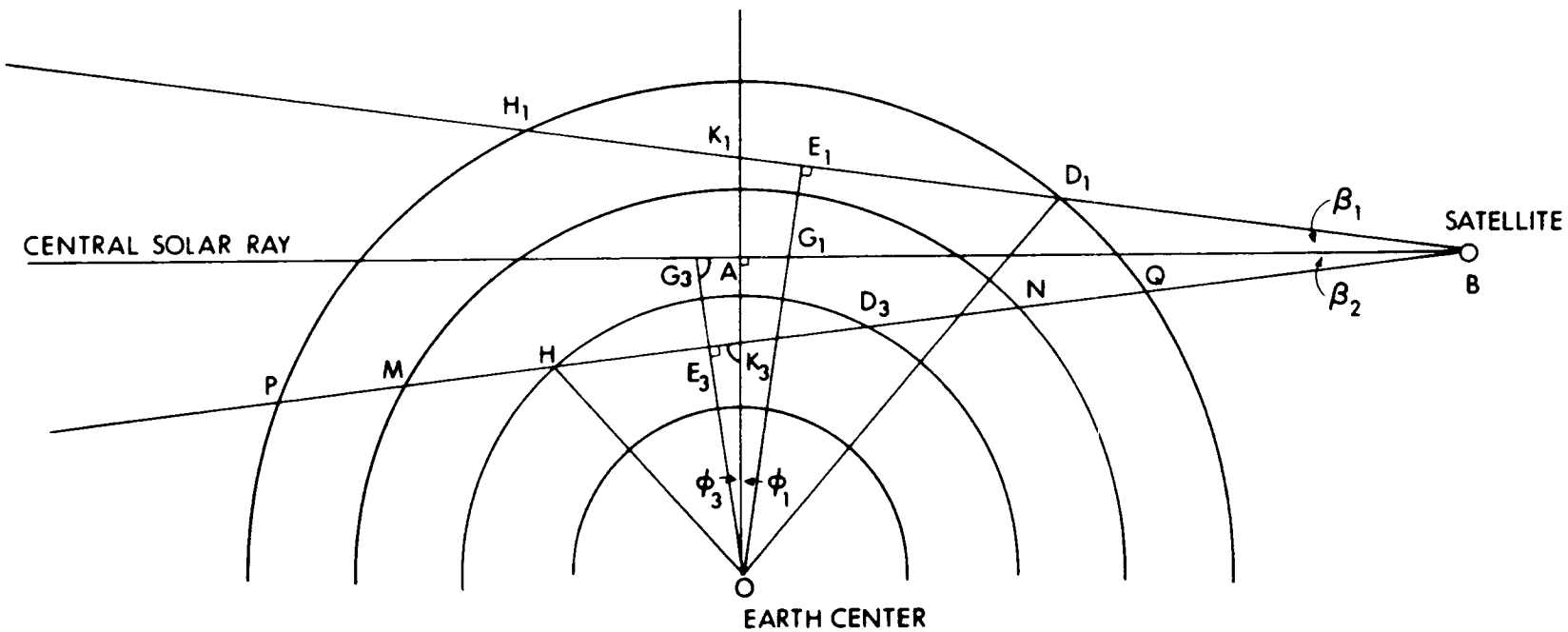

Figure 6-3. Geometry of Solar Rays Traversing Earth's Atmosphere Without Refraction as Observed by a Satellite

Taking the earth's radius as 6375 km, and for a satellite orbital altitude of h_s, the following relationship between h_s and Δh results.

$$\Delta h = 9.30 \times 10^{-3} \left[(6375 + h_s)^2 - (6405)^2 \right]^{1/2} \text{ km.}$$

The altitude range above the sunset point defined by the extreme rays are shown in Table 6-5 for a number of orbital altitudes.

TABLE 6-5

h_s (km)	Δh (km)
200	13.8
400	20.5
600	25.7
800	30.1
1000	34.0
1500	42.6

It can be seen that for any anticipated satellite altitude, the range of altitudes Δh is large with respect to even the coarsest spatial resolution requirements. The analyses of the preceding subsections, on the other hand, are essentially valid only if the tangential or central ray BG_1G_3 is used for the measurement of solar intensities. However, this represents no insurmountable obstacle since optics can be designed which select only a slice of the solar image whose path through the atmosphere approximates that of the central ray. The intensity of solar radiation can be shown to be such that a reduction of 20 or 30 due image-slicing can be tolerated. That is, the large signal-to-noise ratios will still be obtained if photomultiplier detection techniques are used.

However, rather than being limited to the selection of the central ray, a variety of rays could be optically isolated or the entire solar disc could be scanned for any instantaneous position of the satellite. That is, superimposed upon the scanning provided by motion of the satellite a supplementary scanning of the solar disc can be obtained optically. Since this ozone measuring technique is self-calibrating (i.e., the intensity of solar radiation from a segment of the solar disc is measured first when the earth's atmosphere does not intervene and then after it passes through a known path through the atmosphere), the total number of ozone and air molecules can be measured for these additional non-tangential, or slant, paths through the atmosphere. The additional information obtained from these slant paths can be useful in determining any significant departures from spherical symmetry in the ozone concentrations in the individual shells.

This can be most easily shown by referring again to Fig. 6-3. The ozone concentrations in the three shells could be determined by allowing the satellite motion to scan the atmosphere, i.e., select the rays passing through the centers of shells 1, 2, and 3 at three successive satellite positions. This is essentially the technique which has been described in detail in previous portions of this section. An alternate approach would be to allow the satellite, when at the position B, to view the three rays shown in the figure, the central ray, and the two extreme rays. The traverse length of these rays in each shell can again be determined from geometrical principles. This geometry exercise will not be presented in detail here; the important results are:

1. If β_j is the angle that the jth ray makes with the central ray, and h_j is the distance of the central ray from the center of the earth, then the distance of the jth ray from the center of the earth is given by

$b_j = AB \sin\beta_j - (h_j/\cos\beta_j)(\sin^2 \beta_j - 1)$, for rays above the central ray and,

$b_j = -AB \sin\beta_j - (h_j/\cos\beta_j)(\sin^2\beta_j - 1)$, for rays below the central ray. If angles for rays below the central ray are given a negative sign

$$b_j = AB \sin\beta_j - \frac{h_j}{\cos\beta_j}(\sin^2\beta_j - 1), \text{ for all } j.$$

2. If a_{ji} denotes the length that the jth ray traverses in the ith shell, whose top boundary is at a distance c_i from the earth's center, then

$$1/2\ a_{ji} = \left[c_i^2 - b_j^2\right]^{1/2} - \sum_{l=i+1}^{j} a_{jl}$$

3. The results obtained in this form can be used in **INVOZONE**, with minor programming modifications, to yield the vertical profile of the ozone concentrations.

Two essentially independent means of measuring the ozone profile by the differential attenuation technique thus exist. They differ only in the method of scanning the atmosphere. In actual practice, the optimum technique will probably prove to be one which combines both methods of scanning.

In the sample example discussed above, the vertical distribution consists of three concentration values, one for each shell. If the concentration were, in fact, uniform within each shell, the two techniques would yield exactly the same distributions. If different results were obtained by the two methods, however, the assumption of spherical symmetry would obviously be suspect. By comparing the exact paths of each ray in the individual shells, an indication of the locations of

anomalously high or low concentration regions within a shell could be obtained. More information could be obtained by sampling more than just three rays, say seven or eight, at one satellite position. Finally, by performing an optical scan of the entire solar disc at a large number of satellite positions, a high-resolution mapping of the vertical and horizontal ozone distribution could in principle be obtained.

The actual number of rays that are measured in any given satellite passage will, therefore, be determined, in the optimum case, by detector, optical scanning, data recording, reduction, and telemetry limitations. It nevertheless is evident that by exploiting the finite size of the sun's image, the need for assuming spherically symmetric atmospheric shells can in large part be eliminated.

6.5 THE ATMOSPHERIC DISPERSION PROBLEM

The subject of atmospheric refraction was for many years one of the most widely studied problems in astronomy. Simon[175] has recently reviewed the problem, with emphasis on the wavelength dependence (atmospheric dispersion) of the refraction for rays which can be considered to be near-tangential (zenith angles greater than 80°). In earth-bound observations of rays entering the earth's atmosphere from a direction near the horizon, the violet light appears to come from a point nearer the horizon than the red. This must be compensated for either in the reduction of data or by some compensating optics, which exactly shift the two wavelengths of interest by an amount equal to the atmospheric dispersion, before the two wavelengths enter the slit of the recording instrument. In either case, the correct magnitude of the atmospheric dispersion must be known.

In addition to this dispersion problem, atmospheric refraction can introduce two sources of error in the satellite application of the

differential attenuation technique. For a given wavelength component of a ray traversing the earth's atmosphere, refraction can, if not properly accounted for, cause erroneous values to be assumed for:

1. The altitude at which the ray of interest passes above the sunset point, and
2. the lengths traversed by the rays in the individual atmospheric shells.

These problems have been analyzed by Venkateswaran, et. al.[174] who show that the refraction effects can be corrected. Simon[175] also shows that the magnitude of the refraction as a function of wavelength can be computed to any reasonably desired accuracy.

The procedures described by these authors will be incorporated into future analyses of the differential attenuation technique.

6.6 OZONE SIGNAL DETECTION AND MEASUREMENT

Optical detection of attenuated UV and visible solar radiation, in connection with the passive ozone measurement technique described in previous subsections, is quite straightforward and capable of providing high measurement accuracy and precision. In particular, accurate measurements of ozone concentration are achievable since large optical signals are obtained from viewing the solar flux directly after it has been transmitted through the earth's atmosphere. Furthermore, since the sun is the signal source and is viewed directly, the optical receiver in the satellite can be designed to have a field of view which is sufficiently small so that major sources of noise and measurement errors are significantly reduced; and, in addition, the optical receiver spectral bandwidth can be as narrow as practicable so that spectral intensities can be measured with fine spectral resolution. Still further, the available signal intensity and the satellite orbit and measurement geometry are such that several wavelengths can be scanned at modest rates and signals integrated over reasonable times to ensure adequate measurement sensitivity and accuracy.

The subsections which follow contain quantitative discussions of signal detection and factors that affect the measurement system sensitivity and accuracy.

6.6.1 SIGNAL DETECTION

The magnitude of the solar flux that reaches the satellite when the sun's rays are tangential to the earth's atmosphere depend upon the azimuthal position of the satellite with respect to the earth, as was shown in Fig. 6-1. The satellite is shown in a position that is intermediate between the measurement positions of maximum and minimum solar flux attenuation by the earth's atmosphere. As the satellite

makes its transit through each tangential incremental altitude, the sun is tracked and the spectral intensities at several selected UV and optical wavelengths are measured sequentially. In this section we derive an expression for the optical receiver system signal-to-noise ratio (SNR), make certain assumptions about the system design, and then evaluate the system performance.

The optical receiver is assumed to consist simply of an objective lens, a field stop, selectable narrowband optical filters, and a photodetector. The photodetector can be either the photoemissive or solid-state type photodetector, which is sensitive over the spectral region from about 0.25μ to 0.65μ. For the present we consider a photoemissive detector which allows a wide dynamic signal detection range. The overall performance of the optical receiver is determined by the system SNR.

The solar flux on the photodetector produces a photocurrent which is proportional to the intensity of the incident radiation, P_s, given by

$$I_s = \frac{e\,\eta_D\,P_s}{h\nu} \qquad (6\text{-}5)$$

where η_D = detector quantum efficiency
e = electronic charge
$h\nu$ = energy per photon

The intensity of the solar radiation at the photodetector is given by

$$P_s = T_A\,T_o\,A_R\,\Delta_\lambda\,H_\lambda \quad \text{(watts)} \qquad (6\text{-}6)$$

where H_λ = solar spectral irradiance outside the earth's atmosphere in watts/cm^2/Å

Δ_λ = spectral bandwidth of optical filter

A_R = objective aperture

T_o = optical system transmission

T_A = atmospheric transmittance function

Combining Eqs. 6-5 and 6-6 and assuming that a photomultiplier is used with internal gain, G_D, the output signal voltage across the detector load resistor, R_L, is given by

$$V_S = \left(\frac{e\, T_o\, A_R\, \Delta_\lambda\, \eta_D\, G_D\, R_L\, H_\lambda}{h\nu} \right) T_A \qquad (6\text{-}7)$$

Equation 6-9 expresses the responsivity of the system; however, of additional interest is the minimum detectable signal.

The signal voltage must exceed the noise voltage of the optical receiver. For the case of the photomultiplier, assuming noiseless multiplication, the noise of the detector load consists of shot noise produced in the photodetection process and thermal noise produced by the load resistor.

The optical system signal-to-noise ratio is expressed by

$$SNR = \frac{I_S}{\sqrt{2e\, I_t\, \Delta f + 4F_k\, T\, \Delta f / G_D\, R_L}} \qquad (6\text{-}8)$$

where $I_t = I_S + I_{BG} + I_d$

I_{BG} = photocurrent produced by background sources

I_d = detector dark current

F = postdetection noise figure

k = Boltzmann's constant

T = temperature

Δf = electronic bandwidth

Assume that the optical receiver is signal shot noise limited; i.e., $I_S \gg I_d \gg I_{BG}$ and $2e\, I_S\, \Delta f \gg 4F_k\, T\, \Delta f/G_D\, R_L$.

Equation 6-8 now becomes

$$SNR = \left(\frac{I_S}{2e\, \Delta f} \right)^{1/2} = \left(\frac{T_A\, T_o\, A_R\, \Delta_\lambda\, \eta_D\, H_\lambda}{2h\nu\, \Delta f} \right)^{1/2} \qquad (6\text{-}9)$$

The minimum detectable solar flux is given by Eq. 6-9 for the case where SNR = 1. More realistically, the SNR should be greater than unity at a value which is consistent with desired system measurement accuracy. It is apparent from Eq. 6-9 that the minimum detectable signal is determined also by the spectral resolution and sampling rate requirements imposed on the measurements.

For the case just considered, where the optical receiver is signal shot noise limited, the minimum detectable signal is determined by the detector noise equivalent power, NEP, which in turn depends upon the electronic bandwidth requirements of the measurements, given by

$$P_{S_{min}} = NEP = \frac{[A_D\, \Delta f]^{1/2}}{D^*} \quad \text{(watts)} \qquad (6\text{-}10)$$

where
- A_D = detector area
- D^* = detectivity in cm-$Hz^{1/2}$-$watt^{-1}$
- $\Delta f \sim \frac{2}{t_s}$ = electronic bandwidth
- t_s = period of maximum signal frequency

When the system bandwidth requirements are large such that the condition $2e\, I_S\, \Delta f \gg 4F_k\, T\, \Delta f/G_D\, R_L$ or when $I_S \gg I_d \gg I_{DG}$ no longer hold, then the system sensitivity must be determined from Eq. 6-8. We shall not determine the limitation to system bandwidth using the first condition, i.e.,

$$e\ I_S\ \Delta f > \frac{2F_k\ T\ \Delta f}{G_D\ R_L} \tag{6-11}$$

Using Eq. 6-5, Eq. 6-11 can be rewritten

$$P_S > \frac{F_k\ T\ h\nu}{e^2\ \eta_D\ G_D\ R_L} \tag{6-12}$$

where

$$P_{S_{lim}} = NEP > \frac{F_k\ T\ h\nu}{e^2\ \eta_D\ G_D\ R_L} \tag{6-13}$$

The detector load resistance cannot be made arbitrarily large, however, since R_L must also satisfy the bandwidth condition

$$R_L < \frac{2}{\Delta f\ C_S} \tag{6-14}$$

where C_S = effective capacitance of detection system output

Combining Eqs. 6-10 and 6-13, the system electronic bandwidth must satisfy the requirements

$$\Delta f < \left(\frac{e^2\ \eta_D\ G_D\ D^*\ R_L}{F_k\ T\ h\nu\ A_D^{1/2}} \right)^2 \tag{6-15}$$

or from Eqs. 6-14 and 6-15

$$\Delta f < \left(\frac{2e^2\ \eta_D\ G_D\ D^*}{F_k\ T\ h\nu\ A_D^{1/2}\ C_S} \right)^{2/3} \tag{6-16}$$

Summarizing, the optimum selection of photodetector used for the measurements depends upon several factors, most important of which are detector responsivity, detectivity, and frequency response. From Eq. 6-7, it is seen that the signal voltage is proportional to detector quantum efficiency, η_D, multiplication factor, G_D, and load resistance, R_L. The latter is limited by bandwidth considerations as already discussed. In order to increase responsivity then it may be desirable to use a detector with internal gain, such as a photomultiplier, even though quantum efficiencies are typically lower than near-unity gain solid state detectors. Although internal gain does not enter directly into SNR expression (Eq. 6-9) for the case of signal limited operation, it is observed from Eq. 6-15 that internal and noiseless photocurrent gain assists in overcoming thermal noise limitations while broadening allowable electronic bandwidths.

The system electronic bandwidth must be sufficient such that small changes in solar flux are detected, consistent with measurement accuracies. Consider the satellite orbit depicted in Fig. 6-1. With the satellite at an altitude of 1000 km and an orbit velocity of about 100 km/sec, the minimum time of travel of the satellite between incremental altitudes $h_i - h_j = 1$ km is 10 millisecond. Now assume that 10 wavelengths are to be scanned during the travel through each incremental altitude and that the signal integration time per wavelength channel is 1 millisecond. The electronic bandwidth requirement for each observation is, consequently, about 2 kHz.

System performance can now be determined from Eq. 6-9 by making certain system parameter assumptions and by using known values of solar spectral irradiance. Consider the case of a photomultiplier tube (S-5 response) and an optical receiver with the following characteristics:

Receiver collecting area, A_R = 50 cm^2

Optical efficiency, T_o = 0.5

Optical bandwidth, Δ_λ = 10Å

Detector quantum efficiency, η_D = 0.18 (at λ = 2600Å)

Electronic bandwidth, Δf = 2000 Hz

Assume that the atmospheric transmittance through the maximum length of atmosphere is $T_A = 0.1$, which is a worst case value.

The solar flux at λ = 2600Å outside the earth's atmosphere is $N_\lambda = \frac{H_\lambda}{h\nu} = 0.97 \times 10^{12}$ photons/cm^2-sec-Å.

Using Eq. 6-9, the optical system signal to noise is calculated to be

$$SNR = \frac{(0.1)(0.5)(50)(10)(0.18)(0.97 \times 10^{12})}{(2)(2000)} \sim 3 \times 10^4$$

This SNR performance is typical for a measurement solar irradiance at the lowest system sensitivity level and is suitable for reliable and accurate measurements of ozone concentration.

So far the detectability of the detection system has been discussed without detailed mention of the factors affecting the accuracy of the measurements. These factors are now analyzed briefly.

6.6.2 MEASUREMENT ACCURACY

The method of extracting ozone concentration from the measurement data will be reviewed here in order to delineate the factors affecting the measurement accuracy.

For simplicity it will be assumed that solar intensity measurements are made at spectral wavelengths where the ozone absorption is large

$I_i(\lambda_1)$ and completely negligible $I_i(\lambda_2)$, where i corresponds to the ith altitude segment. When the satellite is normal to the sun's tangential rays and in a position where the earth's atmosphere does not intervene, then reference signal intensities are recorded, i.e., $I_o(\lambda_1)$ and $I_o(\lambda_2)$.

Two ratios are formed; namely,

$$R_{io}(\lambda_2) \equiv \frac{I_i(\lambda_2)}{I_o(\lambda_2)} = e^{-N_i(\text{air})\,\beta(\lambda_2)} \qquad (6\text{-}17)$$

where $N_i(\text{air})$ = number of air molecules per receiver viewing area for the optical path at the ith altitude

$\beta(\lambda_2)$ = molecular absorption cross section due to scattering by air molecules at λ_2

and

$$R_{io}(\lambda_1) \equiv \frac{I_i(\lambda_1)}{I_o(\lambda_1)} = e^{-[N_i(\text{air})\,\beta(\lambda_1) + N_i(O_3)\,\sigma(\lambda_1)]} \qquad (6\text{-}18)$$

where $\beta(\lambda_1)$ = molecular absorption cross section due to scattering by air molecules at λ_1

$N_i(O_3)$ = number of ozone molecules per receiver viewing area for optical path at the ith altitude

$\sigma(\lambda_1)$ = ozone absorption cross section

From Eq. 6-17,

$$N_i(\text{air}) = \frac{1}{\beta(\lambda_2)} \ln \frac{1}{R_{io}(\lambda_2)} \qquad (6\text{-}19)$$

and from Eq. 6-18,

$$N_i(O_3) = \frac{1}{\sigma(\lambda_1)}\left[\ln \frac{1}{R_{io}(\lambda_1)} - N_i(\text{air})\,\beta(\lambda_1)\right] \qquad (6\text{-}20)$$

Combining Eqs. 6-17, 6-18, and 6-19 yields the expression for total ozone content given by

$$N_i(O_3) = \frac{1}{\sigma(\lambda_1)} \left[\ln \left(\frac{I_o(\lambda_1)}{I_i(\lambda_1)} \right) - \frac{\beta(\lambda_1)}{\beta(\lambda_2)} \ln \left(\frac{I_o(\lambda_2)}{I_i(\lambda_2)} \right) \right] \quad (6\text{-}21)$$

The measurement error in the total ozone content is obtained by differentiating Eq. 6-21 as follows:

$$d\, N_i(O_3) = \frac{1}{\sigma_1} \frac{d\left(\frac{I_{o1}}{I_{i1}} \right)}{\left(\frac{I_{o1}}{I_{i1}} \right)} + \ln \left(\frac{I_{o1}}{I_{i1}} \right) \left(\frac{-d\sigma_1}{\sigma_1^2} \right) - \frac{\beta_1}{\sigma_1 \beta_2} \frac{d\left(\frac{I_{o2}}{I_{i2}} \right)}{\left(\frac{I_{o2}}{I_{i2}} \right)} -$$

$$\ln \left(\frac{I_{o2}}{I_{i2}} \right) \left[\frac{\sigma_1 \beta_2\, d\,\beta_1 - \beta_1 \sigma_1\, d\,\beta_2 - \beta_1 \beta_2\, d\,\sigma_1}{\sigma_1\, \beta_2^{\,2}} \right]$$

$$= \frac{1}{\sigma_1} \left\{ \frac{d\, I_{o1}}{I_{o1}} - \frac{d\, I_{i1}}{I_{i1}} - \ln \left(\frac{I_{o1}}{I_{i1}} \right) \frac{d\,\sigma_1}{\sigma_1} - \frac{\beta_1}{\beta_2} \frac{d\, I_{o2}}{I_{o2}} + \frac{\beta_1}{\beta_2} \frac{d\, I_{i2}}{I_{i2}} - \right.$$

$$\left. \ln \left(\frac{I_{o2}}{I_{i2}} \right) \left[\frac{d\,\beta_1}{\beta_2} - \frac{\beta_1}{\beta_2} \frac{d\,\beta_2}{\beta_2} - \frac{\beta_1}{\beta_2} \frac{d\,\sigma_1}{\sigma_1} \right] \right\} \quad (6\text{-}22)$$

The maximum error in ozone content is then

$$\Delta N_i(O_3) = \frac{1}{\sigma_1} \left\{ \frac{\Delta I_{o1}}{I_{o1}} + \frac{\Delta I_{i1}}{I_{i1}} + \frac{\beta_1}{\beta_2} \left[\frac{\Delta I_{o2}}{I_{o2}} + \frac{\Delta I_{i2}}{I_{i2}} \right] + \ln \left(\frac{I_{o1}}{I_{i1}} \right) \frac{\Delta\sigma_1}{\sigma_1} + \right.$$

$$\left. \ln \left(\frac{I_{o2}}{I_{i2}} \right) \left[\frac{\Delta\beta_1}{\beta_2} + \frac{\beta_1}{\beta_2} \frac{\Delta\beta_2}{\beta_2} + \frac{\beta_1}{\beta_2} \frac{\Delta\sigma_1}{\sigma_1} \right] \right\} \quad (6\text{-}23)$$

Errors are incurred in the ozone measurements due to uncertainties in measured intensities (including noise in signal), and in known values of absorption and scattering coefficients. It is observed that errors increase for increasing values of β_1/β_2 so that λ_2 should be larger than the largest wavelength selected to correspond with the ozone absorption lines; in this way, the effects of Rayleigh scattering are reduced for the longer wavelengths and β_1/β_2 is minimized.

Consider for the moment the case where absorption and scattering coefficients are accurately known. The maximum percent of error in the ozone measurement is, from Eqs. 6-21 and 6-23,

$$E_{max} = \frac{\Delta N_i(O_3)}{N_i(O_3)} \times 100 = \frac{\left\{\frac{\Delta I_{o1}}{I_{o1}} + \frac{\Delta I_{i1}}{I_{i1}} + \frac{\beta_1}{\beta_2}\left[\frac{\Delta I_{o2}}{I_{o2}} + \frac{\Delta I_{i2}}{I_{i2}}\right]\right\}}{\left\{\ln\left(\frac{I_{o1}}{I_{i1}}\right) - \frac{\beta_1}{\beta_2}\ln\left(\frac{I_{o2}}{I_{i2}}\right)\right\}} \times 100 \quad (6\text{-}24)$$

Errors in intensity measurements arise from three major sources:

a. Variations in sun's intensity across solar disc
b. Directly and indirectly scattered solar radiation
c. Quantum and shot noise

The sun is a relatively stable source of energy so that intensity variations due to source modulation can be neglected. On the other hand, the sun's brightness is significantly lower at the edge of the solar disc than at the center so that solar tracking errors could result in considerable variations in the solar flux being observed at the satellite. Figure 6-4 shows this limb-darkening effect; ultraviolet radiant intensity is particularly reduced at the sun's edge, where the ratio r/R is defined in Fig. 6-5.

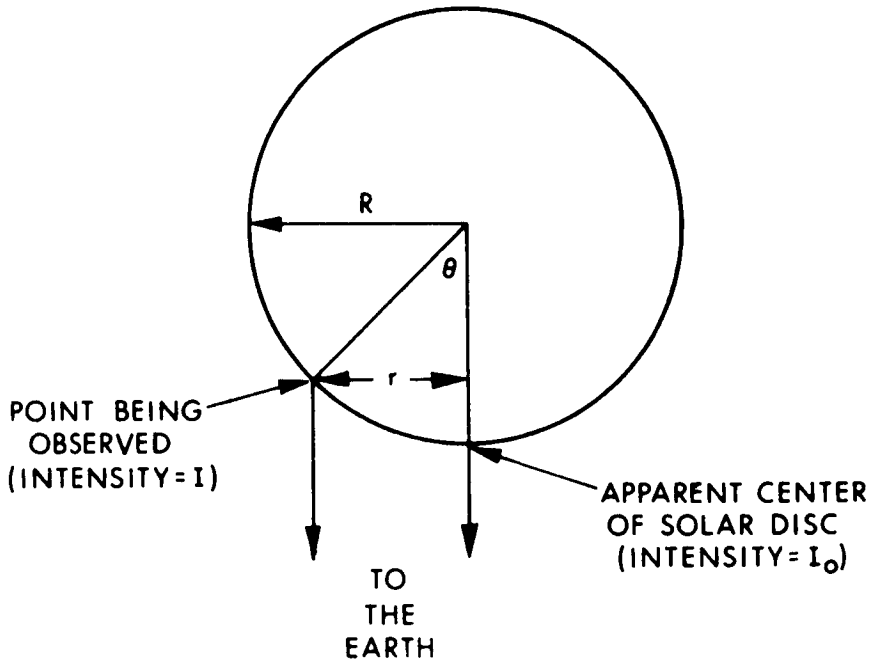

Figure 6-4. Limb Darkening Geometry

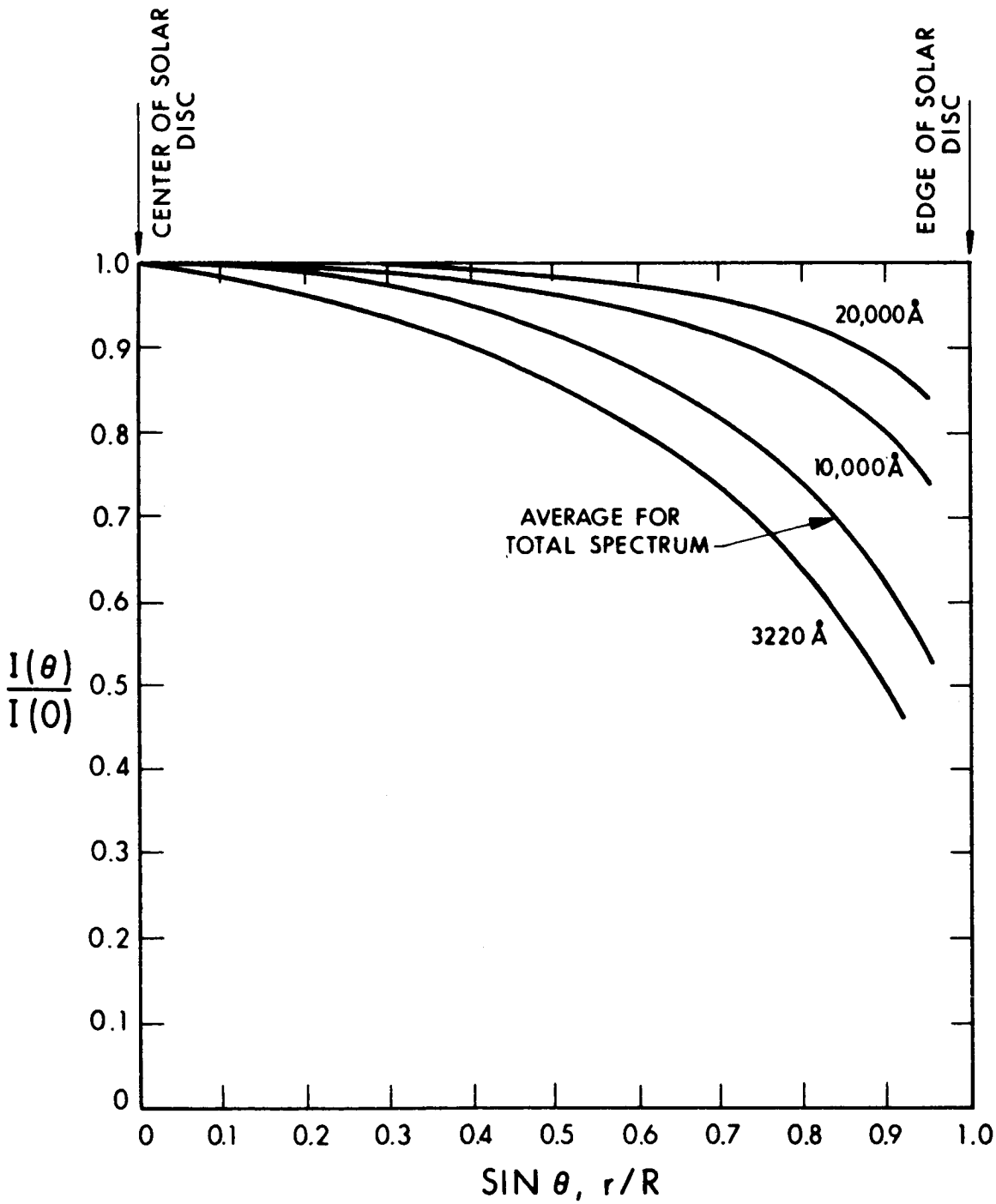

Figure 6-5. Limb Darkening Effect on Solar Disc-Intensity as a Function of Wavelength and Radial Location on Solar Disc

In order to effectively maintain constant source intensity, the sun must be accurately tracked. Furthermore, the sun must continually remain in the optical receiver's field of view during the measurement.

The field of view of the receiver is determined principally by the vertical atmospheric resolution requirements and the altitude of the satellite above the earth. As discussed in a previous report, the vertical increment observed when the satellite is at a height of 1000 km is 34 km when the full sun is observed. In order to improve this vertical resolution, one must observe only a small segment of the sun. Since ample signal-to-noise performance is achievable, then reducing the observational area of the source is practical. The resulting decrease in SNR is given by

$$SNR' = k \left(\frac{A_s}{A_T}\right) SNR \tag{6-25}$$

where

k = limb-darkening coefficient

A_s = observed solar area

A_T = total area of sun

Reducing the optical receiver field of view from about 32 minutes of arc to about one minute of arc has the additional advantage in that the effects of indirect and direct solar scattering are made negligible.

The major source of measurement error arises from quantum and shot noise, which from Eq. 6-9 is

$$\frac{\Delta I}{I} = \frac{N}{S} = \left(\frac{2e\Delta f}{I_s}\right)^{1/2} = \left(\frac{2h\nu\Delta f}{T_A T_o \, k\frac{A_s}{A_T} \, A_R \, \Delta_\lambda \, \eta_D \, H_\lambda}\right)^{1/2} \tag{6-26}$$

6.7 PRELIMINARY INSTRUMENT CONCEPTS

In this subsection, a brief description is given of a spectrometer design which appears to possess features which would allow it to make the type of measurements required in the passive technique under consideration. This instrument design and others will be examined in greater detail in later stages of this program.

The instrument proposed here for the recording of intensities of spectral bands from the ultraviolet to the visible is essentially a Czerny-Turner spectroradiometer. Because of the short time duration allowed for observation of the spectral bands and because of the general undesirability of providing for grating rotation with discrete stops in space applications, all wavelengths are observed simultaneously on a single detector and are sorted through electronic filtering as in Fourier spectroscopy. Thus, with several spectral bands to be scanned in a given time interval, simultaneous wavelength observation increases the obtainable signal-to-noise ratio as compared to sequential wavelength observation. The signal advantage of the larger entrance aperture which is found in interferometer-type spectrometers is offset by the high slits which can be used with the Czerny-Turner spectrometer. It should be emphasized, however, that the main virtue of this approach is not to be found in signal-to-noise considerations, primarily since high radiation fluxes are expected. The virtue of this approach is the mechanical ruggedness and resulting reproducibility of the system. The grating monochromator relieves the instrument of the close tolerances found in the conventional Fourier spectrometer technique of simultaneously producing periodic constructive and destructive interference in many wavelength bands by motion of a plate (change in time of the optical path length difference with constant velocity). Thus the high signal-to-noise advantages of Fourier spectroscopy, with none of its critical, geometrical tolerances, is combined with the more conventional, sturdier grating spectrometer employing a stationary grating.

Scanning would be accomplished by means of a continuously rotating reticle (see Fig. 6-6). The reticle would be segmented into a number of arcs, the number and size depending on the results of the analytical studies and on the compatibility of the instrument with satellite mounting.

Since many of the wavelengths of interest are in the general region of 3000Å and others in the region of 6000Å, the grating can be set to simultaneously image the first-order visible and the second-order ultraviolet wavelengths on the reticle. Each segment needs only modulate its respective wavelengths (alternating segments for visible and ultraviolet) and therefore needs groups of periodically interrupted opaque arcs, each arc being characteristic of the exit aperture height and the wavelength band which it must modulate. The width of these arcs in the direction of the spectral dispersion would be determined by a compromise between spectral resolution and signal requirements.

Ultraviolet and visible transmitting filters would alternately be interposed into the light path between a beam cross section which defines the external baffle and the entrance slit. The period of interposing the filters will be related to the period of the rotating reticle. Filter actuation could be through push-pull solenoids.

Loss of spectral resolution from astigmatic blur can be avoided through the use of curved slits. Strictly speaking, this curve is only a circle when one-to-one magnification collimating and camera mirrors are used and even then only for the central image. For resolution of the degree required for determining spectral intensities in the present application a circular entrance slit would probably be adequate. This feature nicely complements the circular arcs of the periodically interrupted opaque arcs appearing on the reticle.

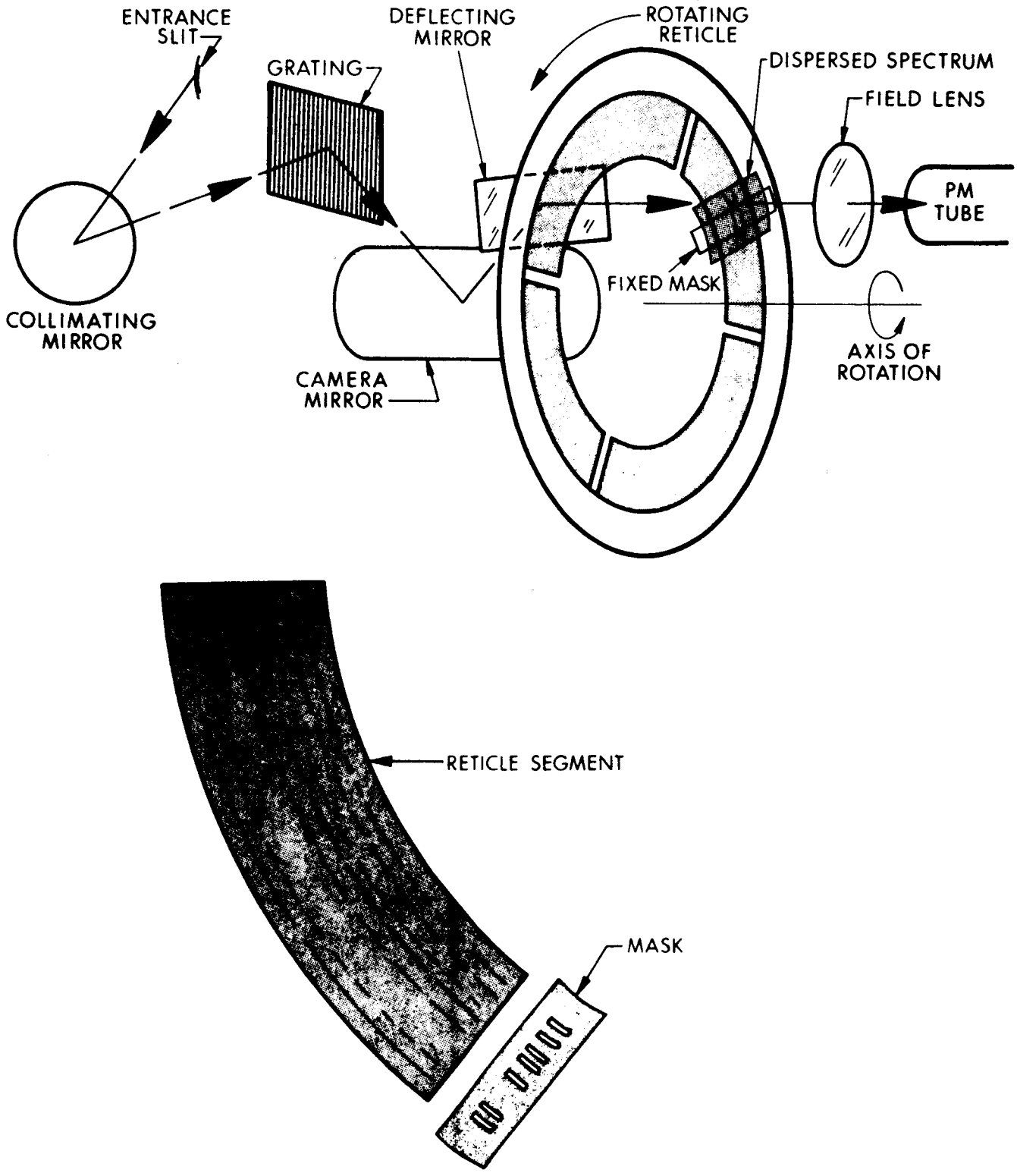

Figure 6-6. Conceptual Design of Spectrometer and Reticle for Measuring Attenuated Solar Radiation at Several Wavelengths

Demagnification in the spectral focusing mirror can be used to reduce the residual coma which is characteristic of the Czerny-Turner mount and would also decrease the required diameter of the reticle disc. A spherical lens, possibly a spherical aberration minimizing doublet, would be used to focus the spectral focusing mirror onto the photocathode. In converting a relatively highly convergent beam from the spectral focusing mirror into an even more highly convergent beam at the photocathode, spherical aberration can result in a significant radiant power loss. The plane deflecting mirror would be mounted on flexural pivots so as to allow slight rotation for wavelength and modulation frequency calibration after launch.

The design concepts discussed here, while admittedly being preliminary in nature, show that measurements of the type required in the differential attenuation technique are entirely feasible from the point of view of spectroscopic instrumentation.

SECTION 7

RAMAN LASERS AS ACTIVE OZONE PROBES

In the long history of ozone measurements by optical techniques, few attempts to use active probes have been made. The various schemes which have been developed or proposed in the past depend mainly on either direct, indirect, reflected, or scattered solar radiation. However, the use of active probes as practical, accurate, and reliable ozone measuring devices has recently become feasible with the advent of the laser. This device emits radiation which is coherent, highly directional, monochromatic, and very intense. This combination of properties warrants serious consideration of the laser for measurements of atmospheric properties. The backscattering of laser radiation has, in fact, recently been used as a means of probing the atmosphere. However, the monochromaticity of laser radiation has proved to be a limitation on the type of information that can be derived from backscattering data.

Since very few materials are capable of emitting pulsed, high-power laser radiation, few wavelengths of intense laser radiation would be available were it not for the phenomenon known as stimulated Raman scattering (this phenomenon will be referred to as SRS and the resulting radiation as Raman laser radiation.) This effect can be exploited to generate intense laser-like radiation at a wide variety of wavelengths and, therefore, to greatly extend the potential usefulness of lasers for atmospheric probes. A brief review of the physics involved in SRS is presented in the following subsection.

Following this, an outline of various methods in which Raman laser radiation could be used to measure the atmospheric ozone content is presented. Subsection 7.3 deals with details of experimental measurements which have been performed for the express purpose of producing wavelengths of Raman laser radiation which coincide with those in the ozone absorption bands. Calculations which show the feasibility of an active probe technique involving ground-based Raman lasers and satellite-based detectors are presented in Subsection 7.4.

7.1 STIMULATED RAMAN SCATTERING AND RAMAN LASERS

The inelastic scattering of photons by molecules is known as Raman scattering. As a result of the act of scattering, an incident photon of energy $h\nu$ is transformed into a scattered photon of energy $h\nu'$. The energy difference, $h|\nu-\nu'|$, represents the separation between a pair of electronic, vibrational, or rotational levels of the scattering molecule. The most commonly encountered forms of Raman scattering involve the latter two types of molecular energy levels. The normal or spontaneous Raman spectrum of a molecule, i.e., that excited by an incoherent source of radiation, generally consists of many spectral lines, each of which is separated from the exciting frequency by the frequency of a vibrational or rotational transition. The number of lines in the normal Raman spectrum depends on the number of atoms in the molecule and on the symmetry of the latter. Figure 7-1 shows the normal vibrational spectra of H_2 and D_2, and Fig. 7-2 shows the normal rotational spectrum of hydrogen.

When giant-pulsed, high intensity laser radiation is used to produce Raman scattering, instead of incoherent radiation from conventional sources, the dominant scattering process may be induced, or stimulated, Raman scattering (SRS). The occurrence of SRS depends

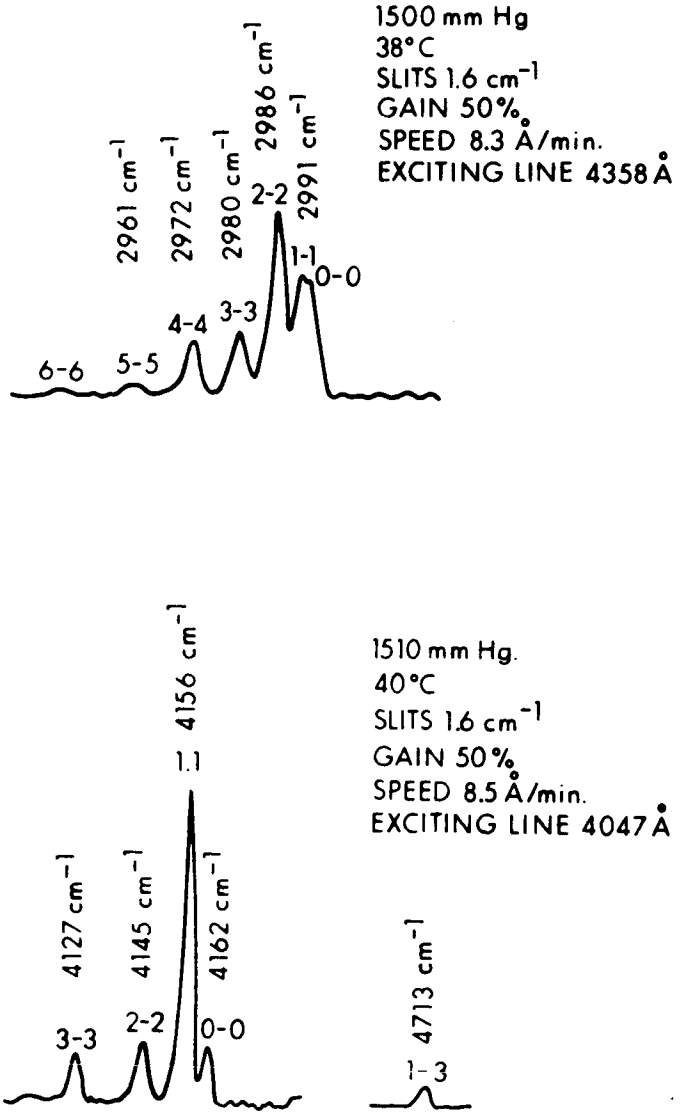

Figure 7-1. The Normal Raman Vibrational Spectra of D_2 and H_2

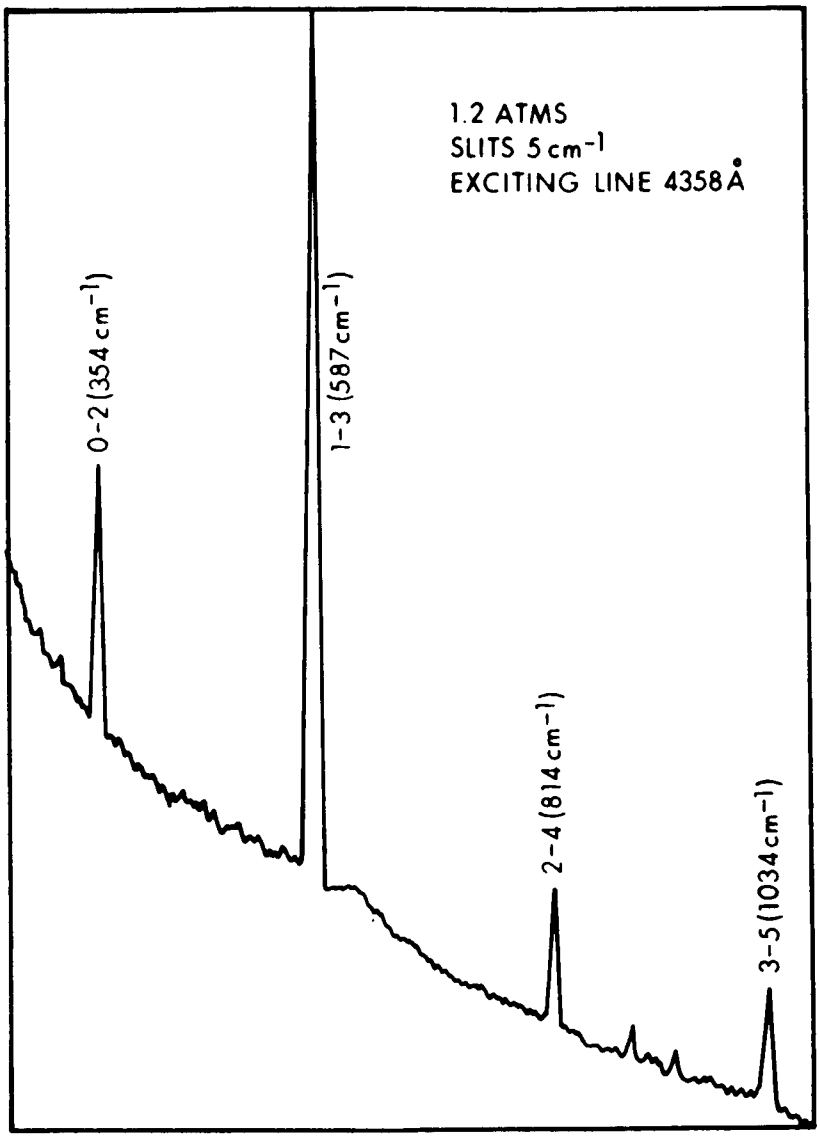

INTENSITY RATIOS OF HYDROGEN ROTATIONAL RAMAN LINES

		OBSERVED	THEORETICAL
ORTHO HYDROGEN	$\frac{3 \rightarrow 5\ (1035\ cm^{-1})}{1 \rightarrow 3\ (588\ cm^{-1})}$	0.112	0.112
PARA HYDROGEN	$\frac{2 \rightarrow 4\ (814\ cm^{-1})}{0 \rightarrow 2\ (355\ cm^{-1})}$	0.438	0.458

Figure 7-2. The Pure Rotational Normal Raman Spectrum of H_2

on the presence of a high density of both incident and Raman-scattered photons and thus had not been observed prior to the development of the laser. Several important differences are observed in the normal and stimulated Raman spectra of any given substance:

a. Only one or two molecular transitions usually participate in SRS. For example, in the SRS spectrum of hydrogen as produced by ruby laser excitation only the Q(1) transition at 4156 cm^{-1} (see Fig. 7-1) appears. This can be seen in Fig. 7-3 which shows the anti-Stokes SRS spectrum of H_2.

b. The efficiency of the Raman process dramatically increases when the transition from normal to stimulated scattering occurs. As much as 50% of the incident radiation may be transformed into Raman shifted wavelengths in SRS, whereas the normal scattering converts only a small fraction of a percent of the incident radiation.

c. In addition to frequency shifts given by $\Delta\nu = |\nu-\nu'|$, where $\Delta\nu$ is the frequency of the molecular transition excited in SRS, the scattered radiation contains components at the frequencies $\nu_L \pm n\Delta\nu$, where ν_L is the frequency of the incident laser and $n = 0, 1, 2, \cdots$. Thus, the emission line at 4400Å which is seen in Fig. 7-3 corresponds to $\nu_L + 2\Delta\nu$ and is referred to as the second anti-Stokes line of H_2 in SRS.

d. The SRS radiation is highly directional, many components having essentially the same angular divergence as that of the initial laser radiation. This is a consequence of the fact that SRS involves the induced emission of radiation by molecules.

The shifts, $\Delta\nu$, most commonly produced in SRS correspond to molecular vibrational frequencies and so their magnitudes vary, depending on

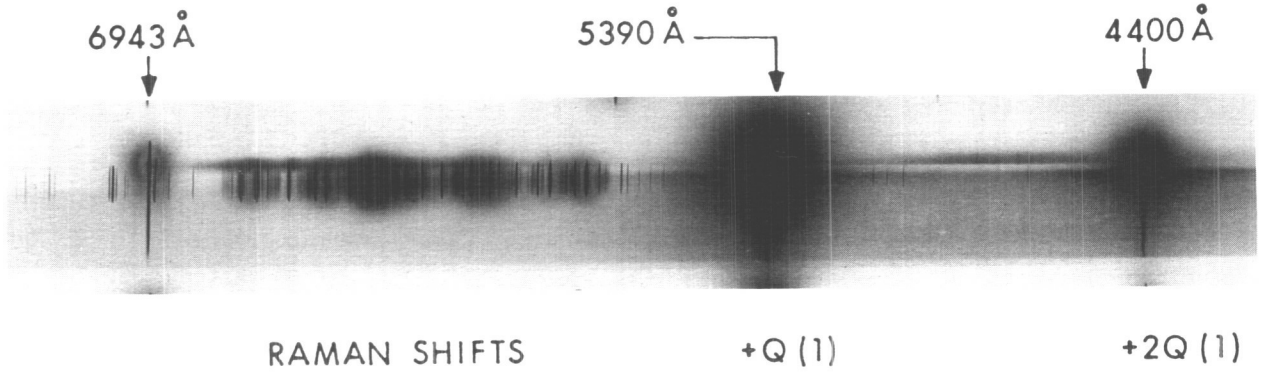

Figure 7-3. Anti-Stokes Spectrum of H_2

the chemical substances that are used as the scattering medium. Fairly complete lists of materials which can be used in SRS, and the shifts that they produce, have been recently published.[176] Thus, a choice from over 100 materials can be made to find one which is capable of providing Raman laser radiation at any wavelength desired for a particular application. From the point of view of ozone probes, the most useful Raman laser will be one which emits wavelengths which lie both within and outside of the absorption bands of ozone. This wavelength requirement also helps to identify the type of laser radiation that should be used as the excitation source for the SRS wavelengths, as will be discussed in the following subsection.

7.2 EXCITATION SOURCES FOR STIMULATED RAMAN SCATTERING

The phenomenon of SRS has been observed to occur only when high-intensity, giant-pulsed laser radiation is used. Thus, relatively low intensity, gas laser radiation can be excluded from consideration in any scheme involving Raman laser probes. The excitation wavelengths which have successfully been used for the production of Raman laser radiation are the primary emission wavelengths of the ruby and neodymium lasers, 6943Å and 10,580Å, respectively, and their so-called second harmonic wavelengths, 3472Å and 5290Å. The latter two wavelengths are produced by passing the primary laser radiation through a crystal which has nonlinear optical properties. The second harmonic (or frequency-doubled) radiation which emerges from the crystal is usually only of the order of a few percent as intense as that of the primary laser, although with internal modulation techniques it is possible to greatly enhance the conversion efficiency.[177] In any case, SRS is not as readily achieved with the second harmonic radiation as it is with the primary laser radiation, mainly because of the lower intensity available at the doubled frequency. Furthermore, complicating effects of two-photon

absorption can also inhibit SRS of laser radiation when the shorter wavelength excitation sources are used[178].

One of the significant findings of the experiments performed during the reporting period is that a "pseudo-SRS" spectrum of the second harmonic radiation can be readily produced, as is described in the appendix. That is, even though the mechanism which produces the spectrum is not truly SRS, coherent radiation is produced at wavelengths that would have been produced by the latter mechanism. If details of the mechanism are not considered, it can be said that the relatively low intensity and the two-photon absorption process are factors which can easily be overcome in the production of Raman laser wavelengths with the second harmonic of giant-pulsed laser radiation. This is explained more fully in the Appendix.

From a consideration of the ozone absorption bands, it is clear that a ruby laser is more suitable than a neodymium laser. The proximity of the Chappuis bands to 6943Å and of the Hartley-Huggins bands to 3472Å ensures that Raman laser radiation generated by these two wavelengths will be within the ozone absorption bands.

7.3 CHOICE OF RAMAN SCATTERING MEDIUM

For the present application, gases were considered to be the ideal scattering media for a number of reasons: (1) The largest frequency shifts in SRS are produced by gases, e.g., H_2 (4155 cm^{-1}) and CH_4 (2915 cm^{-1}). This proves to be important in Raman-shifting laser radiation from 3472Å down to the vicinity of 3000Å. (2) The efficiency of conversion into Raman shifted wavelengths is generally greater when gases are used, as compared to liquids and solids. For example, the first Stokes line of both methane and hydrogen is approximately 20% as intense as the incident laser radiation. When

liquid samples are used, typical conversion efficiencies are between 1% and 5%. (3) The fact that gases are essentially dispersionless allows most Raman frequency components to emerge from the scattering cell with essentially the same angular divergence as the excitation laser radiation. When liquid samples are used, the various anti-Stokes components emerge from the scattering cell with different angular divergences, as the result of certain momentum-matching requirements in the liquid.

The ideal Raman laser probe would appear to be one which produced stimulated Raman frequencies centered about both the 6943Å and 3472Å laser components. The former would be used in conjunction with the visible Chappuis bands and the latter with the ultraviolet Hartley-Huggins bands. The simultaneous production of SRS in gases with two different excitation wavelengths has not been previously reported. The successful generation of Raman laser radiation with 6943Å and 3472Å, as reported in the Appendix, therefore represents a new scientific accomplishment. Because of the results obtained, it can be stated that intense coherent radiation can be produced at the wavelengths listed in Table 7-1.

Any combination of these wavelengths could be used in the active Raman laser probe technique, as will be described in more detail in subsequent reports. Some wavelengths lie within the Chappuis absorption bands, others within the Hartley-Huggins bands, and others in wavelength regions which are free from ozone absorption. All of these wavelengths will be of value in atmospheric ozone measurements. It is also possible to simultaneously generate two sets of wavelengths, using a mixture of two gases, and several wavelengths which are intermediate between those produced by the individual gases[179]. However, unless later analysis proves this to be advantageous, only single component gas scattering media will be considered for use in the active probe technique.

TABLE 7-1

RAMAN LASER WAVELENGTHS AS PRODUCED BY RUBY LASER EXCITATION (6943Å) AND ITS SECOND HARMONIC (3472Å)

Gas Medium		6943Å SRS Wavelengths	3472Å SRS Wavelengths
Hydrogen	S_2	- - -	4879Å
	S_1	9760Å	4057Å
	AS_1	5390Å	3033Å
	AS_2	4400Å	2694Å
Methane	S_2	- - -	4352Å
	S_1	8706Å	3862Å
	AS_1	5774Å	3152Å
	AS_2	4940Å	2887Å
Deuterium	S_2	- - -	4382Å
	S_1	8766Å	3874Å
	AS_1	5748Å	3144Å
	AS_2	4904Å	2874Å

The procedure used and the results obtained in the Raman laser experiments are described in the appendix. The results have also been analyzed in an attempt to identify the nature of the interaction which produces the Raman laser frequencies. On the basis of the results obtained, the analysis presented in the appendix appears to be the correct one. However, one critical measurement which would unambigiously distinguish between the two possible mechanisms, SRS or the mechanism referred to as pseudo-SRS in the Appendix, has yet to be performed. The experiment involves a measurement of the relative intensities of the Stokes and anti-Stokes components of the scattered radiation. According to the interpretation given in the appendix, which is based on an analysis by Giordmaine[180], the Stokes and anti-Stokes components should be of approximately equal intensity. On the other hand, when the lines are produced by SRS, the Stokes intensity is an order of magnitude greater than the anti-Stokes intensity. Preliminary attempts to measure the relative intensities proved to be unsatisfactory. Since the efficiency of the Raman laser probe technique depends on the intensities of the Raman-shifted components, the experiments will be repeated.

The availability of high-intensity, directional Raman laser radiation at wavelengths which are pertinent to the ozone optical absorption bands opens several possibilities regarding worldwide ozone monitoring by optical means. Experimental configurations in which Raman lasers could be employed include those in which the laser is flown in a satellite and detectors placed in another satellite or at ground stations. The attenuation of the different wavelength components would serve as a measure of the ozone content between the laser emitter and the detectors. The backscattering of Raman laser radiation by the atmosphere could also be examined by placing detectors aboard the same satellite as the Raman laser. However,

the simplest and probably the most reliable use of Raman lasers for atmospheric ozone measuring appears to be one in which Raman laser radiation is transmitted from ground stations to an orbiting satellite aboard which several photomultiplier tube detectors are placed. Figure 7-4 illustrates the geometry involved.

Calculations designed to show that the Raman intensities are readily detectable are presented in the following subsection, where the specific examples of 3472Å and 3034Å are used. For these calculations, intensities of the emitted radiation were used which are typical of those measured in the experiments described in the appendix. In subsequent reports the limits of accuracy of this proposed technique will be established and a survey of recent developments in Raman laser technology will be given to show that the intensities can be considerably enhanced.

7.4 ACTIVE PROBE SIGNAL INTENSITY

This subsection describes the calculation of the number of signal photons received when an actual system employing a Raman-shifted frequency-doubled ground-based laser is used as described in the preceding subsection. The geometry associated with such a system is shown in Fig. 7-4. The area A subtended by the laser beam of divergence and at a slant range R is given as

$$A = \frac{\alpha R^2 \pi}{4} \tag{7-1}$$

As a result, the incident signal power P_I on a detector of area a in a system employing a laser of power P_R is given as

$$P_I = \frac{P_R 4at}{\alpha R^2 \pi} \tag{7-2}$$

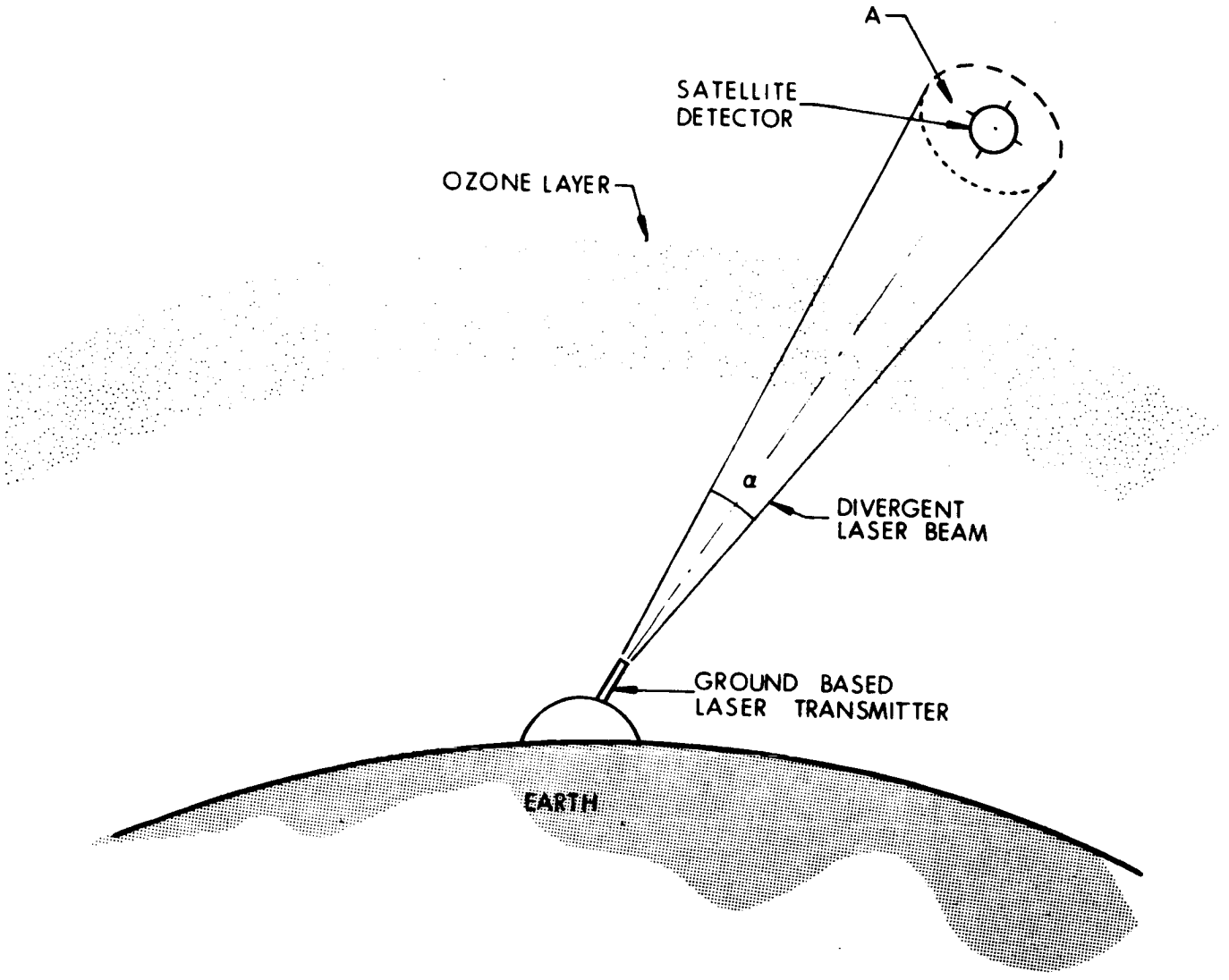

Figure 7-4. Geometry of Ground-Based Laser with Orbiting Detector

where t is the atmospheric transmission at the wavelength of the laser radiation, and a is the detector aperture.

Figure 7-5 shows slant ranges as a function of zenith angle for a 1000km orbit. The atmospheric transmission for light at several laser wavelengths of interest were determined by considering clear air atmospheric scattering and ozone absorption as a function of zenith angle.

The actual detected signal power P_D is given by

$$P_D = P_I \, Eq \tag{7-3}$$

where E is the optical efficiency of the detector system and q is the quantum efficiency of the phosphor.

Calculations were performed to determine the number of detected photons for a system in which

$a = 6$ in.^{2}
$E = 0.9$
$q = 0.12$ at 3472Å
$P_R = 0.5$ megawatt at 3472Å

The results of this calculation are shown in Table 7-2.

Similar calculations were performed for a system radiating at 3034Å and using vertical ozone contents which differed by a factor of three. The results of the calculations are summarized in Fig. 7-6.

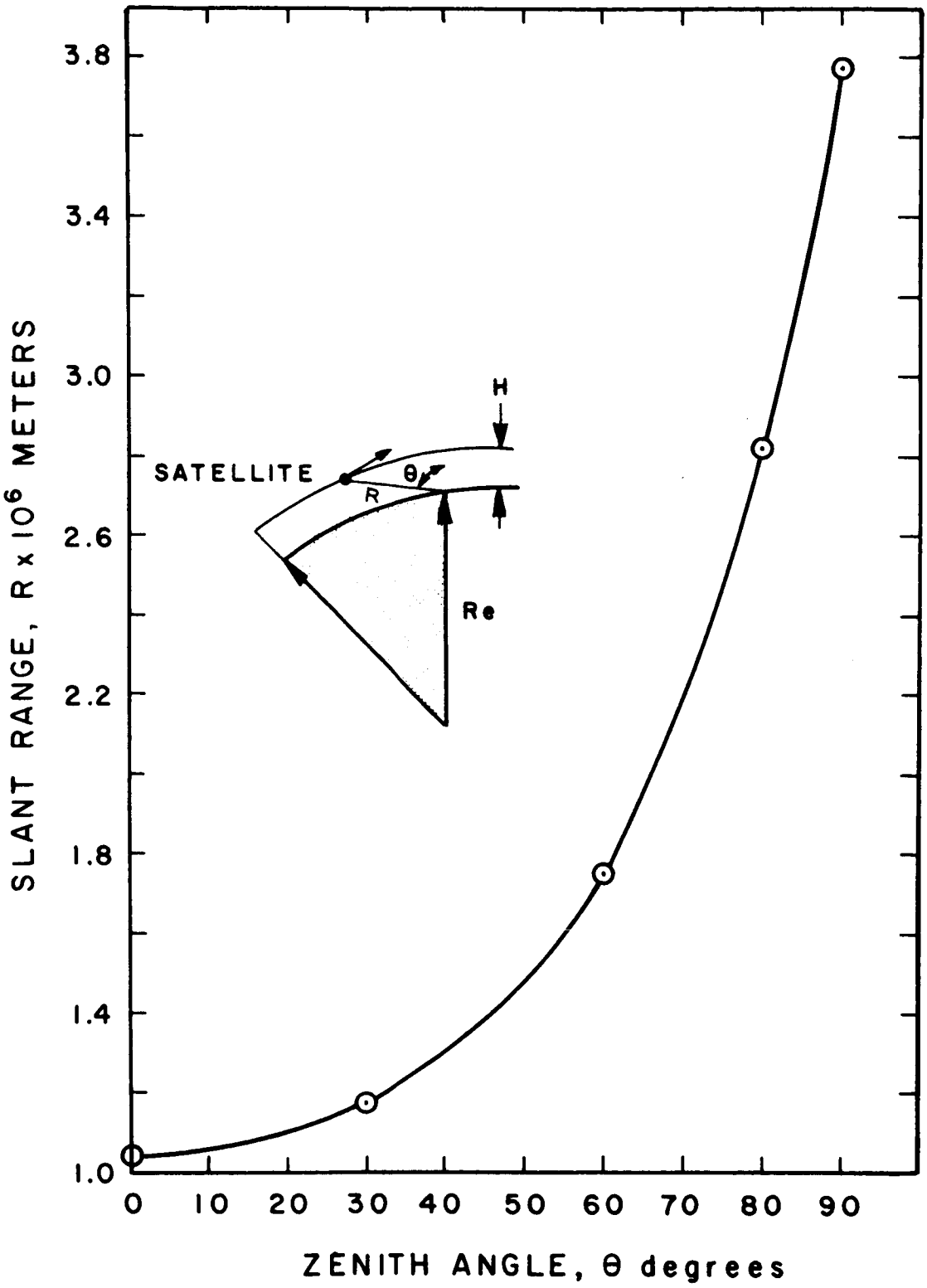

Figure 7-5. Slant Range versus Zenith Angle for 1000 km Orbit

TABLE 7-2

SIGNAL INTENSITY FOR VARYING ZENITH ANGLE

θ = Zenith Angle	Range	Signal Photoelectrons/ Pulse At 3472Å
0°	1×10^6 m	2.24×10^9
10°	1.04×10^6 m	2.07×10^9
20°	1.10×10^6 m	1.86×10^9
30°	1.18×10^6 m	1.44×10^9
40°	1.30×10^6 m	1.06×10^9
50°	1.46×10^6 m	0.74×10^9
60°	1.74×10^6 m	0.45×10^9
70°	2.14×10^6 m	0.25×10^9
80°	2.80×10^6 m	0.03×10^9
90°	--	--

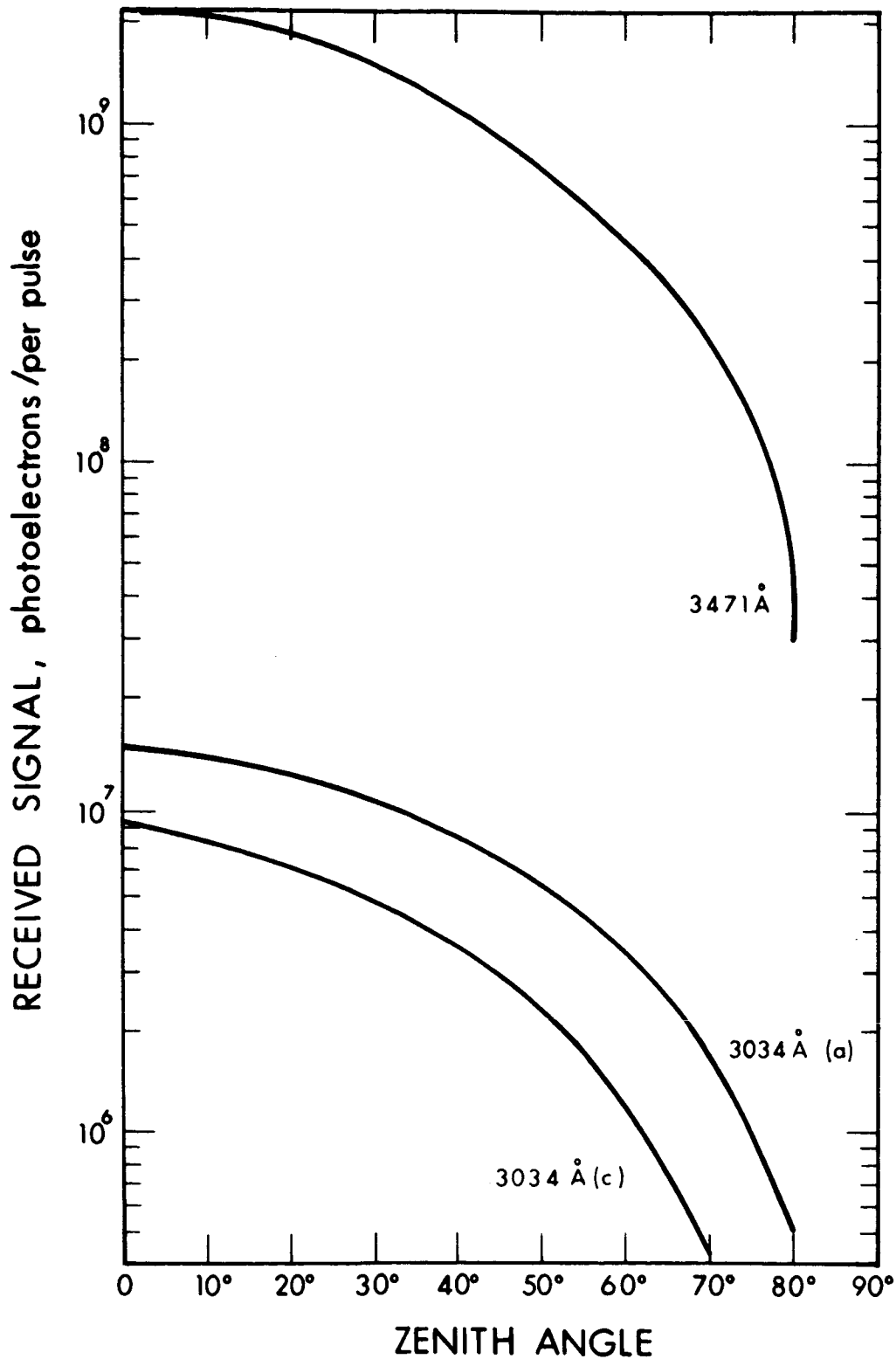

Figure 7-6. Received Signal versus Zenith Angle

The calculations were performed for the purpose of demonstrating the detectability of the Raman laser radiation as transmitted to a satellite through various atmospheric slant paths. The results show that the received signal is well above the noise level of the detector system, including background radiation. Similar calculations for the other wavelengths shown in Table 7-1 will be performed during the next year, and the limits of the accuracy with which the atmospheric ozone can be measured will be established. For the present, it should be pointed out that the technique under evaluation would be especially valuable for determining variations in the horizontal distribution of ozone. If used in conjunction with a technique which measures the vertical distribution with high accuracy, the distribution of atmospheric ozone over large geographical areas could be well mapped from a single satellite.

SECTION 8

CONCLUSIONS

The work performed during the period covered by this interim report consisted in large part of a compilation and examination of the vast amount of literature that has been published on the spectroscopy of ozone, the measurement of its atmospheric concentrations by optical means, its role in atmospheric dynamics, and its potential use as a tracer for atmospheric winds. Guided by the information derived from this literature, two ozone measuring techniques have been selected as the most promising, from among the various optical techniques, for use in conjunction with an orbiting satellite. These are: (1) the passive technique which utilizes solar radiation, as described in Section 6, and (2) the active probe method utilizing Raman laser radiation, as described in Section 7. The former offers great advantages in terms of determining vertical ozone distributions on a worldwide basis and the latter technique appears to be especially promising for measuring the total ozone content. The analyses performed, some of which were based on laboratory measurements, confirmed the practicality and reliability of the selected methods.

On the basis of well developed theories, which suffer only from a lack of supporting observational data for practical implementation, the monitoring of ozone distributions promises to be a unique and invaluable means of defining and predicting atmospheric circulations and other meteorological behavior.

The approach most likely to yield significant information on the motion of ozone on a global scale is to map the vertical ozone distribution, or ozone profile, at numerous geographical locations and to continuously monitor this information as the satellite orbits around the earth.

8.1 ADVANTAGES OFFERED BY OPTICAL MEASURING TECHNIQUES

During the course of program effort, and as detailed in this report, a number of distinct advantages of using radiation in the optical regime for ozone atmospheric measurements became apparent. These are listed in the following subsections.

8.1.1 ACCURACY OF OZONE ABSORPTION COEFFICIENTS

Ozone molecule exhibits broad absorption bands in the infrared, visible and near UV, whose coefficients have been carefully measured by many workers. The measurements have been independently repeated, compared and refined. They have been critically evaluated in connection with meteorological applications. There exists a general agreement as to the most reliable set of values, and the coefficients are now considered to be known to a high degree of precision.

8.1.2 RANGE OF VALUES OF OPTICAL ABSORPTION COEFFICIENTS

Large differences exist in the absolute magnitudes of ozone cross-sections at visible and UV wavelengths ($\sigma \sim 10^{-21}$ cm^2 at 4800Å, $\sigma \sim 10^{-17}$ cm^2 at 2600Å.) This means, in effect, that variations of over four orders of magnitude in the total ozone content in an optical path can be measured by absorption measurements. This range also insures that:

a. Ozone concentrations at altitudes as high as 75-80 km can be measured from a satellite by using the larger cross-section values.

b. Solar radiation which traverses the layer of maximum ozone concentration will emerge with an attenuation that can accurately be measured by using the smaller cross-section values.

8.1.3 METEOROLOGICAL APPLICATION OF OZONE ABSORPTION SPECTROSCOPY

Optical techniques have been used to measure atmospheric ozone content for over 45 years. All of the information we now possess concerning atmospheric ozone was first obtained by optical means (total ozone content, its vertical distribution, variations in these latter two quantities, and, in fact, the very existence and the approximate height of the ozone layer were first determined through optical spectroscopic measurements.) The history of ozone spectroscopy and measurements of its atmospheric content are, in fact, inseparable. The physics and optical principles involved in optical ozone measurements have been well developed and analyzed, corrections have been introduced, and the principles are thus well understood. Measurements from a satellite would not involve any radical or revolutionary concepts, but rather an adaptation or modification of some well-established technique. Satellite measurements do, however, offer the promise of greater accuracy and precision in ozone measurements by optical methods, as well as global coverage on a continuous basis.

8.1.4 SOLAR RADIATION AS A SOURCE FOR ABSORPTION MEASUREMENTS

The solar emission spectrum possesses a broad maximum in the visible and near UV and IR spectral region and thus constitutes a very strong source of radiation which can be used in atmospheric ozone absorption measurements. The solar radiation is so intense that

narrow wavelength intervals can be taken, high spatial resolution optics can be incorporated into the optical system, and yet very large signal-to-noise ratios will be obtained by photomultiplier tube detectors.

8.1.5 LASERS AS SOURCES FOR ABSORPTION MEASUREMENTS

Since discrete wavelengths of radiation are generally used to measure atmospheric ozone (even when the sun is used as a source) recently developed sources of intense, collimated, monochromatic radiation (Raman lasers) can be employed as sources for absorption measurements. Significant progress has recently been made at EOS in the understanding of the physics involved in the production of visible and near UV Raman laser radiation. (See Appendix and references cited therein.) The availability of intense radiation at desired wavelengths for ozone determination opens new possibilities with respect to the relative positioning of the emission source and the detectors used for measuring the radiation which is attenuated by the atmospheric ozone.

8.2 PROJECTION OF PROGRAM CONTINUATION

In order to be able to exploit optical techniques to the limit of their capability, the analyses described herein will be continued and refined during the second-year effort of this study and preliminary design program. In particular, the accuracy and rate at which measurements can be taken from a satellite will be clearly established by performing an instrument design study, including instrument-satellite interface considerations. The spectroscopic and physical principles involved will also be examined in greater detail in order to fully define the accuracy limits of each technique, and the type of information that can be derived from each technique. Further

considerations will be given to the problem of defining the optimum orbits and ground station locations that would lead to a mapping of the atmospheric ozone-air mass circulation. Laboratory measurements of Raman laser wavelengths and intensities will be continued if such measurements appear to be desirable. Finally, the interrelationships between atmospheric ozone and meteorological parameters will be thoroughly investigated in order to clearly document the value of monitoring the worldwide distributions of ozone. Foremost among these interrelationships will be the manner in which the atmospheric circulation and the ozone distributions react with one another.

SECTION 9

BIBLIOGRAPHY AND REFERENCES

This section contains a compilation of references to literature articles which pertain to the topics discussed in this report. The references are grouped into categories depending upon whether the main emphasis is on ozone photochemistry, meteorological significance, spectroscopy, etc. However, the classification of the articles under one heading is somewhat arbitrary, since most of the articles deal with more than one of the above topics. It is to be noted that not all literature references appearing in this bibliography have been cited in the text of this report. For convenience, references which have been cited are collected in Subsection 9.6, "Cited References."

9.1 Atmospheric Ozone Photochemistry

1. S. Chapman, "On Ozone and Atomic Oxygen in the Upper Atmosphere," Phil. Mag. 10, 369-383 (1930).

2. S. Chapman, "A Theory of Upper Atmospheric Ozone," Mem. R. Met. Sox. 3, 103-125 (1930).

3. O. R. Wulf and L. S. Deming, Terr. Mag. 41, 299, 375 (1936); 42, 195 (1937).

4. E. Regener, Meteor. Z., 35, 788 (1943).

5. H. U. Dütsch, "Photochemische Theorie des Atmosphärischem Ozons' unter Berücksichtigung von Nichtgleichgewichts - Zuständen and Luftbewegungen," Ph.D. Dissertation, Zurich (1946).

6. D. R. Bates and M. Nicolet, "The Photochemistry of Atmospheric Water Vapor," J. Geophys. Res. 55, 301-327 (1950).

7. R. A. Craig, "The Observations and Photochemistry of Atmospheric Ozone and their Meteorological Significance," A.M.S. Met. Monographs, Vol. 1, No. 2, pp. 50 (1950).

8. Bowen and Regener, J. Geophys. Res. 56 (1951).

9. H. K. Paetzold, Geophys. p.e. Appl. 24, 1 (1953).

10. H. K. Paetzold, Geophys. p.e. Appl. 24, 15 (1953).

11. H. K. Paetzold, J. Atm. Terr. Phys. 3, 131 (1953).

12. H. K. Paetzold, Mitt. Astron. Ges., p. 19 (1953).

13. M. Nicolet, in The Earth as a Planet, Ed. G. P. Kuiper, Univ. of Chicago Press, Chicago, p. 666 (1954)

14. H. K. Paetzold, "New Experimental and Theoretical Investigations on the Atmospheric Ozone Layer," J. Atm. Terr. Phys. 1, 128-140 (1955).

15. F. N. Frenkiel, J. Chem. Phys. 23, 2440 (1955).

16. R. R. Reeves, G. Mannella, and P. Harteck, "Rate of Recombination of Oxygen Atoms," J. Chem. Phys. 32, 632-633 (1960).

17. H. U. Dütsch, "Current Problems of the Photochemical Theory of Atmospheric Ozone," Chemical Reactions in the Lower and Upper Atmosphere (proceedings of an international symposium at Stanford Research Institute), New York, Interscience Pub., 167-180 (1961).

18. H. K. Paetzold, "Photochemistry of the Atmospheric Ozone Layer," in Chemical Reactions in the Lower and Upper Atmosphere (proceedings of an international symposium at Stanford Research Institute), New York, Interscience Pub., 181-195 (1961).

19. F. S. Johnson, "Atmospheric Chemistry and Composition," Upper Atmosphere and Space Physics Seminar, Southwest Center for Advanced Studies, Dallas, Texas, 1-10 (1962).

20. J. E. Blamont and T. M. Donahue, J. Geophys. Res. 69, 4093 (1964).

21. C. Leovy, "Radiative Equilibrium of the Mesosphere," J. Atm. Sci. 21, 238 (1964).

22. J. Hampson, "Chemical Instability of the Atmosphere," Atmospheric Radiation Symposium, Leningrad (1964)

23. R. A. Craig, The Upper Atmosphere, Meteorology and Physics, International Geophysics Series, Vol. 8, Academic Press, New York and London (1965).

24. B. G. Hunt, "A Nonequilibrium Investigation Into the Diurnal Photochemical Atomic Oxygen and Ozone Variations in the Mesophere," J. Atmos. Terr. Phys. 21, 133-144 (1965).

25. R. Lindzen and R. Goody, "Radiative and Photochemical Processes in Mesopheric Dynamics. Part I, Models for Radiative and Photochemical Processes," J. Atm. Sci. 22, 341 (1965).

26. P. L. Roney, "On the Influence of Water Vapour on the Distribution of Stratospheric Ozone," J. Atmos. Terr. Phys. 27, 1177-1190 (1965).

27. S. W. Benson and A. E. Axworthy, "Reconsideration of the Rate Constants from the Thermal Decomposition of Ozone," J. Chem. Phys. 42, 2614-2615 (1965).

28. V. S. Whitehead, M. D. Miller, and W. J. Saucier, "A Consideration of Some of the Factors Affecting Atmospheric Composition, Static Stability and Motion between 20 km and 100 km," Final Report, Contract AF 19(628)-4767 (1966).

29. B. G. Hunt, "Photochemistry of Ozone in a Moist Atmosphere," J. Geophys. Res. 71, 1385 (1966).

30. B. G. Hunt, "The Need for a Modified Photochemical Theory of the Ozonosphere," J. Atmospher. Sci., 23 (1966).

9.2 Ozone Distributions and Atmospheric Circulations

31. W. L. Godson, "Total Ozone and the Middle Stratosphere over Arctic and Sub-Arctic Areas in Winter and Spring," Quart. J. Roy, Meteor. Soc., 86, 301-317 (1960).

32. J. P. Funk and G. L. Garnham, "Australian Ozone Observations and a Suggested 24 Month Cycle," Tellus 14, 378-382 (1962).

33. R. N. Kulkarni, "Comparison of Ozone Variations and of its Distribution with Height over Middle Latitudes of the Two Hemispheres," Quart. J. Roy, Meteor. Soc., 88, 522-534 (1962).

34. J. London, "The Distribution of Total Ozone over the Northern Hemisphere," Sun at Work 7, No. 2, 11-12 (1962).

35. J. London, "The Distribution of Total Ozone in the Northern Hemisphere," Beitr. Phys. Atmos., 36, 254-263 (1963).

36. R. N. Kulkarni, P. D. Angreji, and K. R. Ramanathan, "Comparison of Ozone Amounts measured at Delhi (28½°N), Srinagar (34°N), and Tateno (36°N) in 1957-1958," Pap. Meteor. Geoph., Meteor. Res. Inst., Japan 10, 85-92 (1959).

37. G. Perl and H. Dütsch, "Die 30-Jährige Arosa Ozonmessreihe, " Ann. Schweiz. Meteor. Zentralamstalt, 1958, 8 (1959).

38. R. A. Craig, The Upper Atmosphere, Meteorology and Physics, Ch. 5 (Academic Press, 1965).

39. C. L. Mateer and W. L. Godson, "The Vertical Distribution of Atmospheric Ozone over Canadian Stations from Umkehr Observations," Quart. J. Roy. Meteor. Soc. 86, 512-518 (1960

40. H. U. Dütsch, "Mittelwerte and Wetterhafte Schwankungen des Atmospharischen Ozongehaltes in Verschiedenen Höhen über Arosa," Archiv. Meteor., Geoph., Biokl, A13, 167-185 (1962).

41. F.W.P. Götz, A. R. Meetham, and G.M.B. Dobson, "The Vertical Distribution of Ozone in the Atmosphere," Proc. Roy. Soc. A145, 416-446 (1934).

42. R. V. Karandikar and K. R. Ramanathan, "Vertical Distribution of Atmospheric Ozone in Low Latitudes," Proc. Ind. Acad. Sci, 29, 330-348 (1949).

43. E. Tonsberg and K. Langh, Geophys. Publ. 13, No. 12 (1944)

44. Results of preliminary examination of data from a V2 rocket flight over New Mexico in October, 1947, by Durant and Colleagues, as cited by C. Normand (see reference)

45. V. Regener, "Vertical Distribution of Atmospheric Ozone," Nature 167, 276-277 (1951)

46. C. Normand, "Some Recent Work on Ozone," Quart. J. Roy. Meteor. Soc. 77, 474-478 (1951).

47. J. Reed, "The Role of Vertical Motions in Ozone-Weather Relationships," J. Meteorol, 7, 263-267 (1950).

48. O. R. Wulf, "The Distribution of Atmospheric Ozone," Proc. Eighth Amer. Sci. Cong., Washington, 439-446 (1945).

49. W. W. Kellogg and G. F. Schilling,"A Proposed Model of the Circulation in the Upper Atmosphere," J. Meteor, 8, 222-230 (1951).

50. H. K. Paetzold, "Vertical Atmospheric Ozone Distribution," Adv. in Chemistry Series, No. 21, Am. Chem. Soc., p. 352 (1959).

51. K. R. Ramanathan, "Atmospheric Ozone and the General Circulation of the Atmosphere," in Sci. Proc. Intern. Assoc. Meteorol. Rome (1954). pp. 3-24 (Butterworth's, London, 1956).

52. R. M. Goody and W. T. Roach, "The Determination of Tropospheric Ozone from Infrared Emission Spectra," Quart. J. Roy. Meteor. Soc. 82, 217-221 (1958).

53. I. A. Khvostikov, Uspekhi fiz. nauk, 59, No. 2 (1956).

54. V. M. Berezen and Y. A. Shafrin, Geomagn-i Aeronamiya, 4, No. 1 131 (1964).

55. V. I. Bekoryukov, "Computation of the Effect of Closed Air Circulation on the Equilibrium Distribution of Ozone in the Earth's Atmosphere," Geomagn. and Aeronomy (USA) Vol. 5, No. 3, 357-361 (May-June 1965).

56. C. Prabhakara, "Effects of Nonphotochemical Processes on the Meriodinal Distribution and Total Amount of Ozone in the Atmosphere," Mon. Wea. Rev., 91, 411-431 (1963).

57. H. K. Paetzold, "The Mean Vertical Ozone Distribution Resulting from the Photochemical Equilibrium, Turbulence, and Currents of Air," J. Atm. Terr. Phys. 3, 125-131 (1953).

58. J. London and C. Prabhakara, "The Effect of Stratospheric Transport Processes on the Ozone Distribution," Proc. Intern. Symp. Stratospheric and Mesopheric Circulation, Freien Universitat, Berlin, 291-297 (1963).

59. W. L. Godson, "The Representation and Analysis of Vertical Distributions of Ozone," Quart. J. Roy. Meteorol. Soc. 88, 220 (1962)

60. R. Penndorf, "The Annual Variation of the Amount of Ozone Over Northern Norway," Ann. Geophys., 6, 4 (1950).

61. K. Allington, B.W. Boville, and F.K. Hare, "Midwinter Ozone Variations and Stratospheric Flow Over Canada," Tellus, 12, 266-273 (1958-1959).

62. B. W. Boville and F. K. Hare, "Total Ozone and Perturbations in the Middle Stratosphere," Quart. J. Roy. Meteor. Soc., 87, 490-501 (1961).

63. W. W. Coblentz and R. Stair, "Distribution of Ozone in the Stratosphere," J. Res. Natl. Bur. Stand. 22, 573-606 (1939).

64. H. U. Dütsch, "Das Atmosphärische Ozon als Indikator für Strömungen in der Stratosphare," Archiv. Meteor., Geoph. Biokl A9, 87-119 (1956).

65. C. E. Junge, "Global Ozone Budget and Exchange between Stratosphere and Troposphere," Tellus 14, 363-377 (1962).

66. R. E. Newell, "Transfer through the Tropopause and within the Stratosphere," Quart. J. Roy. Meteor. Soc. 89, 167-204 (1963).

67. H. K. Paetzold and F. Piscalar, "Meridionale Ozonverteilung und Stratosphärische Zirkulation," Naturwiss 48, 474 (1961).

68. A. Vassy and I. Rasool, "Rapartition Verticale de l'ozone Atmosphérique à différentes latitudes," Ann. Geoph. 16, 262-263 (1960).

69. W. S. Hering, "Ozonesonde Observations over North America, Vol. 1, AFCRL-64-30, pp. 517 (1964).

70. E. Vigroux, M. Migeotte, and P. Vermande, "Variations de l'Ozone Atmosphérique," Annal Geophys. 22, 15 (1966).

71. W. L. Godson and R. Lee, Beitr. Phys. Atmos. 31, 40-68 (1958).

72. R. Lee and W. L. Godson, J. Met. 12, 95-106 (1957).

73. K. P. Pogosyan, Met. and Hydrol. (Leningrad), No. 2 15-21 (Met. Transl. Toronto 1960 No. 4, pp. 13-22).

74. C.W.B. Normand, Quart. J. R. Met. Soc. 79, 39-50 (1953).

75. C.W.B. Normand, Proc. Toronto Met. Conf. 1953, pp. 4-8 (1954).

76. E. Schroer, Ber. Deutsch Wetterd. U.S. Zone, 2, No. 11, pp 13-22 (1949).

77. H. Moser, Ber. Deutsch Wetterd. U.S. Zone, 2, No. 11, pp 28-37 (1949).

78. K. Langlo, Geofys. Publ., 18, No. 6 (1952).

9.3 Ozone and Its Relation to the Atmospheric Radiative Budget and Other Parameters.

79. W. W. Webb, "Stratospheric Solar Response," J. Atm. Sci., 21, 582-591 (1964).

80. J. London, "Ozone Variations and their Relations to Stratospheric Warming," Proc. Intern. Symp. Stratospheric and Mesospheric Circulation, Freien Universität Berlin, 299-310 (1963).

81. R. J. Murgatroyd and R. M. Goody, "Sources and Sinks of Radiative Energy from 30 to 90 km," Quart. J. R. Meteor. Soc. 84, 225-234 (1958).

82. A. R. Curtis, "The Computation of Radiative Heating Rates in the Atmosphere," Proc. Roy. Soc. A236, 156-159 (1956).

83. A. R. Curtis and R. M. Goody, "Thermal Radiation in the Upper Atmosphere," Proc. Roy. Soc. A236, 193-206 (1956).

84. E. H. Gowan, "Ozonosphere Temperatures under Radiative Equilibrium," Proc. Roy. Soc. A190, 219-225 (1947)

85. F. S. Johnson, "High Altitude Diurnal Temperature Changes due to Ozone Absorption," Bull. Amer. Meteor. Soc. 34, 106-110 (1956).

86. R. V. Karandikar, "Radiation Balance of the Lower Stratosphere, I," Proc. Ind. Acad. Sci., 23, 70-96 (1946).

87. A. Manabe and F. Möller, "On the Radiative Equilibrium and Heat Balance of the Atmosphere," Mon. Wea. Rev. 89, 503-531 (1961).

88. W. W. Kellog, "Warming of the Polar Mesosphere and Lower Ionosphere in Winter," J. Meteor., 18, 373-381 (1961).

89. P. A. Davis, "An Analysis of the Atmospheric Heat Budget," J. Atm. Sci., 20, 5 (1963).

90. G. Ohring, "The Radiation Budget of the Stratosphere," J. Meteor., 15, 440-451 (1958).

91. G. N. Plass, "The Influence of the 9.6μ Ozone Band on the Atmospheric Infrared Cooling Rate," Quart. J. R. Meteor. Soc. 82, 30-44 (1956).

92. J. Pressman, "The Latitudinal and Seasonal Variations in the Absorption of Solar Radiation by Ozone," J. Geophys. Res., 59, 485-498 (1954).

93. J. Pressman, "Diurnal Temperature Variations in the Middle Atmosphere," Bull. Amer. Meteor. Soc. 36, 220-223 (1955).

94. R. A. Craig and G. Ohring, "The Temperature Dependence of Ozone Radiational Heating Rates in the Vicinity of the Mesopeak," J. Meteor., 15, 59-62 (1958).

95. J. G. Breiland, "Vertical Distribution of Atmospheric Ozone and Its Relation to Synoptic Meteorological Conditions," J. Geophys. Res., 69, 3801 (1964).

96. P. R. Sticksel, "The Vertical Distribution of Ozone over Tallahassee, Florida," Sci. Rep. No. 1, Contract AF 19(628)-4953 (1966).

97. A. R. Meetham, Quart. J. Roy. Met. Soc. 85, 393-404 (1937).

98. R. Penndorf, Met. Rund. 3, 49-54 (1950).

99. H. Johansen, Geofys. Publ. 19, No. 5 (1955).

100. H. Johansen, "On the Relation between Meteorological Conditions and Total Amount of Ozone over Tromsö," J. Atm. Terr. Phys., Suppl. 1957, Proc. of the Polar Atm. Symposium.

101. D. W. Martin and A. W. Brewer, Sci. Proc. Int. Ass. Met. Rome 1954 pp. 177-180 (1956).

102. D. W. Martin and A. W. Brewer, Quart. J. Roy. Met. Soc. 77, 474-478 (1951).

103. J. K. Angell and J. Kosshover, "Quasibiennial Variations in Temperature, Total Ozone, and Tropopause Height," J. Atm. Sci. 21, 479 (1964).

104. R. A. Craig, "Radiative Temperature Changes in the Ozone Layer," Compendium of Meteorology, Amer. Meteorological Soc., 292, Boston (1951).

105. D. L. Brooks, "The Distribution of Carbon Dioxide Cooling (and Ozone Heating) in the Lower Stratosphere," J. Meteor. 15, 210 (1958).

106. G.M. B. Dobson and D. N. Harrison, "Measurements of the Amount of Ozone in the Earth's Atmosphere and its Relation to other Geophysical Conditions," Proc. Roy. Soc. A110, 660-693 (1926).

107. G.M.B. Dobson, D.N. Harrison, and J. Lawrence, "Measurements of the Amount of Ozone in the Earth's Atmosphere and its Relation to other Geophysical Conditions, Part II," Proc. Roy. Soc., A114, 521-541 (1927).

108. G.M.B. Dobson, D.N. Harrison, and J. Lawrence, "Measurements of the Amount of Ozone in the Earth's Atmosphere and its Relation to other Geophysical Conditions, Part III," Proc. Roy. Soc. A122, 456-486 (1929).

109. G.M.B. Dobson, "Observations of the Amount of Ozone in the Earth's Atmosphere and Its Relation to Other Geophysical Conditions, Part IV," Proc. Roy. Soc., A129, 411 (1930).

110. G.M.B. Dobson, A.W. Brewer, and B.M. Cwilong, "Meteorology of the Lower Stratosphere," Proc. Roy. Soc. London, A185, 144 (1946).

111. R. M. Endlich, "The Mesocale Structure of Some Regions of Clear-Air Turbulence," J. Appl. Meteor. 3, 261 (1964).

112. O. R. Wulf, "On the Relation Between Geomagnetism and the Circulatory Motions of the Air in the Atmosphere," Terr. Magn. Atm. of Electr., 50, 185 (1945).

113. W. S. Hering, "Ozone Measurements for Diagnostic Studies of Atmospheric Circulation," Proc. AIAA Second Annual Meeting, San Francisco (1965), 8 pp.

114. R. E. Newell, "The Transport of Trace Substances in the Atmosphere and Their Implications in the General Circulation of the Stratosphere," Geofis. Pura e Appl. 49, 137 (1961).

115. K. R. Ramanathan and R. N. Kulkarni, "Mean Meridional Distributions of Ozone in Different Seasons Calculated from Umkehr Observations and Probable Vertical Transport Mechanisms," Quart. J.R. Met. Soc. 86, 144 (1960).

116. H. U. Dütsch, "Ozone Distribution and Stratospheric Temperature Field over Europe during the Sudden Warming in January/February 1958," Beitr. Phys. Atmos. 35, 87-107 (1962).

117. A. Eucken and F. Patat, "Die Temperaturabhängigkeit der Photochemischen Ozonbildung," Z. Phys. Chem. B33, 459-474 (1936).

118. J. L. Kroening and E. P. Ney, "Atmospheric Ozone," J. Geoph. Res. 67, 1867-1875 (1962).

119. D. W. Martin and A. W. Brewer," A Synoptic Study of Day-To-Day Changes of Ozone over the British Isles," Quart. J. Roy. Meteor. Soc. 85, 393-403 (1959).

120. A. R. Meetham, "The Correlation of the Amount of Ozone with other Characteristics of the Atmosphere," Quart. J. Roy. Meteor. Soc., 63, 289-307 (1937).

121. Y. Miyake and K. Kawamura, "Studies on Atmospheric Ozone at Tokyo," Sci. Proc. Int. Assoc. Meteor., Rome, 1954, 172-176 (1956).

122. G. Ohring and H. S. Muench, "Relationships between Ozone and Meteorological Parameters in the Lower Stratosphere," J. Meteor. 17, 195-206 (1960).

123. W. W. Kellogg, "Warming of the Solar Mesosphere and Lower Ionosphere in Winter," J. Meteor, 18, 373-381 (1961).

124. A. V. Yakovleva, L. A. Kudryavtseva, A. S. Britaev, V. F. Gerasev, V. P. Kachalov, A. P. Kuznetzov, N. A. Pavlenko, and V. A. Iozenas, "Spectrometric Investigation of the Ozone Layer up to a Height of 60 km," Planet. Space Sci., 11, 709-721 (1963).

125. R. Berggren and K. Lalutzke, "A Detailed Study of the Horizontal and Vertical Distribution of Ozone," Tellus 18, 761-772 (1966).

9.4 Ozone Absorption Spectroscopy

126. G. Herzberg, Molecular Spectra and Molecular Structure, Vol. III, "Electronic Spectra and Electronic Structure of Polyatomic Molecules," pp. 511-12, D. Van Nostrand Co., Inc., Princeton, New Jersey (1966).

127. R. Trambarulo, S. N. Ghosh, C. A. Burrus, Jr., and W. Gordy, "The Molecular Structure, Dipole Moment, and g factor of Ozone from its Microwave Spectrum," J. Chem. Phys. 21, 851 (1953).

128. G. W. Robinson, Ch. 2.4 "Electronic Spectra," Methods of Experimental Physics, V. 3, Academic Press, New York and London (1962).

129. R. H. Hughes, "The Microwave Spectrum and Structure of Ozone," J. Chem. Phys., 21, 959 (1953).

130. W. Shand and R. A. Spurr, J. Chem. Soc., 65, 179 (1943).

131. Chappius, Ann. de l'ecole normale sup. 11 , 137 (1882); Compt. rend. 91, 985 (1880); 94, 858 (1882).

132. E. Vigroux, "Contribution a' l' étude Experimentale de l' Absorption de l'Ozone," Ann. Phys. 8, 709-762 (1953).

133. Annals of the IGY 5, 46 (1957) "Observer's Handbook for the Ozone Spectrophotometer."

134. E.C.Y. Inn and Y. Tanaka, "Comparison of Recently Recorded Ozone Absorption Coefficients in the Visible and Ultraviolet Regions," Conference on Ozone, Armour Research Foundation (Dec. 1956).

135. G.M.B. Dobson, Royal Met. Soc. Quart. Journ. 89, 409 (1963).

136. R. A. Hamilton and J. M. Walker, J. Atm. Terr. Phys. 28, 667 (1962).

137. USAF Handbook of Geophysics, Ch. 16, Macmillan Co., New York.

138. W. H. Eberhardt and W. Shand, Jr., "On the Ultraviolet Absorption Spectrum of Ozone," J. Chem. Phys. 14, 525 (1946).

139. J. Strong, "On a New Method of Measuring the Mean Height of the Ozone in the Atmosphere," J. Franklin Inst. 231, 121-156 (1941).

140. S. A. Klough and F. X. Kneizys, J. Chem. Phys. 44, 1855 (1966); AFCRL Report, AF Cambridge Laboratories (1965).

141. C. D. Walshaw, "Integrated Absorption by the 9.6μ Band of Ozone," Quart. J. Roy. Meteor. Soc., 83, 315-321 (1957).

142. O. R. Wulf, "The Band Spectrum of Ozone in the Visible and Photographic Infrared," Proc. Nat'l Acad. Sci. (U.S.), 16, 507 (1930).

143. Schoene, J. Russ. Phys., Chem. Soc. 16, 250 (1884); J. Chem. Soc. 48, 713 (1884); Chem. News, 69, 289 (1894).

144. Ladenburg and Lehmann, Ann. Phys. 21, 305 (1906) · Verh. d · deutsch. Phys. Ges. 8, 125 (1906).

145. M. G. Colange, J. Phys. et le rad. 8, 254 (1927), "Etude de l' Absorption Par l' Ozone dans le Spectre Visible."

146. L. Lefebvre, "The Absorption Spectrum of Ozone in the Photographic Infrared Region," Compt. Rend. Acad. Sci. 200, 1743 (1935).

147. R. S. Mulliken, Rev. Mod. Phys., 14, 204 (1942).

148. Hartley, J. Chem. Soc. 39, 57 (1881).

149. Y. Tanaka, E.C.Y. Inn, and K. Watanabe, "Absorption Coefficients of Gases in the Extreme Ultraviolet, Part IV: Ozone," J. Chem. Phys. 21 1651-1653 (1953).

150. E. Von Bahr, Ann. d. Physik 29, 780 (1909).

151. F. E. Fowle, Smithsonian Misc. Coll. 68, No. 8, p. 41 (1917).

152. J. Devaux, Compt. rend. 193, 1207 (1931); 198, 1595 (1934); 201, 1500 (1935).

153. A. Adel, V. M. Slipher, and E. F. Barber, Phys. Rev. 47, 580 (1935).

154. A. Adel and C.O. Lampland, Astrophys. J. 91, 481 (1940).

155. J. Strong, Phys. Rev. 55, 1114 (1939).

156. J. Strong and K. Watanabe, Phys. Rev. 57, 1049 (1940).

157. A. Adel and D. M. Dennison, J. Chem. Phys. 14, 379 (1946).

158. M. K. Wilson and R. M. Badger, J. Chem Phys. 16, 741 (1948).

159. O. R. Wulf and E. H. Melvin, "The Effect of Temperature Upon the Ultraviolet Band Spectrum of Ozone and the Structure of this Spectrum," Phys. Rev. 38, 330 (1931).

160. A. Fowler and G. Strutt, Proc. Roy. Soc. 93, 729 (1917).

161. D. Chalonge and L. Lefebvre, Compt. rend. 197, 444 (1933).

162. L. Lefebvre, Compt. rend. 199, 456 (1934).

163. A. Jakowlewa and K. Kondratjew, Phys. Zeits. Sowjetunion 9, 106 (1936).

164. D. Melcher, Helv. Phys. Acta 18, 72 (1945).

165. E. Jones and O. R. Wulf, J. Chem. Phys. 5, 873 (1937).

166. T. Z. Ny and S. P. Choong, Chinese J. Phys. 1, 38 (1933).

167. Huggins, Proc. Roy. Soc. 48, 216 (1890).

168. Meyer, Anna. de Physik 12, 849 (1903).

169. Kriger and Moeller, Physik. Zeits 13, 729 (1912).

170. Fabry and Buisson, "L' Absorption de l' Ultraviolet par l' Ozone et la Limite du Spectre Solaire," Jour. de Phys. Rad. 3, 196 (1913).

171. Shaver, Proc. Roy. Soc. Canada 15, Sec. III, 5 (1921).

172. Lambert, Dejardin, and Chalonge, Compt. rend. 183, 800 (1926).

173. Lauchli, Zeits. f. Physik 53, 92 (1929).

174. Lambry and Chalonge, Gerland's Beitrage Z. Geophysik 24, 42 (1929).

175. Dutheil, Jour. de Phys. rad. 7, 414 (1926).

176. T. Z. Ny and S. P. Choong, Compt. rend. 195, 309 (1932); 196, 916 (1933).

177. Barbier, Chalonge, and Vassy, Revue d' Optique, 14, 425 (1935).

178. M. E. Vassy, Compt. rend. 204, 1426 (1936).

179. E.C.Y. Inn and Y. Tanaka, "Absorption Coefficients of Ozone in the Ultraviolet and Visible Regions," J. Opt. Soc. Amer., 43, 870-873 (1953).

180. K. Angstrom, Arch. f. Math., Astron. och. Phys. I, 345 & 395 (1904).

181. D. Simpson, Trans. Faraday Soc. 41, 209 (1945); J. Chem. Phys. 14, 379 (1946).

182. G. Hettner, R. Pohlmann, and H. J. Schumacher, Zeits. f. Electro Chemie 41, 524 (1933).

183. S. L. Gerhard, Phys. Rev. 42, 622 (1933).

184. A. Adel, et al, Astrophys. J. 89, 320 (1930); 94, 451 (1941); Phys. Rev. 49, 288 (1936).

9.5 Determination of Atmospheric Abundance and Vertical Distribution

185. D. Barbier, D. Chalonge, and E. Vigroux;"Utilisation des éclipses de lune a' l' étude de la haute atmosphere," Compt. rend., 214, 983-984 (1942).

186. BarBarbier, D. Chalonge, and E. Vigroux;"Étude spectrophotometrique de l' éclipse de lune des 2 et 3 mars 1942," Ann. Astrophys., 5, 1-22 (1942).

187. D. Chalonge,"Exploration de l' atmosphere terrestre au moyen des éclipses de lune," L'Astronomic, 69, 319-336 (1955).

188. L.S. Flugge and J.G. Bartels, Band XLVIII, Geophysik II, pp 384-386 (1957).

189. Penndorf, R.,"Uber die Ermittlung der vertikalen Ozonverteilung bei Mondfinsternissen,"Veroffentl. Geophys. Inst., Univ. Leipzig, Weickmannheft (1957).

190. Penndorf, R., "Effects of the Ozone Shadow," J. Meteorol., 5, 152-160 (1948).

191. J. Dufay, "Le Spectra de la lune éclipse," Compt. rend., 193, 711, (1931).

192. G. Fabry, "Etude de l' Ozone Atmospherique par l' Observation des Éclipses de lune, L' Ozone Atmospherique," Chapt. 6, du C.N.R.S., Paris, 202-206 (1950).

193. Fesenkov, V.G., "On the Optical State of the Atmosphere Illuminated by Twilight," Astron. Zhur., 36, 201-207, or Soviet Astronomy (English translation), 3 (2), 207-213 (1959)

194. V.G. Fesenkov, On the Investigation of Atmospheric Ozone by Photometry of Lunar Eclipses, Astron. Zhur., 36 (4), 564-572, or Soviet Astronomy (English translation), 3 (4), 554-562 (1959).

195. A.E.S. Green, "Attenuation by Ozone and the Earth's Albedo in the Middle Ultraviolet," Applied Optics, 3, 203 (1964).

196. E. L. Hubbard, "Calculation of the Intensity of Light Scattered in the Atmosphere in the Wavelength Region 2300Å to 3100Å with Absorption by Oxygen and Ozone Considered," Report LAS-TR-199-48, Univ. of Chicago Lab. Appl. Sci. (Sept. 1963).

197. J.V. Dave and C.L. Mateer, "The Determination of Ozone Parameters from Measurements of the Radiation Backscattered by the Earth's Atmosphere," unpublished.

198. Fesenkov, V.G., "On the theory of the lunar eclipses," Summary appearing in Symposium on Atmospheric Ozone, Oxford, July 1959, Union Géodésique et Géophysique Internationale, Monograph 3 (1960).

199. Götz, F.W.P., "Die vertikale Verteilung des atmosphärischen Ozons," Erggeb. kosn. Physik, 3 253-325 (1938).

200. F. Link, "Théorie photométrique des éclipses de lune," Bull. astron., 8, 77-107 (1932).

201. F. Link, "Occtulations et éclipses par les planétes," Bull. astron., "mémoires et variétés," 227-249 (1931).

202. F. Link, "Exploration de la haute atmosphere a 1' aide des éclipses de lune," premier partie, Ann. Géophys., 4 (1), 47-64 (1948).

203. F. Link, "Die Mondfinsternisse," Probleme der kosmischen Physik, 28, Akademische Verlagsgesellschaft, Goest and Portig, Leipzig (1956).

204. Paetzold, H. K., "Über die Erfassung der atmosphärischen Ozonverteilung durch Benutzung von Mondfinsternissen," Z. Naturforsch., 6a (11), 639-648 (1951).

205. Paetzold, H. K., "Die durch die atmosphärischen Ozonschicht bewirkte Farbung des Erdschattens auf dem verfinsterten Mond," Naturwissenschaften, 38 (23) 544-545 (1951).

206. Paetzold, H.K., "Erfassung der vertikalen Ozonverteilung in verschiedenen geographischen Breiten bei Mondfinsternissen," J. Atmospheric and Terrest. Phys., 3, 183 (1952).

207. Paetzold, H.K., "Weitere Bestimmungen der vertikalen Ozonverteilung bei Mondfinsternissen," Z. Naturforsch., 7a (5), 325-328 (1952).

208. Paetzold, H.K., "Schwankungen der vertikalen Ozonverteilung in 0^{o} and 60^{o} geographischen Breite nach Mesungen bei Mondfinsternissen," Deut. Wetterdienst in der U.S. Zone, 38, 292-294, Berichte (1952).

209. Paetzold, H.K., "Über die Möglichkeit der Benutzung von Mondfinsternissen zur Erfassung de vertikalen Ozonverteilung in verschiedenen Breiten," Union Géodésique et Géophysique Internationale, Nuevième Assemblée Générale Procés-Verbaux des Séances de l'Association de Météorologie, Mémoires et Discussion, Publication AIM, no. 9/c, 333-336, Brussels (1953).

210. Paetzold, H.K. and E. Regener, "Ozon in der Erdatmosphäre" (see Sec. 9). Bestimmung der vertikalen Ozonverteilung, Methods der Mondfinsternissen in Handbuch der Physik.

211. Van de Hulst, H.C., "Scattering in the atmospheres of the earth and the planets," see section D, Exploration of the high atmosphere by optical methods, The Atmospheres of the Earth and Planets, ed. G.P. Kuiper, Univ. of Chicago Press, Chapt. 3, 85-88 (1952).

212. Vigroux, E., "Photométrie d'une éclipse de lune: répartition de l'ozone," Compt. rend., 239 (4), 339-341 (1954).

213. Vigroux, E., "Spectrophotométrie de l'éclipse de lune du 29-30 Janvier, 1953," Ann. astrophys., 17, 399-415 (1954).

214. L. Spitzer, Jr., "Earth Satellites as Research Vehicles," Franklin Institute Monograph 2, 69 (1956).

215. F. S. Johnson, J. D. Russell, R. Tousey, and K. Watanabe, "Direct Measurements of the Vertical Distribution of Atmospheric Ozone to 70 Kilometers Altitude," J. Geophys. Res. 57, 157-176 (1952).

216. S. V. Venkateswaran, J. G. Moore, and A. J. Krueger, "Determination of the Vertical Distribution of Ozone by Satellite Photometry," J. Geophys. Res. 66, 1751 (1961).

217. S. F. Singer and R. C. Wentworth, "A Method for the Determination of the Vertical Ozone Distribution from a Satellite," J. Geophys. Res. 62, 299 (1957).

218. E. Regener and V. H. Regener, Physik Zs. 35, 778 (1934).

219. J. A. Van Allen and J.J. Hopfield, Mein. Soc. Rog. Sci. Liege 12, 179 (1952).

220. W. S. Hering and H. U. Dütsch, "A Comparison of Chemiluminescent and Electrochemical Observations," J. Geophys. Res. 70, 5483-5490 (1965).

221. H. E. Bennett and W. R. McBride, "Use of Filters for Suppressing Scattered Light in Spectrometers used in the Ultraviolet," Appl. Opt. 3, 919 (1964).

222. I. G. Bowen and V. H. Regener, "On the automatic Chemical Determination of Atmospheric Ozone," J. Geophys. Res. 56, 307-324 (1951).

223. A. W. Brewer, "Ozone Concentration Measurements from an Aircraft in N. Norway," Quart. J. Roy. Meteor. Soc. 83, 266-268 (1957).

224. A.W. Brewer and J.R. Milford, "The Oxford-Kew Ozone Sonde," Proc. Roy. Soc. A256, 470-495 (1960).

225. A. W. Brewer, H. Dütsch, J. R. Milford, M. Migeotte, H.K. Paetzold, F. Piscalar, and E. Vigroux, "Distribution Verticale de l' ozone atmosphérique. Comparison de Diverses Méthodes," Ann. Geoph. 16, 196-222 (1960)

226. G.M.B. Dobson, "A Photoelectric Spectrophotometer for Measuring the Amount of Atmospheric Ozone," Proc. Phys. Soc. 43, 324-339 (1931).

227. H. Dütsch, "Vertical Ozone Distribution from Umkehr Observation," Archiv Meteor., Geoph. Biokl. A11, 240-251 (1959).

228. E.S. Epstein, C.Osterberg, and A. Adel, "A New Method for the Determination of the Vertical Distribution of Ozone from a Ground Station," J. Meteor. 13, 319-334 (1956).

229. R.M. Goody and W.T. Roach, "The Determination of Tropospheric Ozone from Infrared Emission Spectra," Quart. J. Roy. Meteor. Soc. 84, 108-117 (1958).

230. M. Griggs, "Measurements of the Vertical Distribution of Atmospheric Ozone at Nairobi," Quart. J. Roy. Meteor. Soc. 89, 284-286 (1963).

231. F.S. Johnson, J.D. Purcell, and R. Tousey, "Measurements of the Vertical Distribution of Atmospheric Ozone from Rockets," J. Geoph. Res. 56, 583-594 (1951).

232. F.S. Johnson, J.D. Purcell, and R. Tousey,"Studies of the Ozone Layer above New Mexico," in Rocket Exploration of the Upper Atmosphere (R.L.F. Boyd and M.J. Seaton, eds.), 189-199, Pergamon Press, New York (1954).

233. R.H. Kay, "The Measurement of Ozone Vertical Distribution by a Chemical Method to Heights of 12 km from Aircraft," in Rocket Exploration of the Upper Atmosphere (1954).

234. C.L. Mateer, "A Rapid Technique for Estimating the Vertical Distribution of Ozone from Umkehr Observations," Quart. Circ. No. 3291, Meteor. Branch, Dept. Transport, Toronto (1960).

235. H.K. Paetzold and F. Piscalar, "Die Messung der Vertikalen Ozonverteilung mittels einer Optischen Radiosonde," Beitr. Phys. Atmos. 34, 53-68 (1961).

236. A.B. Pittock, "Determinations of the Vertical Distribution of Ozone by Twilight Balloon Photometry," J. Geoph. Res. 68, 5143-5155 (1963).

237. K.R. Ramanathan and J.V. Dave, "The Calculation of the Vertical Distribution of Ozone by Götz Umkehr-Effect (Method B), Ann. I.G.Y. 5, 23-45 (1957).

238. E. Regener, H.K. Paetzold, and A. Ehmert, "Further Investigations on the Ozone Layer," in Rocket Exploration of the Upper Atmosphere (1954).

239. V.N. Regener, "Neue Messungen der Vertikalen Verteilung des Ozons in der Atmosphäre," Z. Phys. 109, 642-670 (1938).

240. V.H. Regener, "On a Sensitive Method for the Recording of Atmospheric Ozone," J. Geophys. Res. 65, 3975-3977 (1960).

241. Z. Sekera and J.V. Dave, "Determination of the Vertical Distribution of Ozone from the Measurement of Diffusely Reflected Ultraviolet Solar Radiation," Plan. Space Sci., 5, 122-136 (1961).

242. Z. Sekera and J.V. Dave, "Diffuse Transmission of Solar Ultraviolet Radiation in the Presence of Ozone," Ap. J. 133, 210-227 (1961).

243. S. Twomey, "On the Deduction of the Vertical Distribution of Ozone by Ultraviolet Spectral Measurements from a Satellite," J. Geoph. Res. 66, 2153-2162 (1961).

244. E. Vigroux, "Distribution Verticale de l'ozone atmospherique d'apres les observations de la bande 9.6μ," Ann. Geophys. 15, 516-538 (1959).

245. E. Vigroux and A. Debaix, "Resultats d'observations de l'ozone Atmospherique par la Méthode Infra-Rouge," Ann. Geophys. 19, 31-52 (1963).

246. C.D. Walshaw, "The Accuracy of Determination of the Vertical Distribution of Atmospheric Ozone from Emission Spectrophotometry in the 1043 cm^{-1} Band at High Resolution," Quart. J. Roy. Meteor. Soc. 86, 519-529 (1960).

247. G.F. Walton, "The Calculation of the Vertical Distribution of Ozone by Götz Umkehr-Effect (Method A)," Ann. I.G.Y. 5, 9-22 (1957).

248. R. Frith, "Measuring the Ozone above the Earth," Discovery, 390-391 (September 1961).

249. R. D. Rawcliffe, G. E. Meloy, R. M. Friedman, and E. H. Rogers, J. Geophys. Res., 68, 6425 (1963).

9.6 Cited References

1. S. Chapman, "On Ozone and Atomic Oxygen in the Upper Atmosphere," Phil. Mag. 10, 369-383 (1930).

2. B. G. Hunt, "A Nonequilibrium Investigation Into the Diurnal Photochemical Atomic Oxygen and Ozone Variations in the Mesophere," J. Atmos. Terr. Phys. 21, 133-144 (1965).

3. B. G. Hunt, "Photochemistry of Ozone in a Moist Atmosphere," J. Geophys. Res. 71, 1385 (1966).

4. V. S. Whitehead, M. D. Miller, and W. J. Saucier, "A consideration of Some of the Factors Affecting Atmospheric Composition, Static Stability and Motion between 20 km and 100 km," Final Report, Contract AF 19(628)-4767 (1966).

5. F. S. Johnson, "Atmospheric Chemistry and Composition," Upper Atmosphere and Space Physics Seminar, Southwest Center for Advanced Studies, Dallas, Texas, 1-10 (1962).

6. R. A. Craig, "The Observations and Photochemistry of Atmospheric Ozone and their Meteorological Significance," A.M.S. Met. Monographs, Vol. 1, No. 2, pp. 50 (1950).

7. H. K. Paetzold, Geophys. p.e. Appl. 24, 1 (1953).

8. H. K. Paetzold, Geophys. p.e. Appl. 24, 15 (1953).

9. H. K. Paetzold, J. Atm. Terr. Phys. 3, 131 (1953).

10. H. K. Paetzold, Mitt. Astron. Ges., p. 19 (1953).

11. H. K. Paetzold, "New Experimental and Theoretical Investigations on the Atmospheric Ozone Layer," J. Atm. Terr. Phys. 1, 128-140 (1955).

12. H. K. Paetzold, "Photochemistry of the Atmospheric Ozone Layer," in Chemical Reactions in the Lower and Upper Atmosphere (proceedings of an international symposium at Stanford Research Institute), New York, Interscience Pub., 181-195 (1961).

13. M. Nicolet, in The Earth as a Planet, Ed. G. P. Kuiper, Univ. of Chicago Press, Chicago, p. 666 (1954)

14. F. N. Frenkiel, J. Chem. Phys. 23, 2440 (1955).

15. J. E. Blamont and T. M. Donahue, J. Geophys. Res. 69, 4093 (1964).

16. S. Chapman, "A Theory of Upper Atmospheric Ozone," Mem. R. Met. Sox. 3, 103-125 (1930).

17. O. R. Wulf and L. S. Deming, Terr. Mag. 41, 299, 375 (1936); 42, 195 (1937).

18. B. G. Hunt, "The Need for a Modified Photochemical Theory of the Ozonosphere," J. Atmospher. Sci., 23 (1966).

19. J. Hampson, "Chemical Instability of the Atmosphere," Atmospheric Radiation Symposium, Leningrad (1964)

20. P. L. Roney, "On the Influence of Water Vapour on the Distribution of Stratospheric Ozone," J. Atmos. Terr. Phys. 27, 1177-1190 (1965).

21. R. R. Reeves, G. Mannella, and P. Harteck, "Rate of Recombination of Oxygen Atoms," J. Chem. Phys. 32, 632-633 (1960).

22. W. L. Godson, "Total Ozone and the Middle Stratosphere over Arctic and Sub-Arctic Areas in Winter and Spring," Quart. J. Roy, Meteor. Soc., 86, 301-317 (1960).

23. J. P. Funk and G. L. Garnham, "Australian Ozone Observations and a Suggested 24 Month Cycle," Tellus 14, 378-382 (1962).

24. R. N. Kulkarni, "Comparison of Ozone Variations and of its Distribution with Height over Middle Latitudes of the Two Hemisphereas," Quart. J. Roy, Meteor. Soc., 88, 522-534 (1962).

25. J. London, "The Distribution of Total Ozone over the Northern Hemisphere," Sun at Work 7, No. 2, 11-12 (1962).

26. J. London, "The Distribution of Total Ozone in the Northern Hemisphere," Beitr. Phys. Atmos., 36, 254-263 (1963).

27. R. N. Kulkarni, P. D. Angreji, and K. R. Ramanathan, "Comparison of Ozone Amounts measured at Delhi (28 1/2^{o}N), Srinagar (34^{o}N), and Tateno (36^{o}N) in 1957-1958," Pap. Meteor. Geoph., Meteor. Res. Inst., Japan 10, 85-92 (1959).

28. G. Perl and H. Dütsch, "Die 30-Jährige Arosa Ozonmessreihe," Ann. Schweiz. Meteor. Zentralamstalt, 1958, 8 (1959).

29. R. A. Craig, The Upper Atmosphere, Meteorology and Physics, Ch. 5 (Academic Press, 1965).

30. R. A. Craig, The Upper Atmosphere, Meteorology and Physics, International Geophysics Series, Vol. 8, Academic Press, New York and London (1965).

31. C. L. Mateer and W. L. Godson, "The Vertical Distribution of Atmospheric Ozone over Canadian Stations from Umkehr Observations," Quart. J. Roy. Meteor. Soc. 86, 512-518 (1960).

32. H. U. Dütsch, "Mittelwerte and Wetterhafte Schwankungen des Atmospharischen Ozongehaltes in Verschiedenen Höhen über Arosa," Archiv. Meteor., Geoph., Biokl, A13, 167-185 (1962).

33. F. W. P. Götz, A. R. Meetham, and G. M. B. Dobson, "The Vertical Distribution of Ozone in the Atmosphere," Proc. Roy. Soc. A145, 416-446 (1934).

34. R. V. Karandikar and K. R. Ramanathan, "Vertical Distribution of Atmospheric Ozone in Low Latitudes," Proc. Ind. Acad. Sci, 29, 330-348 (1949).

35. E. Tönsberg and K. Langlo, Geophys. Publ. 13, No. 12 (1944).

36. Results of preliminary examination of data from a V2 rocket flight over New Mexico in October, 1947 by Durant and colleagues, as cited by C. Normand.

37. V. Regener, "Vertical Distribution of Atmospheric Ozone," Nature 167, 276-277(1951).

38. C. Normand, "Some Recent Work on Ozone," Quart. J. Roy. Meteor. Soc. 77, 474-478 (1951).

39. H. U. Dütsch, "Photochemische Theorie des Atmosphärischem Ozons' unter Berücksichtigung von Nichtgleichgewichts - Zuständen and Luftbewegungen," Ph.D. Dissertation, Zurich (1946).

40. J. Reed, "The Role of Vertical Motions in Ozone-Weather Relationships," J. Meteorol, 7, 263-267 (1950).

41. O. R. Wulf, "The Distribution of Atmospheric Ozone," Proc. Eighth Amer. Sci. Cong., Washington, 439-446 (1945).

42. W. W. Kellogg and G. F. Schilling," A Proposed Model of the Circulation in the Upper Atmosphere," J. Meteor, 8, 222-230 (1951).

43. H. K. Paetzold, "Vertical Atmospheric Ozone Distribution," Adv. in Chemistry Series, No. 21, Am. Chem. Soc., p. 352 (1959).

44. K. R. Ramanathan, "Atmospheric Ozone and the General Circulation of the Atmosphere," in Sci. Proc. Intern. Assoc. Meteorol. Rome (1954), pp. 3-24 (Butterworth's, London, 1956).

45. R. M. Goody and W. T. Roach, "The Determination of Tropospheric Ozone from Infrared Emission Spectra," Quart. J. Roy. Meteor. Soc. 82, 217-221 (1958).

46. V. M. Berezen and Y. A. Shafrin, Geomagni-i Aeronamiya, 4, No. 1 131 (1964).

47. V. I. Bekoryukov, "Computation of the Effect of Closed Air Circulation on the Equilibrium Distribution of Ozone in the Earth's Atmosphere," Geomagn. and Aeronomy (USA) Vol. 5, No. 3, 357-361 (May-June 1965).

48. C. Prabhakara, "Effects of Nonphotochemical Processes on the Meriodinal Distribution and Total Amount of Ozone in the Atmosphere," Mon. Wea. Rev., 91, 411-431 (1963).

49. H. K. Paetzold, "The Mean Vertical Ozone Distribution Resulting from the Photochemical Equilibrium, Turbulence, and Currents of Air," J. Atm. Terr. Phys. 3, 125-131 (1953).

50. J. London and C. Prabhakara, "The Effect of Stratospheric Transport Processes on the Ozone Distribution," Proc. Intern. Symp. Stratospheric and Mesopheric Circulation, Freien Universitat, Berlin, 291-297 (1963).

51. W. L. Godson, "The Representation and Analysis of Vertical Distributions of Ozone," Quart. J. Roy. Meteorol. Soc. 88, 220 (1962).

52. R. Penndorf, "The Annual Variation of the Amount of Ozone Over Northern Norway," Ann. Geophys., 6, 4 (1950).

53. K. Allington, B. W. Boville, and F. K. Hare, "Midwinter Ozone Variations and Stratospheric Flow Over Canada," Tellus, 12, 266-273 (1958-1959).

54. B. W. Boville and F. K. Hare, "Total Ozone and Perturbations in the Middle Stratosphere," Quart. J. Roy. Meteor. Soc., 87, 490-501 (1961).

55. W. W. Coblentz and R. Stair, "Distribution of Ozone in the Stratosphere," J. Res. Natl. Bur. Stand. 22, 573-606 (1939).

56. H. U. Dütsch, "Das Atmosphärische Ozon als Indikator für Strömungen in der Stratosphare," Archiv. Meteor., Geoph. Biokl A9, 87-119 (1956).

57. C. E. Junge, "Global Ozone Budget and Exchange between Stratosphere and Troposphere," Tellus 14, 363-377 (1962).

58. R. E. Newell, "Transfer through the Tropopause and within the Stratosphere," Quart. J. Roy. Meteor. Soc. 89, 167-204 (1963).

59. H. K. Paetzold and F. Piscalar, "Meridionale Ozonverteilung und Stratosphärische Zirkulation," Naturwiss 48, 474 (1961).

60 A. Vassy and I. Rasool, "Rapartition Verticale de l'ozone Atmosphérique à différentes latitudes," Ann. Geoph. 16, 262-263 (1960).

61. W. S. Hering, "Ozonesonde Observations over North America, Vol. 1, AFCRL-64-30, pp. 517 (1964).

62. E; Vigroux, M. Migeotte, and P. Vermande, "Variations de l'Ozone Atmosphérique," Annal Geophys. 22, 15 (1966).

63. W. L. Godson and R. Lee, Beitr. Phys. Atmos. 31, 40-68 (1958).

64. R. Lee and W. L. Godson, J. Met. 12, 95-106 (1957).

65. K. P. Pogosyan, Met. and Hydrol. (Leningrad), No. 2 15-21 (Met. Transl. Toronto 1960 No. 4, pp. 13-22).

66. C.W.B. Normand, Quart. J. R. Met. Soc. 79, 39-50 (1953).

67. C.W.B. Normand, Proc. Toronto Met. Conf. 1953, pp. 4-8 (1954).

68. E. Schroer, Ber. Deutsch Wetterd. U.S. Zone, 2, No. 11, pp. 13-22 (1949).

69. H. Moser, Ber. Deutsch Wettered. U.S. Zone, 2, No. 11, pp. 28-37 (1949).

70. K. Langlo, Geofys. Publ., 18, No. 6 (1952).

71. W. W. Webb, "Stratospheric Solar Response," J. Atm. Sci., 21, 582-591 (1964).

72. C. Leovy, "Radiative Equilibrium of the Mesosphere," J. Atm. Sci. 21, 238 (1964).

73. J. London, "Ozone Variations and their Relations to Stratospheric Warming," Proc. Intern. Symp. Stratospheric and Mesospheric Circulation, Freien Universität Berlin, 299-310 (1963).

74. R. J. Murgatroyd and R. M. Goody, "Sources and Sinks of Radiative Energy from 30 to 90 km," Quart. J. R. Meteor. Soc. 84, 225-234 (1958).

75. A. R. Curtis, "The Computation of Radiative Heating Rates in the Atmosphere," Proc. Roy. Soc. A236, 156-159 (1956).

76. J. Pressman, "The Latitudinal and Seasonal Variations in the Absorption of Solar Radiation by Ozone," J. Geophys. Res., 59, 485-498 (1954).

77. A. R. Curtis and R. M. Goody, "Thermal Radiation in the Upper Atmosphere," Proc. Roy. Soc. A236, 193-206 (1956).

78. E. H. Gowan, "Ozonosphere Temperatures under Radiative Equilibrium," Proc. Roy. Soc. A190, 219-225 (1947).

79. F. S. Johnson, "High Altitude Diurnal Temperature Changes due to Ozone Absorption," Bull. Amer. Meteor. Soc. 34, 106-110 (1956).

80. R. V. Karandikar, "Radiation Balance of the Lower Stratosphere, I," Proc. Ind. Acad. Sci., 23, 70-96 (1946).

81. A Manabe and F. Möller, "On the Radiative Equilibrium and Heat Balance of the Atmosphere," Mon. Wea. Rev. 89, 503-531 (1961).

82. W. W. Kellog, "Warming of the Polar Mesosphere and Lower Ionosphere in Winter," J. Meteor., 18, 373-381 (1961).

83. P. A. Davis, "An Analysis of the Atmospheric Heat Budget," J. Atm. Sci., 20, 5 (1963).

84. G. Ohring, "The Radiation Budget of the Stratosphere," J. Meteor., 15, 440-451 (1958).

85. G. N. Plass, "The Influence of the 9.6μ Ozone Band on the Atmospheric Infrared Cooling Rate," Quart. J. R. Meteor. Soc. 82, 30-44 (1956).

86. J. Pressman, "Diurnal Temperature Variations in the Middle Atmosphere," Bull. Amer. Meteor. Soc. 36, 220-223 (1955).

87. R. A. Craig and G. Ohring, "The Temperature Dependence of Ozone Radiational Heating Rates in the Vicinity of the Mesopeak," J. Meteor., 15, 59-62 (1958).

88. R. Lindzen and R. Goody, "Radiative and Photochemical Processes in Mesopheric Dynamics. Part I, Models for Radiative and Photochemical Processes," J. Atm. Sci. 22, 341 (1965).

89. J. G. Breiland, "Vertical Distribution of Atmospheric Ozone and Its Relation to Synoptic Meteorological Conditions," J. Geophys. Res., 69, 3801 (1964).

90. P. R. Sticksel, "The Vertical Distribution of Ozone over Tallahassee, Florida," Sci. Rep. No. 1, Contract AF 19(628)-4953 (1966).

91. W. S. Hering, "Ozone Measurements for Diagnostic Studies of Atmospheric Circulation," Proc. AIAA Second Annual Meeting, San Francisco (1965), 8 pp.

92. A. R. Meetham, Quart. J. Roy. Met. Soc. 85, 393-404 (1937).

93. D. W. Martin and A. W. Brewer, Quart. J. Roy. Met. Soc. 77, 474-478 (1951).

94. G. Herzberg, Molecular Spectra and Molecular Structure, Vol. III, "Electronic Spectra and Electronic Structure of Polyatomic Molecules," pp. 511-12, D. Van Nostrand Co., Inc., Princeton, New Jersey (1966).

95. R. Trambarulo, S. N. Ghosh, C. A. Burrus, Jr., and W. Gordy, "The Molecular Structure, Dipole Moment, and g factor of Ozone from its Microwave Spectrum," J. Chem. Phys. 21, 851 (1953).

96. G. W. Robinson, Ch. 2.4 "Electronic Spectra," Methods of Experimental Physics, V. 3, Academic Press, New York and London (1962).

97. R. H. Hughes, "The Microwave Spectrum and Structure of Ozone," J. Chem. Phys., 21, 959 (1953).

98. W. Shand and R. A. Spurr, J. Chem. Soc., 65, 179 (1943).

99. Chappius, Ann. de l'ecole normale sup. 11, 137 (1882); Compt. rend. 91, 985 (1880); 94, 858 (1882).

100. E. Vigroux, "Contribution a' l' étude Experimentale de l' Absorption dė l'Ozone," Ann. Phys. 8, 709-762 (1953).

101. Annals of the IGY 5, 46 (1957) "Observer's Handbook for the Ozone Spectrophotometer."

102. E. C. Y. Inn and Y. Tanaka, "Comparison of Recently Recorded Ozone Absorption Coefficients in the Visible and Ultraviolet Regions," Conference on Ozone, Armour Research Foundation (Dec. 1956).

103. G. M. B. Dobson, Royal Met. Soc. Quart. Journ. 89, 409 (1963).

104. R. A. Hamilton and J. M. Walker, J. Atm. Terr. Phys. 28, 667 (1962).

105. USAF Handbook of Geophysics, Ch. 16, Macmillan Co., New York.

106. W. H. Eberhardt and W. Shand, Jr., "On the Ultraviolet Absorption Spectrum of Ozone," J. Chem. Phys. 14, 525 (1946).

107. J. Strong, "On a New Method of Measuring the Mean Height of the Ozone in the Atmosphere," J. Franklin Inst. 231, 121-156 (1941).

108. S. A. Klough and F. X. Kneizys, J. Chem. Phys. 44, 1855 (1966); AFCRL Report, AF Cambridge Laboratories (1965).

109. C. D. Walshaw, "Integrated Absorption by the 9.6μ Band of Ozone," Quart. J. Roy. Meteor. Soc., 83, 315-321 (1957).

110. O. R. Wulf, "The Band Spectrun of Ozone in the Visible and Photographic Infrared," Proc. Nat'l Acad. Sci. (U.S.), 16, 507 (1930).

111. Schoene, J. Russ. Phys., Chem. Soc. 16, 250 (1884); J. Chem. Soc. 48, 713 (1884); Chem. News, 69, 289 (1894).

112. Ladenburg and Lehmann, Ann. Phys. 21, 305 (1906) · Verh. d · deutsch. Phys. Ges. 8, 125 (1906).

113. M. G. Colange, J. Phys. et le rad. 8, 254 (1927), "Etude de l' Absorption Par l' Ozone dans le Spectre Visible."

114. L. Lefebvre, "The Absorption Spectrum of Ozone in the Photographic Infrared Region," Compt. Rend. Acad. Sci. 200, 1743 (1935).

115. R. S. Mulliken, Rev. Mod. Phys., 14, 204 (1942).

116. Hartley, J. Chem. Soc. 39, 57 (1881).

117. Y. Tanaka, E. C. Y. Inn, and K. Watanabe, "Absorption Coefficients of Gases in the Extreme Ultraviolet, Part IV: Ozone," J. Chem. Phys. 21 1651-1653 (1953).

118. E. Von Bahr, Ann. d. Physik 29, 780 (1909).

119. F. E. Fowle, Smithsonian Misc. Coll. 68, No. 8, p. 41 (1917).

120. J. Devaux, Compt. rend. 193, 1207 (1931); 198, 1595 (1934); 201, 1500 (1935).

121. A Adel, V. M. Slipher, and E. F. Barber, Phys. Rev. 47, 580 (1935).

122. A. Adel and C. O. Lampland, Astrophys. J. 91, 481 (1940).

123. J. Strong, Phys. Rev. 55, 1114 (1939).

124. J. Strong and K. Watanabe, Phys. Rev. 57, 1049 (1940).

125. A. Adel and D. M. Dennison, J. Chem. Phys. 14, 379 (1946).

126. M. K. Wilson and R. M. Badger, J. Chem Phys. 16, 741 (1948).

127. O. R. Wulf and E. H. Melvin, "The Effect of Temperature Upon the Ultraviolet Band Spectrum of Ozone and the Structure of this Spectrum," Phys. Rev. 38, 330 (1931).

128. A. Fowler and G. Strutt, Proc. Roy. Soc. 93, 729 (1917).

129. D. Chalonge and L. Lefebvre, Compt. rend. 197, 444 (1933).

130. L. Lefebvre, Compt. rend. 199, 456 (1934).

131. A. Jakowlewa and K. Kondratjew, Phys. Zeits. Sowjetunion 9, 106 (1936).

132. D. Melcher, Helv. Phys. Acta 18, 72 (1945).

133. E. Jones and O. R. Wulf, J. Chem. Phys. 5, 873 (1937).

134. T. Z. Ny and S. P. Choong, Chinese J. Phys. 1, 38 (1933).

135. Huggins, Proc. Roy. Soc. 48, 216 (1890).

136. Meyer, Anna. de Physik 12, 849 (1903).

137. Kriger and Moeller, Physik. Zeits 13, 729 (1912).

138. Fabry and Buisson, "L'Absorption de l'Ultraviolet par l'Ozone et la Limite du Spectre Solaire," Jour. de Phys. Rad. 3, 196 (1913).

139. Shaver, Proc. Roy. Soc. Canada 15, Sec. III, 5 (1921).

140. Lambert, Dejardin, and Chalonge, Compt. rend. 183, 800 (1926).

141. Lauchli, Zeits. f. Physik 53, 92 (1929).

142. Lambry and Chalonge, Gerland's Beitrage Z. Geophysik 24, 42 (1929).

143. Dutheil, Jour. de Phys. rad. 7, 414 (1926).

144. T. Z. Ny and S. P. Choong, Compt. rend. 195, 309 (1932); 196, 916 (1933).

145. Barbier, Chalonge, and Vassy, Revue d'Optique, 14, 425 (1935).

146. M. E. Vassy, Compt. rend. 204, 1426 (1936).

147. E. C. Y. Inn and Y. Tanaka, "Absorption Coefficients of Ozone in the Ultraviolet and Visible Regions," J. Opt. Soc. Amer., 43, 870-873 (1953).

148. K. Angstrom, Arch. f. Math., Astron. och. Phys. I, 345 & 395 (1904).

149. D. Simpson, Trans. Faraday Soc. 41, 209 (1945); J. Chem. Phys. 14, 379 (1946).

150. G. Hettner, R. Pohlmann, and H. J. Schumacher, Zeits. f. Electro Chemie 41, 524 (1933).

151. S. L. Gerhard, Phys. Rev. 42, 622 (1933).

152. A. Adel, et al, Astrophys. J. 89, 320 (1930); 94, 451 (1941); Phys. Rev. 49, 288 (1936).

153. H. Dütsch, "Vertical Ozone Distribution from Umkehr Observation," Archiv Meteor., Geoph. Biokl. A11, 240-251 (1959).

154. C. L. Mateer, "A Rapid Technique for Estimating the Vertical Distribution of Ozone from Umkehr Observations," Quart. Circ. No. 3291, Meteor. Branch, Dept. Transport, Toronto (1960).

155. K. R. Ramanathan and J. V. Dave, "The Calculation of the Vertical Distribution of Ozone by Götz Umkehr-Effect (Method B), Ann. I.G.Y. 5, 23-45 (1957).

156. E. Vigroux and A. Debaix, "Resultats d'observations de l'ozone Atmospherique par la Méthode Infra-Rouge," Ann. Geophys. 19, 31-52 (1963).

157. Paetzold, H. K., "Über die Erfassung der atmosphärischen Ozonverteilung durch Benutzung von Mondfinsternissen," Z. Naturforsch., 6a (11), 639-648 (1951).

158. Paetzold, H. K., "Die durch die atmosphärischen Ozonschicht bewirkte Farbung des Erdschattens auf dem verfinsterten Mond," Naturwissenschaften, 38 (23) 544-545 (1951).

159. Paetzold, H. K., "Erfassung der vertikalen Ozonverteilung in verschiedenen geographischen Breiten bei Mondfinsternissen," J. Atmospheric and Terrest. Phys., 3, 183 (1952).

160. Paetzold, H. K., "Weitere Bestimmungen der vertikalen Ozonverteilung bei Mondfinsternissen," Z. Naturforsch., 7a (5), 325-328 (1952).

161. Paetzold, H. K., "Schwankungen der vertikalen Ozonverteilung in 0^{o} and 60^{o} geographischen Breite nach Mesungen bei Mondfinsternissen," Deut. Wetterdienst in der U.S. Zone, 38, 292-294, Berichte (1952).

162. Paetzold, H. K., "Über die Möglichkeit der Benutzung von Mondfinsternissen zur Erfassung de vertikalen Ozonverteilung in verschiedenen Breiten," Union Géodésique et Géophysique Internationale, Nuevième Assemblée Générale Procés-Verbaux des Séances de l'Association de Météorologie, Mémoires et Discussion, Publication AIM, No. 9/c, 333-336, Brussels (1953).

163. Paetzold, H. K. and E. Regener, "Ozon in der Erdatmosphäre" (see Sec. 9). Bestimmung der vertikalen Ozonverteilung, Methods der Mondifinsternissen in Handbuch der Physik.

164. V. H. Regener, "On a Sensitive Method for the Recording of Atmospheric Ozone," J. Geophys. Res. 65, 3975-3977 (1960).

165. R. M. Goody and W. T. Roach, "The Determination of Tropospheric Ozone from Infrared Emission Spectra," Quart. J. Roy. Meteor. Soc. 84, 108-117 (1958).

166. E. Vigroux, "Distribution Verticale de l'ozone atmospherique d'apres les observations de la bande 9.6μ," Ann. Geophys. 15, 516-538 (1959).

167. C. D. Walshaw, "The Accuracy of Determination of the Vertical Distribution of Atmospheric Ozone from Emission Spectrophotometry in the 1043 cm^{-1} Band at High Resolution," Quart. J. Roy. Meteor. Soc. 86, 519-529 (1960).

168. S. F. Singer and R. C. Wentworth, "A Method for the Determination of the Vertical Ozone Distribution from a Satellite," J. Geophys. Res. 62, 299 (1957).

169. Z. Sekera and J. V. Dave, "Determination of the Vertical Distribubution of Ozone from the Measurement of Diffusely Reflected Ultraviolet Solar Radiation," Plan. Space Sci., 5, 122-136 (1961).

170. Z. Sekera and J. V. Dave, "Diffuse Transmission of Solar Ultraviolet Radiation in the Presence of Ozone," Ap. J. 133, 210-227 (1961).

171. S. Twomey, "On the Deduction of the Vertical Distribution of Ozone by Ultraviolet Spectral Measurements from a Satellite," J. Geoph. Res. 66, 2153-2162 (1961).

172. R. Frith, "Measuring the Ozone above the Earth," Discovery, 390-391 (September 1961).

173. R. D. Rawcliffe, G. E. Meloy, R. M. Friedman, and E. H. Rogers, J. Geophys. Res., 68, 6425 (1963).

174. S. V. Venkateswaran, J. G. Moore, and A. J. Krueger, "Determination of the Vertical Distribution of Ozone by Satellite Photometry," J. Geophys. Res. 66, 1751 (1961).

175. G. W. Simon, "A Practical Solution of the Atmospheric Dispersion Problem," J. Astron, 71, 190-194 (1966).

176. G. Eckhardt, IEEE J. Quantumm Electronics, QE-2, 1 (1966); M. D. Martin and E. L. Thomas, IEEE J. Quantuum Electronics, QE-2, 196 (1966).

177. R. L. Kohn and R. H. Pontell, Appl. Phys. Letters, 8, 231 (1966).

178. J. A. Duardo and F. M. Johnson, J. Chem. Phys. 45, 2325 (1966).

179. J. A. Duardo, L. J. Nugent, and F. M. Johnson, to be published in J. Chem. Phys., May 1, 1967.

180. J. A. Giordmaine and W. Kaiser, Phys. Rev., 144, 676 (1966).

APPENDIX

The phenomenon of stimulated Raman scattering (SRS) can potentially be used to great advantage in molecular spectroscopy investigations, since it results in the production of pulsed, intense, coherent, collimated, and monochromatic radiation. In most instances, SRS has been produced by using either 6943Å ruby laser or 1.058μ neodymium laser radiation. On the other hand, the so-called second harmonic radiation of these laser sources, at 3472Å and 5290Å, respectively, would provide a more useful set of discrete SRS wavelengths, i.e., "laser-like" radiation in the ultraviolet spectral region where the electronic absorption bands of a great number of molecules are located. However, few experiments of SRS involving the second-harmonic of giant-pulsed laser radiation have been reported. One reason for this is that the powers available at the second harmonic wavelength are an order of magnitude or two lower than those of the primary laser radiation. In certain cases, quenching processes, such as two-photon absorption, may also serve to inhibit SRS of the second harmonic radiation.

This appendix describes experiments which demonstrate that when ruby laser radiation (6943Å) and its second harmonic (3472Å) are simultaneously passed through an SRS active material, a "pseudo-SRS" spectrum of the 3472Å radiation can be produced. That is, coherent radiation is made to appear at wavelengths identical to those which would be produced by SRS of the 3472Å radiation.

However, power measurements indicate that the mechanism responsible for the interaction is more properly described as a modulation of the 3472Å radiation by molecular vibrations which are coherently driven by the 6943Å laser radiation. The effect is similar to that which has been shown to account for the Raman-type scattering of a probe light by coherently driven lattice vibrations[1]. In the present case, the effect was used to produce second harmonic pseudo-SRS spectra of hydrogen and methane gases and of a number of liquid substances.

The experimental arrangement is as shown in Fig. A-1. The ruby laser was Q-switched by means of a rotating prism and produced between 40 and 90 megawatts of 6943Å radiation during a 34-nanosecond pulse. The 3472Å radiation was produced by passing the ruby laser radiation through a 2.5 cm KDP crystal whose z-axis was oriented so as to allow the production of 3472Å through a nonlinear polarization, phase-matching mechanism[2]. The power and energy measuring devices shown in the figure were used to monitor the intensities of the 6943Å and 3472Å radiation components incident on the scattering medium. A variety of filters were used to differentially attenuate the two radiation components before they entered the scattering medium in order to determine the intensity combinations which produced second harmonic SRS spectra. The occurrence or nonoccurrence of SRS was determined spectrographically, by means of an f/6.3, 0.75m Jarrell-Ash spectrograph. The discussion below will deal only with the results obtained for the specific example of hydrogen gas.

The threshold power for SRS of laser radiation by hydrogen gas is determined by such factors as gas pressure and temperature[3], the effective focal volume of the lens system used[4], and the linewidth and polarization of the incident laser radiation[5,6]. With the

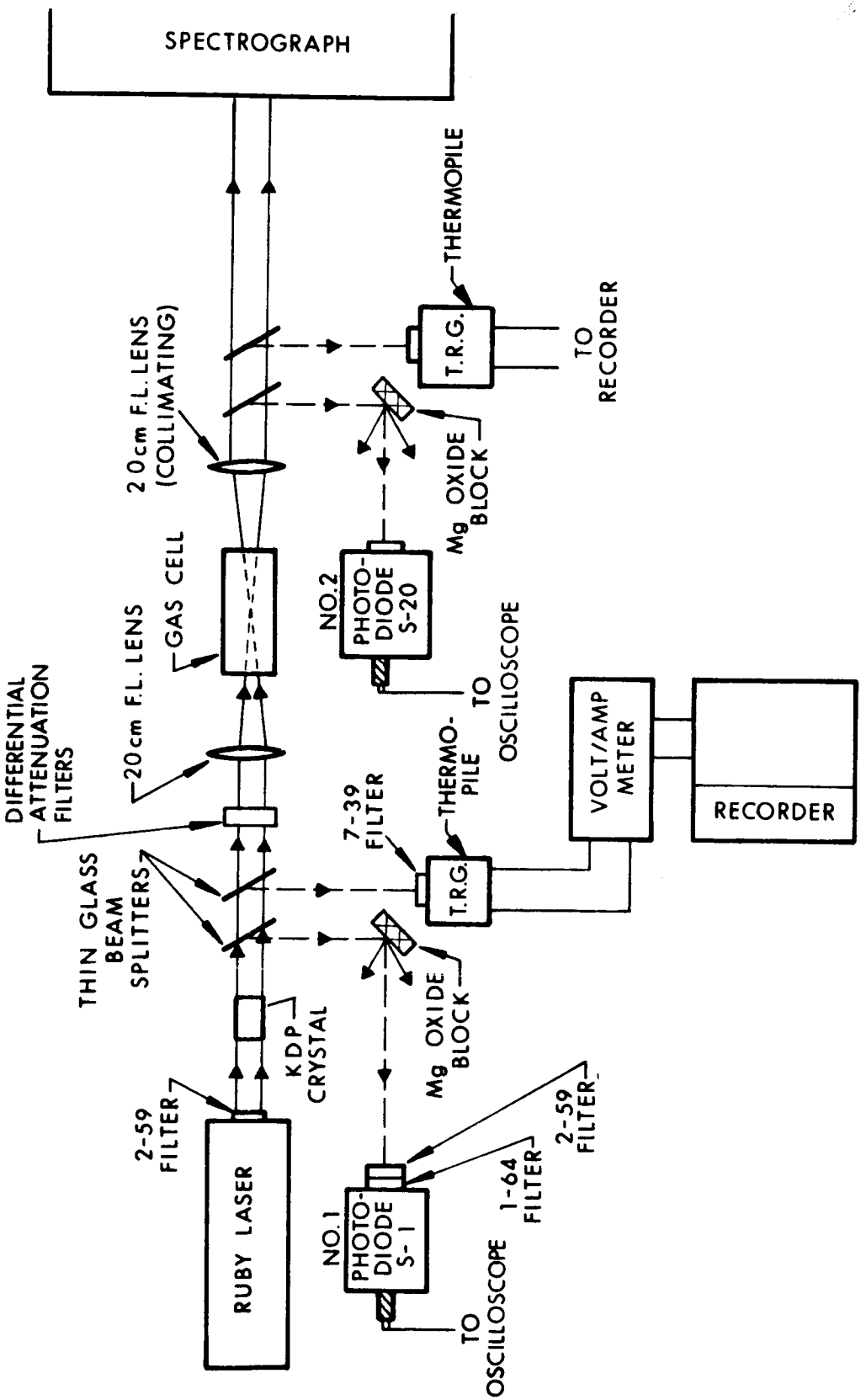

Figure A-1. Experimental Arrangement used in the Determination of Threshold Values for SRS of 6943Å and 3472Å Laser Radiation

7087-IR-1

coherent radiation can be caused to occur at $\nu' \pm n\nu_R$, where ν_R is the Raman shift characteristic of the scattering material. This technique was also used to produce pseudo-SRS spectra of methane and of carbon disulfide, benzene and ethyl iodide. Experiments, which will be described elsewhere, show that ν' need not necessarily be the second harmonic of indident laser radiation, but may also be the anti-Stokes SRS component of a preliminary scattering material, i.e., when two scattering media are used in tandem.[7]

The mechanism responsible for the effect referred to herein as pseudo-SRS is a general one and was first described in terms of classical scattering theory by Garmire,[4] et al, to account for the production of multiple vibrational frequency shifts in SRS. Since then, extensions of the theory have been used to explain: (1) the detection of laser-stimulated lattice vibrations, or optical phonons, by low-intensity monochromatic probes;[1] (2) the appearance of combination (sum and difference) vibrational Raman shifts in the SRS spectra of two gases, which may either be two components in a gas mixture or different gases in separate cells[3]; and (3) the production of a complex vibrational-rotational SRS spectrum of hydrogen when excited by giant-pulsed 1.058μ laser radiation[8].

Since the hydrogen gas can be considered to be essentially dispersionless, a simplified form of the theory, which neglects momentum-matching requirements, can be used in the present case. The frequencies emitted by the hydrogen gas can then be deduced by analyzing the time-dependence of the oscillating electric dipole moment associated with coherently driven molecular vibrations. This dipole moment, $\vec{\mu}$, is given by

$$\vec{\mu} = q\left(\frac{\delta\alpha}{\delta q}\right)_o \vec{E} \qquad (1)$$

hydrogen gas at 40 atmospheres and at room temperature, and with the experimental arrangement shown in Fig. A-1, the threshold power for SRS of 6943Å was determined to be 30 MW ± 3 MW. This threshold value was obtained whether or not the 3472Å radiation was simultaneously passed through the hydrogen sample. The onset of 6943Å SRS was determined by the appearance of spectral lines at the frequencies $\nu_L \pm n\nu_{H_2}$, where ν_L is the laser frequency, 14,400 cm^{-1}, ν_{H_2} = 4155 cm^{-1} and n = 0, 1, 2, ... The maximum intensity of 3472Å produced by the KDP crystal was 1 megawatt. It was not found possible to excite an SRS spectrum with this second harmonic radiation, as long as the intensity of 6943Å radiation simultaneously incident on the hydrogen sample was kept lower than 30 MW by differential filtering. That is, the powers available at the second harmonic wavelength were clearly below the threshold power required for the production of SRS. (The actual threshold for 3472Å SRS was not determined, due to the limited second harmonic generation efficiency attained in the experiments described here.)

However, even though the 3472Å intensity was below the SRS threshold, the second harmonic SRS frequencies, $2\nu_L \pm n\nu_{H_2}$, appeared in the spectrum whenever the incident 6943Å radiations was sufficiently intense to produce the primary SRS frequencies, $\nu_L \pm n\nu_{H_2}$. That is, once the 6943Å SRS threshold was exceeded, the 3472Å SRS also occurred simultaneously, with no apparent additional threshold requirement. The pseudo-SRS spectrum was observed when powers as low as 0.2 megawatt of 3472Å radiation were used, providing that more than 30 megawatts of 6943Å were simultaneously incident on the sample.

The results described above are taken as evidence that if relatively low intensity radiation of frequency ν' is transmitted through a medium in which SRS is excited by high intensity laser radiation,

where q is the amplitude of the molecular vibration which is driven by a force which is proportional to the square of the total electric field[3,4], and $(\frac{\delta\alpha}{\delta q})_o$ is the polarizability derivative with respect to q, which is assumed to be isotropic for simplicity. It has been shown[3] that with the gas pressures used, in the present experiments the driving force is due primarily to the electric field components associated with the high-intensity laser radiation (6943Å) and its Raman-shifted frequencies. When the time dependence of q and the components of $\vec{E}$ are explicitly inserted into Eq. 1, it is readily seen that if there is a component of the field corresponding to the frequency ν', the frequencies $\nu' \pm n\nu_R$ will be emitted by the oscillating dipole, provided that the frequencies ν_R are excited in SRS by the ruby laser.

REFERENCES

1. J. A. Giordmaine and W. Kaiser, Phys. Rev., 144, 676 (1966).
2. A. Savage and R. C. Miller, Appl. Opt. 1, 661 (1962).
3. J. A. Duardo, L. J. Nugent, and F. M. Johnson to be published in J. Chem. Phys. May 1, 1967.
4. E. Garmire, F. Pandarese and G. H. Townes, Phys. Rev. Ltrs., 11, 160 (1963).
5. R. W. Minck, R. W. Terhune, and W. G. Rado, Appl. Phys. Ltrs. 3, 181 (1963).
6. R. V. Wick, J. A. Wiggins, and D. H. Rank, Appl. Opt. 5, 473 (1966).
7. J. A. Duardo and F. M. Johnson (to be published).
8. F. M. Johnson, J. A. Duardo, and G. L. Clark, Appl. Phys. Ltrs., 10, 157 (1967).